15

0-315-15925-1

National Library of Canada
Bibliothèque nationale du Canada

Canadian Theses Division
Division des thèses canadiennes

Ottawa, Canada
K1A 0N4

63834

PERMISSION TO MICROFILM — AUTORISATION DE MICROFILMER

• Please print or type — Écrire en lettres moulées ou dactylographier

Full Name of Author — Nom complet de l'auteur

DOUGLAS. NORMAN ABRAMS

Date of Birth — Date de naissance

JULY 14, 1952

Country of Birth — Lieu de naissance

CANADA

Permanent Address — Résidence fixe

27 Bluebird Crescent
Sherwood Park, Alberta, Canada

Title of Thesis — Titre de la thèse

Synthesis and Evaluation of Some Radiohalogenated 2'-Halo-2'-deoxyuridine and 6-Halouracil Analogues as Tumor Diagnostic Radiopharmaceuticals

University — Université

University of Alberta

Degree for which thesis was presented — Grade pour lequel cette thèse fut présentée

Ph. D.

Year this degree conferred — Année d'obtention de ce grade

1983

Name of Supervisor — Nom du directeur de thèse

Dr. L.I. Wiebe and Dr. E.E. Knaus

Date

March 7, 1983

Signature

D Abrams

NL-91 (4/77)

THE UNIVERSITY OF ALBERTA

SYNTHESIS AND EVALUATION OF SOME RADIOHALOGENATED 2'-HALO-2'-DEOXYURIDINE AND 6-HALOURACIL ANALOGUES AS TUMOR DIAGNOSTIC RADIOPHARMACEUTICALS

by

DOUGLAS NORMAN ABRAMS

A THESIS

SUBMITTED TO THE FACULTY OF GRADUATE STUDIES AND RESEARCH

IN PARTIAL FULFILLMENT OF THE REQUIREMENTS FOR THE DEGREE

OF DOCTOR OF PHILOSOPHY

IN

PHARMACEUTICAL SCIENCES

(BIONUCLEONICS)

FACULTY OF PHARMACY AND PHARMACEUTICAL SCIENCES

EDMONTON, ALBERTA

SPRING 1983

THE UNIVERSITY OF ALBERTA

RELEASE FORM

NAME OF AUTHOR - DOUGLAS NORMAN ABRAMS

TITLE OF THESIS - SYNTHESIS AND EVALUATION OF SOME RADIOHALOGENATED 2'-HALO-2'-DEOXYURIDINE AND 6-HALOURACIL ANALOGUES AS TUMOR DIAGNOSTIC RADIOPHARMACEUTICALS

DEGREE FOR WHICH THESIS WAS PRESENTED - Ph.D.

YEAR THIS DEGREE GRANTED - 1983

. . . D Abrams . . . . . .

PERMANENT ADDRESS:

Douglas N. Abrams
27 Bluebird Crescent
Sherwood Park, Alberta
T8A 0E6

DATED March 3. 19 83

THE UNIVERSITY OF ALBERTA

FACULTY OF GRADUATE STUDIES AND RESEARCH

The undersigned certify that they have read, and recommend to the Faculty of Graduate Studies and Research, for acceptance, a thesis entitled "Synthesis and Evaluation of Some Radiohalogenated 2'-Halo-2'-Deoxyuridine and 6-Halouracil Analogues as Tumor Diagnostic Radiopharmaceuticals" submitted by Douglas Norman Abrams in partial fulfillment of the requirements for the degree of Doctor of Philosophy in Pharmaceutical Sciences (Bionucleonics).

.....

Supervisor

Edward E. Knaus

.....

Supervisor

A.R.P. Paterson

.....

Douglas M. Sheppard

.....

M.J. Robins

.....

Peter Timan

.....

External Examiner

DATE March 2 1983

DEDICATION

To

Sharon,
Kory and Ryan

ABSTRACT

Several radiohalogenated nucleosides and pyrimidine bases were synthesized and evaluated as potential radiopharmaceuticals for non-invasive tumor diagnosis. 2'-[^{18}F]-Fluoro-2'-deoxyuridine (2'-[^{18}F]-FUdR), 2'-[^{34m}Cl]-chloro-2'-deoxyuridine (2'-[^{34m}Cl]-ClUdR) and 2'-[^{123}I]-iodo-2'-deoxyuridine (2'-[^{123}I]-IUdR) were synthesized via reaction of the appropriate radiohalide with 2,2'-cyclouridine in acidic media. 6-[^{123}I]-Iodouracil and 6-[^{36}Cl]-chlorouracil were prepared via non-isotopic halide exchange reactions with 6-chlorouracil and 6-iodouracil respectively.

Methods for the recovery of ^{18}F and ^{34m}Cl from the production targets, in a chemical form compatible with the proposed labelling techniques, were investigated. The production of anhydrous hydrogen fluoride-18 via the $^{16}O(^{3}He,n)^{18}Ne \xrightarrow{\beta^+} {}^{18}F$, $^{20}Ne(d,\alpha)^{18}F$, $^{6}Li(n,t)\alpha$-$^{16}O(t,n)^{18}F$ nuclear reactions were evaluated. The highest recovery (69.3%) of ^{18}F was obtained when the $^{20}Ne(d,\alpha)^{18}F$ nuclear reaction was used and the irradiated target was purged with a mixture of anhydrous hydrogen fluoride in neon. The utility of ^{34m}Cl produced via the $^{35}Cl(p,pn)^{34m}Cl$, $^{34}S(d,2n)^{34m}Cl$ and $^{34}S(p,n)^{34m}Cl$ nuclear reactions was examined. The $^{34}S(p,n)^{34m}Cl$ reaction, with hydrogen sulfide as the target gas, afforded the best compromise between absolute yield (13.0 MBq $\mu A^{-1}h^{-1}$) and specific activity (from 300 MBq $mmol^{-1}$ to no-carrier-added) of ^{34m}Cl.

The *in vivo* tissue distribution of each radiohalogenated nucleoside or nucleobase was evaluated in a murine tumor model to determine its' potential for use in non-invasive tumor imaging. The tissue

distribution of 6-[^{123}I]-iodouracil, 2'-[^{123}I]-IUdR and 6-[^{3}H]-2'-FUdR were studied in a Walker 256 carcinosarcoma model in male Wistar rats. The tissue distribution of 2'-ClUdR was determined with 2'-[^{36}Cl]-2'-ClUdR in a Lewis Lung carcinoma model in male BDF_1 mice. The analogues tested showed low absolute uptake of radioactivity by the tumor (maximum tumor uptake of 6-[^{123}I]-iodouracil = 1.58, 2'-[^{123}I]-IUdR = 0.55, 6-[^{3}H]-2'-FUdR = 0.41 and 2'-[^{36}Cl]-ClUdR = 2.42 % of the injected radioactivity dose) and persistently high blood levels of radioactivity (6-[^{123}I]-iodouracil = 5.52, 2'-[^{123}I]-IUdR = 2.78, 6-[^{3}H]-2'-FUdR = 4.29 and 2'-[^{36}Cl]-ClUdR = 0.72 % of injected radioactive dose 2 hours after injection). These two factors did not provide a sufficient concentration gradient between the tumor and surrounding tissue suitable for satisfactory gamma camera imaging procedures with these new radiolabelled analogues.

ACKNOWLEDGEMENTS

I wish to express my thanks to Drs. E.E. Knaus and L.I. Wiebe for their direction and guidance during the course of this research and the preparation of this manuscript. Without their help and patience the completion of this study would not have been possible.

Es ist mir ein Anliegen, mich bei Dr. Helus, Dr. Maier-Borst and Dr. Sahm für ihre Hilfe und Unterstützung zu bedanken. Ich danke Herr Gasper, Herr Winniwisser und Fräulein Winkler für ihre technische Hilfe. Ich möchte mich auch bei Dr. Schumacher und Dr. Sinn für ihre technische Beratung bedanken und ich danke Dr. Wolber, Herr Konowalchuk und Herr Weber für ihre Hilfe mit dem Zyklotron. Zuletzt, will ich Franz Oberdorfer, Heinrich Bauer, Jurgen Schoer, George Zubal und Michael Treiber für ihre Freundschaft danken.

I wish to thank Connie Turner, Gilbert Matte and Pam Zabel for their help with the drawings, Chris Ediss and Steve McQuarrie for their technical and mathematical consultation, John Mercer, Richard Flanagan, Yip Lee and Tom Sykes for their willingness to lend a helping hand, Dr. Wolowyk, his staff, Dr. Noujaim and Barb Hepperle for their help with the tissue culture work. I would also thank Bev Johnson for her patience during the typing of this manuscript.

Financial assistance from the University of Alberta, the Deutscher Akademischer Austauschdienst, the Alberta Heritage Foundation for Medical Research and the Dissertation Fellowship is gratefully acknowledged.

TABLE OF CONTENTS

Page

Page

Page

Page

Page

LIST OF TABLES

LIST OF FIGURES

LIST OF SCHEMES

LIST OF PLATES

LIST OF ABBREVIATIONS

Abbreviation	Term
α	Alpha
Ac	Acetyl
AHF	Anhydrous hydrogen fluoride
ara-A	9-β-D-Arabinofuranosyladenine
ara-C	1-β-D-Arabinofuranosylcytosine
ara-5FU	1-β-D-Arabinofuranosyl-5-fluorouracil
ara-H	9-β-D-Arabinofuranosylhypoxanthine
ara-U	1-β-D-Arabinofuranosyluracil
atm	Atmosphere
β^+	Positron
β^-	Electron
Bq	Becquerel; 1 Disintegration per second
2'-BrUdR	1-(2'-Bromo-2'-deoxy-β-D-ribofuranosyl)-uracil
5-BrUdR	5-Bromo-2'-deoxyuridine
C	Carrier
CA	Carrier added
cc	Centrifugal chromatography
CdR	2'-Deoxycytosine
CDP	Cytidine-5'-diphosphate
CF	Carrier free
Ci	Curie, 3.7×10^{10} disintegrations per second
6-ClU	6-Chlorouracil
2'-ClUdR	1-(2'-Chloro-2'-deoxy-β-D-ribofuranosyl)-uracil

CMP	Cytidine-5'-monophosphate
cm	Centimeter
cpm	Count per minute
CR	Cytidine
CTP	Cytidine-5'-triphosphate
d	Deuteron; deuterium; ^2H
dCDP	2'-Deoxycytidine-5'-diphosphate
dCMP	2'-Deoxycytidine-5'-monophosphate
dCTP	2'-Deoxycytidine-5'-triphosphate
dec	Decomposition
DMF	Dimethylformamide
DMSO-d_6	Deuterated dimethylsulfoxide
DNA	Deoxyribonucleic acid
DPC	Diphenylcarbonate
dpm	Disintegration per minute
dps	Disintegration per second
dTDP	2'-Deoxythymidine-5'-diphosphate
dTMP	2'-Deoxythymidine-5'-monophosphate
dTTP	2'-Deoxythymidine-5'-triphosphate
dUDP	2'-Deoxyuridine-5'-diphosphate
dUMP	2'-Deoxyuridine-5'-monophosphate
dUTP	2'-Deoxyuridine-5'-triphosphate
EC	Electron capture
EOB	End of bombardment
2'-FCdR	1-(2'-Fluoro-2'-deoxy-β-D-ribofuranosyl)-cytosine
2'-FdCDP	1-(2'-Fluoro-2'-deoxy-β-D-ribofuranosyl)-cytosine-5'-diphosphate

2'-FdUDP	1-(2'-Fluoro-2'-deoxy-β-D-ribofuranosyl)-uracil-5'-diphosphate
2-FDG	2-Fluoro-2-deoxyglucose
2'-FUdR	1-(2'-Fluoro-2'-deoxy-β-D-ribofuranosyl)-uracil
5-FUdR	5-Fluoro-2'-deoxyuridine
5-FUMP	5-Fluorouridine-5'-monophosphate
γ	Gamma ray
g	Gram
GBq	Gigabecquerel; 10^9 disintegrations per second
^{1}H nmr	Proton nuclear magnetic resonance
Hz	Hertz
IT	Isomeric transition
6-IU	6-Iodouracil
2'-IUdR	1-(2'-Iodo-2'-deoxy-β-D-ribofuranosyl)-uracil
5-IUdR	5-Iodo-2'-deoxyuridine
J	Coupling constant
kBq	Kilobecquerel; 10^3 disintegrations per second
keV	Kiloelectron volt
λ	Decay constant
lit	Literature
lsc	Liquid scintillation counting
μA	Microampere
μl	Microliter
μM	Micromolar
μmol	Micromole
MBq	Megabecquerel; 10^6 disintegrations per second
mEq	Milliequivalent

mg	Milligram
min	Minute (time)
ml	Milliliter
mm	Millimeter
mmol	Millimole
mp	Melting point
ms	Mass spectroscopy
n	Neutron
NBMPR	Nitrobenzylthioinosine
NCA	No carrier added
nm	Nanometer
OMP	Orotidine-5'-monophosphate
p	Proton; ^{1}H
pmol	Picomole
rbc	Erythrocyte
rp-hplc	Reverse phase high pressure liquid chromatography
RNA	Ribonucleic acid
s	Second
T	Thymine
t	Triton; ^{3}H
$T_{\frac{1}{2}}$	Half-life
TBq	Terabecquerel; 10^{12} disintegrations per second
TdR	2'-Deoxythymidine
tlc	Thin layer chromatography
TMS	Trimethylsilyl derivative
TPP	Toluene : diphenyloxazole : p-bis-[2-(5-phenyl-oxazolyl)]benzene

tRNA	Transfer RNA
U	Uracil
2'-UdR	2'-Deoxyuridine
UDP	Uridine-5'-diphosphate
UMP	Uridine-5'-monophosphate
UTP	Uridine-5'-triphosphate
UR	Uridine
uv	Ultraviolet
v/v	Volume/volume
w/w	Weight/weight

I. INTRODUCTION

Two aspects of cancer treatment are of particular interest to radiopharmacy and nuclear medicine. These are early detection of the disease and evaluation of the subsequent response to treatment. Clinically the degree of tumor regression is the parameter most often used to evaluate a therapeutic modality. However the methods currently in use are subject to error and are not applicable to a wide population of tumors[1]. For example, the rate of cell loss from a tumor is not always proportional to the number of cells killed and may be characteristic of each individual tumor[2]. Therefore tumor volume regression is not a very sensitive indicator in many tumor systems. A method more applicable to the clinical setting would allow quantitation of the proliferative potential of a tumor mass with non-invasive techniques. The possibility of localizing primary or metastatic tumors and assessing, non-invasively, changes in the proliferative states of malignant tissues with radionuclide tracers (tumor diagnostic agents) would be very useful clinically[3,4].

Radioisotope techniques are often the methods of choice for examining patients with suspected tumors. The techniques are non-invasive, atraumatic, give little radiation hazard in relation to the nature of the disease and yield results with an accuracy comparable to other more expensive or more complicated tests[5]. However most of the tumor imaging agents studied have been discovered empirically and are non-specific. For example, radioactive gallium, which was first introduced as a bone scanning agent, is widely used clinically as a general tumor imaging agent but is known to accumulate in abscesses as well[6,7].

A more rational approach to the development of tumor diagnostic agents has been based on the knowledge that exogenously supplied nucleosides are incorporated into cellular DNA and RNA via the salvage pathway[3,4,8] in a manner proportional to the number of dividing cells. Thus thymidine, labelled with ^{11}C [9,10], has been studied as a potential radiopharmaceutical for the determination of DNA synthesis in intact organisms. The short half-life of ^{11}C limits the usefulness of this radiotracer to medical centers which have close access to a cyclotron. A second disadvantage of ^{11}C-labelled thymidine is the observation that it is rapidly catabolized and the ^{11}C labelled catabolites are reutilized to label sites other than DNA, such as lipids and proteins[3,10]. The thymidine analogue, 5-iodo-2'-deoxyuridine (5-IUdR)[11] has been investigated as an alternative to ^{11}C-labelled thymidine since it is not subject to the same limitations[3]. The authors concluded that measurement of the total uptake of 5-IUdR by a tumor before and after treatment should give an indication of the tumor response to the therapy.

The rapid loss of radioiodide, low tumor specificity and the length of time required to evaluate tumor therapy using radiolabelled 5-IUdR stimulated the study of alternative halogenated nucleosides. Thus, the feasibility of using ^{18}F-labelled 5-fluoro-analogues of uracil[12,13], uridine[4] and 2'-deoxyuridine[14,15] to provide an index of the proliferative potential (fraction of cells in a tumor capable of repopulating the tumor) of tumor tissue was investigated. The rationale for using the fluorinated analogues is different than that for 5-IUdR. The 5-fluoro-analogues are known to be metabolically

phosphorylated and thereby trapped inside the cells. Intracellularly, 5-fluorouracil and 5-fluoro-2'-deoxyuridine are converted to 5-fluoro-2'-deoxyuridine-5'-monophosphate which binds to and inhibits the enzyme thymidylate synthetase [16]. 5-Fluorouridine and 5-fluorouracil are anabolized to the nucleoside triphosphate and incorporated into RNA [4].

The objective of this project was to synthesize and evaluate a series of radiohalogenated pyrimidine bases and nucleosides as radiopharmaceuticals for the non-invasive delineation of a tumor. The 2'-halo-2'-deoxyuridine analogues chosen (2'-FUdR, 2'-ClUdR and 2'-IUdR) are considered to be analogues of uridine [17,18] and the 6-halouracil derivatives (6-chlorouracil and 6-iodouracil) may be considered uracil or orotic acid analogues[19]. Although the biochemical fate of these analogues is not well understood, they have the potential to enter the pyrimidine metabolic pathways via the salvage pathway and therefore interact with the cellular metabolic process. The specific goals of the project were to:

1. determine if the radiohalogenated analogues chosen could be synthesized and purified within the time frames imposed by the short-lived radionuclides selected;
2. determine if ^{18}F and ^{34m}Cl could be recovered in a chemical form suitable for the synthesis of the fluoro and chloro derivatives; and
3. determine if the radiolabelled analogues would demonstrate sufficient tumor selectivity and absolute incorporation into

the tumor, within the time constraints of each radionuclide, to make non-invasive gamma camera imaging practical in a clinical setting.

II. LITERATURE SURVEY

A. Historical Development of Nuclear Medicine and Radiopharmacy

In 1896, Antoine Henry discovered a naturally occurring radioactive uranium salt. Five years later in 1901, Henri Alexander Danlos reported the first medical use of a radioisotope with the introduction of radium therapy. Henri Ludwig Blumgart pioneered the diagnostic use of radioactivity *in vivo* in 1924 by attempting to determine blood velocity in man by injecting a solution of radon in normal saline intravenously. However nuclear medicine would probably not have evolved into a viable diagnostic tool without the development of artificial radioisotopes. In 1934, Jean Frederic Joliot-Curie and his wife Irene became the first radiochemists to produce the artificial radioisotope ^{30}P. One year later Hevesey used this new radiophosphorous radionuclide for metabolic studies in rats[20]. Radiophosphorous was later shown to accumulate in tumors and by 1941 Kroll *et al*. had predicted a bright future for the detection of tumors with radionuclides[21].

The nuclear reactor first built by Fermi and his colleagues in 1942 soon became the mainstay of the radiopharmaceutical industry even though E.O. Lawrence had developed the cyclotron many years earlier in 1930. Most radionuclides used in medicine, industry and research today are extracted from the fission products of reactors or are produced specifically by slow (thermal) neutron irradiation of selected target materials inside the reactor[20].

The recent interest in cyclotron produced radionuclides is a result of the latest requirements demanded by nuclear medicine physicians for radiopharmaceuticals. The initial approach in

nuclear medicine was to visualize, non-invasively, the *in vivo* physiological distribution of radioactivity in a particular organ or localize a suspected abnormality[22]. Therefore the majority of the procedures were designed to reveal anatomical or physiological function abnormalities. However, the development of X-ray computed tomography, ultrasonography and the potential of nuclear magnetic resonance imaging techniques, provides the medical community with a comprehensive battery of methods to determine the gross abnormalities of specific organs, of which nuclear medicine plays only a part[23]. Therefore the focus of nuclear medicine has shifted towards the more subtle aspects of organ function. The major objective is to elucidate how efficiently an organ or system is functioning[24], by quantification of various parameters such as metabolism[25], membrane transport[26] and the viable fraction of a cell mass[3].

The advent of single photon emission computed tomography (SPECT)[27] and positron emission tomography (PET)[28] has greatly increased the accuracy with which accumulated data can be quantitated. The increased accuracy is due to the inherent superiority of contrast resolution demonstrated by tomographic techniques in comparison to planar scintigraphy. Whereas the gamma camera provided two dimensional analysis of the three dimensional phenomenon of *in vivo* tracer distribution, PET and SPECT techniques allow the third dimension to be measured. This allows the contribution of activity above and below the region of interest (ROI) to be rejected and the activity within the ROI to be more precisely determined[29]. A relatively long imaging time is required to accumulate statistically significant data during

which time a steady state concentration of radiotracer within the ROI is necessary for accurate interpretation of the results. The challenge for nuclear medicine and radiopharmacy therefore lies in the design and synthesis of radiopharmaceuticals that will fulfill the requirements imposed by the imaging instrumentation and answer the specific questions related to tissue function asked by physicians.

B. Radiopharmaceutical Design

The concept of a "magic bullet" has provided incentive for the development of new, more specific chemotherapeutic agents and diagnostic techniques in all areas of medical research. The design of new radiopharmaceuticals is no exception. New approaches rely upon an understanding of the pharmacology, biochemistry, physiology and anatomy unique to the subject in question. The structure-activity relationship information elucidated from current agents is also important.

The design of radiopharmaceuticals is further complicated by the choice of a suitable radioactive label. The half-life of the radionuclide must be long enough for the radiopharmaceutical to be synthesized and purified, to allow the radiopharmaceutical sufficient time to localize and concentrate in the organ of interest and to provide an observed level of radioactivity which does not decrease significantly via physical decay during the imaging procedure. These factors must be compromised to minimize the radiation dose to the patient[30]. The mode of decay of the radionuclide must be suitable for external detection purposes. Thus α and β^- emissions and very low energy γ rays and X rays which cannot be detected outside the body are undesirable components of a radionuclide decay scheme. Very high energy γ emissions are also undesirable because they are poorly detected (low sensitivity), cause high background count rates and result in high radiation fields during synthesis and purification of the product[27,31]. Furthermore the specific activity of the radiopharmaceutical must be sufficiently high to preclude induction of an undesirable pharmacological response or saturation of the biological system being studied[32].

Most biologically active compounds consist of carbon, hydrogen, oxygen and nitrogen. This composition represents a major obstacle to the synthesis of radiopharmaceuticals containing "natural" labels. There are no γ emitting radioisotopes of hydrogen and the clinically useful radioisotopes of oxygen, nitrogen and carbon have very short half-lives ($T_{\frac{1}{2}}$ ^{15}O = 2 min, ^{13}N = 10 min and ^{11}C = 20 min)[33]. Therefore frequent use is made of "foreign" labels to design analogues of physiologically active compounds in anticipation that they will behave biologically similar to the parent molecule.

The radiohalogens ^{18}F, ^{34m}Cl, ^{77}Br and ^{123}I are particularly well suited as "foreign" labels for radiopharmaceuticals and are potentially the cyclotron-produced nuclides of choice in nuclear medicine[34,35]. The advantages of the halogen family as radiolabels are based on both their chemical and physical characteristics. Halogen chemistry is well documented and in many instances is directly applicable to radiochemical labelling techniques. The advantageous physical attributes of radiohalogens include their short half-lives and emission characteristics (Table I) which are particularly well suited for either the widely available single photon instrumentation or the newer SPECT and PET techniques[34,35].

The design of radiohalogenated pyrimidine nucleosides and nucleobases for potential use as tumor imaging agents requires consideration of:

1. the general metabolism of natural nucleosides;
2. the metabolic and structural perturbations that may occur with the introduction of the halogen label;

TABLE I. Physical Characteristics of Some Medically Useful Radiohalogens[33].

Radionuclide	Half-Life	Major Emissions	Abundancy %	Energy MeV
^{18}F	109.9 min	β^+	97	0.635
		γ^1	194	0.511
^{34}Cl	1.5 s	β^+	100	4.45
		γ^1	200	0.511
^{34m}Cl	32.0 min	β_1^+	26	2.5
		β_2^+	26	1.3
		$\gamma_{(IT)}$ [2]	47	0.145
		$\gamma_{(\beta^+)}$	12	1.17
		$\gamma_{(\beta^+)}$	38	2.13
		$\gamma_{(\beta^+)}$	12	3.32
		γ^1	104	0.511
^{77}Br	57 h	$\gamma_{(EC)}$ [3]	22.8	0.24
		$\gamma_{(EC)}$ [3]	22.1	0.52
^{123}I	13 h	$\gamma_{(EC)}$ [3]	82.9	0.159

1. Annihilation photon: photon produced by the annihilation of a positron and an electron.

2. Isomeric transition: a transition between two isomeric states of a nucleus or from an isomeric state to the ground state.

3. Electron capture: a radioactive transformation whereby a nucleus captures one of its orbital electrons[36].

3. the synthetic routes available for introducing the label into the desired position; and
4. the availability of the radiohalogens in the chemical form required for the synthesis.

C. The Metabolism of Pyrimidine Nucleosides

The ability to synthesize pyrimidine nucleotides required for DNA and RNA synthesis (Scheme 1) [37,38] is an almost universal trait among living cells [39]. However, it is via the salvage reactions (Scheme 2) [37,40,40a,41] that many nucleobase and nucleoside analogues gain entry into the metabolic reactions depicted in Scheme 1. For example, 5-fluorouracil can be converted directly to the ribonucleoside monophosphate, 5-fluorouridine-5'-monophosphate (5-FUMP) by pyrimidine phosphoribosyltransferase [42]. 5-Fluorouracil can also be converted directly to 5-FUMP via a two step synthesis. First 5-fluorouracil is converted to the ribonucleoside, 5-fluorouridine (5-FUR), by uridine phosphorylase. Then, 5-FUR is phosphorylated by uridine-cytidine kinase to 5-FUMP. However, the 2'-deoxyribonucleoside-5'-monophosphate derivative of a pyrimidine base cannot be obtained directly from the free base in one step. For example, 5-fluorouracil must first be converted to the deoxyribonucleoside, 5-fluoro-2'-deoxyuridine (5-FUdR) by either uridine phosphorylase or thymidine phosphorylase. The deoxyribonucleoside 5-FUdR is then phosphorylated by thymidine kinase to 5-FdUMP. Uridine phosphorylase and thymidine phosphorylase have overlapping specificity. 5-Fluorouracil, 5-FUR and 5-FUdR must be converted to nucleotides to exert their cytotoxicity [42,44]. However, it is not necessary for all nucleosides to be phosphorylated to exert a biological effect. For example, the physiological nucleoside adenosine has been implicated in a variety of regulatory functions [45].

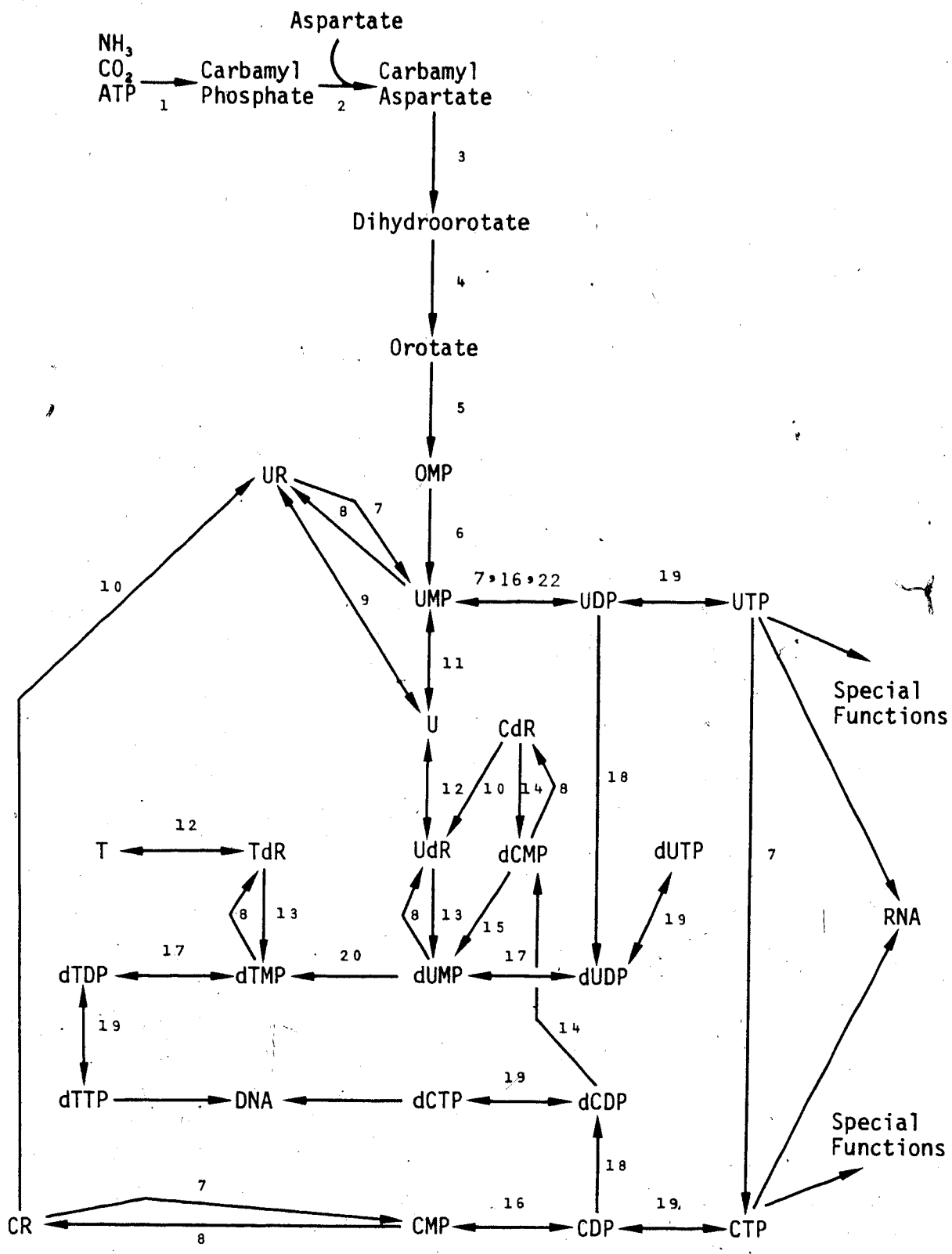

Scheme 1. Pyrimidine Metabolic Pathways[37, 38, 40, 40a]

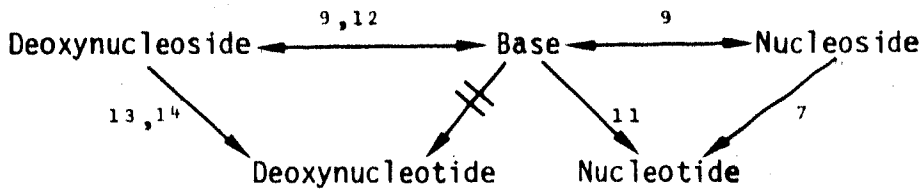

Scheme 2. Salvage Pathway for Pyrimidine Metabolism[37,40,41,40a]

Enzymes in Schemes 1 and 2

	Enzyme Trivial Name	Enzyme Commission Number[43]
1	Carbamyl Phosphate Synthetase II	2.7.2.2
2	Aspartate Carbamyltransferase	2.1.3.2
3	Dihydroorotase	3.5.2.3
4	Dihydroorotate Dehydrogenase	1.3.3.1
5	Orotate Phosphoribosyltransferase	2.4.2.10
6	Orotidine-5'-phosphate decarboxylase	4.1.1.23
7	Uridine-Cytidine Kinase	2.7.1.48
8	5'-Nucleotidase	3.1.3.5
9	Uridine Phosphorylase	2.4.2.3
10	Cytidine Deaminase	3.5.4.5
11	Uracil Phosphoribosyltransferase	2.4.2.9
12	Thymidine Phosphorylase	2.4.2.4
13	Thymidine Kinase	2.7.1.2
14	Deoxycytidine Kinase	2.7.1.74
15	Deoxycytidylate Deaminase	3.5.4.12
16	Cytidylate Kinase	2.7.4.14
17	Thymidylate Kinase	2.7.4.9
18	Ribonucleotide Reductase	1.17.4.1
19	Nucleoside Diphosphate Kinase	2.7.4.6
20	Thymidylate Synthetase	2.1.1.45
21	CTP Synthetase	6.3.4.2
22	Nucleosidemonophosphate Kinase	2.7.4.4

Pyrimidine bases are not anabolized in vivo as efficiently as the corresponding nucleosides. The incorporation of 5-iodouracil into DNA was found to be less efficient than 5-IUdR[46], while the uptake of 5-fluorouracil into various murine tumors was reported to be less than that of either 5-FUdR[13,14] or 5-FUR[4]. This discrepancy can be attributed in part to the catabolic pathway of pyrimidine nucleobases. The first step in the degradation of the free base is irreversible reduction to the 5,6-dihydropyrimidine, while the first step in nucleoside degradation is reversible cleavage of the nucleoside glycosidic bond to yield the free base and ribose-1-phosphate or deoxyribose-1-phosphate[41]. Other factors that contribute to the differential tumor uptake of bases and nucleosides are differences in their rates and mechanisms of entry into cells and differences in their rates of metabolic trapping inside the cells[47-49].

The complex metabolism of physiological nucleotides makes it difficult to predict the ultimate fate of exogenous pyrimidine nucleoside analogues entering the metabolic pathways. This was demonstrated by Hunting et al.[50], who determined quantitatively the metabolic fates of uridine, 2'-deoxyuridine, thymidine, cytidine and 2'-deoxycytidine in cultured Chinese hamster ovary cells. The results indicated a much more complicated metabolic fate for the ribonucleosides compared to the deoxyribonucleosides. Uridine was incorporated, in at least trace amounts, into all of the pyrimidine nucleotides. Cytidine was converted into all of the pyrimidine nucleotides excepting the phosphorylated deriviatives of thymidine. However, conversion of cytidine to thymidine nucleotides would not

have been detected under the experimental conditions employed because 5-[^{3}H]-cytidine was used and the tritium label would have been lost from the C-5 position during the synthesis of thymidylate[50]. In contrast, 2'-deoxycytidine and thymidine were converted to their respective mono-, di- and triphosphates only. 2'-Deoxyuridine was anabolized almost as efficiently as thymidine into the thymidine nucleotides. These were the only interconversions between the deoxyribonucleosides observed[50]. Although it is difficult to accurately predict the biological fate of pyrimidine analogues, the biological activity of new compounds can be directed towards specific goals by synthesizing new analogues having structural alterations based on the biological activity of currently known nucleosides.

D. Pyrimidine Nucleobase and Nucleoside Analogues

Almost every structural feature of a nucleoside plays an important role in determining its metabolic fate and biological activity. Indeed, the pyrimidine heterocycle has been modified at every position in the ring by replacement or interchange of the skeletal carbons and nitrogens or by modification of the substituents at each position. A similar, but less extensive study of the ribofuranosyl moiety has included substituent modification at all five carbon positions and replacement of the ring heterocyclic oxygen.

The extent and nature of the biological transformations that a nucleoside or base analogue may undergo is difficult to determine *a priori*. However, a number of structural features are known to be important determinants in the metabolic fate of pyrimidine nucleoside analogues. These are[51,52]:

1. the anomeric configuration of the glycosidic bond between the base and the sugar;
2. the enantiomeric configuration of the sugar;
3. the conformation of the base and sugar rings;
4. the conformational relationship between the base and the sugar about the C-1'-N-1 glycosidic bond;
5. the sites of attachment of the base and sugar;
6. the substituents on the base and sugar;
7. the configuration of the C-2' and [illegible]' substituents on the sugar.

The physiological nucleosides and nucleoside antibiotics isolated from natural sources exist primarily in the β anomeric configuration

(Figure 1). However the β-configuration is not an absolute requirement for biological activity. For example the α-anomer of 2'-deoxythioguanosine is known to undergo metabolic phosphorylation and eventual incorporation into the terminal positions of RNA and DNA[52]. Nucleosides

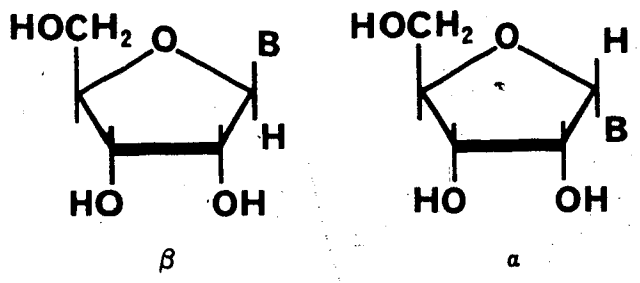

Figure 1. Anomeric Configurations of the Glycosidic Bond

which have the L-enantiomeric configuration are metabolized, but to a lesser extent than the natural D-isomers[53]. The conformation of the sugar and the conformation between the base and sugar are strongly influenced by the last three structural features listed. It is the alteration of these structural features, due to chemical modification of naturally occuring nucleosides, that is responsible for the wide range of biological actions observed for the various nucleoside and nucleobase analogues.

1. C-6 Substituted Pyrimidines

The majority of nucleoside analogues synthesized have been modified in the pyrimidine heterocycle. Pyrimidine bases are essentially planar, and functional group substitution or interchange of annular atoms has little effect on the ring conformation as long as the aromaticity of the base is retained[39].

Pyrimidines which have undergone substitution in the C-6 position are potential analogues of uracil (1a) or orotic acid (1b) and may interfere with de novo pyrimidine metabolism at the orotate phosphoribosyltransferase or orotidine-5'-phosphate decarboxylase enzyme level[54].

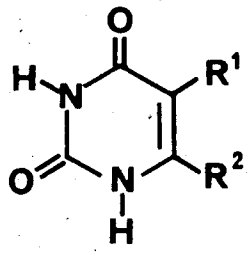

	R^1	R^2
a	H	H
b	H	COOH
c	CH_3	H

1

Alternatively, the pyrimidine C-6 position has been implicated as the site of enzyme attack in the initiation of various metabolic events in which natural and synthetic nucleosides and nucleobases are involved. These include the synthesis of of thymidine monophosphate (inhibited by 5-FUdR)[55], the deamination of cytosine nucleosides (metabolism of ara-C) [56], and the general catabolism of pyrimidines [57]. A number of C-6 mono-substituted analogues of uracil, cytosine (2) and thymine (1c) have been synthesized.

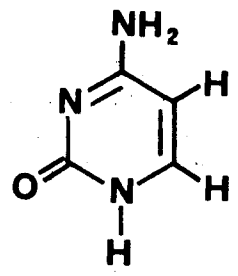

2

The 6-methyluracil derivatives (3a-e) were initially prepared as possible antimetabolites[58,59,60]. 6-Methyluracil (3a) was reported to have no antimicrobial or cancerostatic activity[58] and 6-methyluridine (3b) did not exhibit bacteriostatic activity[59]. The bulky methyl group of 3b decreased its susceptibility to cleavage

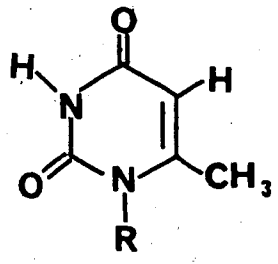

	R
a	H
b	ribose
c	2'-deoxyribose
d	ribose-5'-monophosphate
e	ribose-5'-diphosphate

3

(8.5%) of the glycosidic bond under similar conditions that resulted in 50% degradation of uridine to uracil. The monophosphate derivative 3d was a substrate for a number of phosphatases[59]. The biological activity of 3c[60] and 3e[59] was not reported.

The 6-methyl cytosine analogues (4a-c) were prepared to determine whether the methyl group would hinder deamination in vitro[56]. This proved true with the free base 4a, but the bulky methyl group increased the rate of non-enzymatic cleavage of the cytosine nucleosides 4b,c to the free base. This was ascribed to steric rather than electronic factors in which the 5'-hydroxyl is forced into a position where it can hydrogen bond with the C-2 carbonyl. This effect stabilizes the base oxonium ion formation and makes the pyrimidine a better leaving group[56].

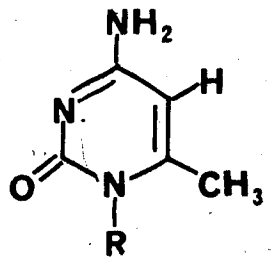

	R
a	H
b	ribose
c	deoxyribose

4

The introduction of halogen substituents into the C-6 position of pyrimidine nucleobases was of interest because of the biological effects observed with these substituents in the C-5 position. 6-Fluorouracil (5a) was inactive against a variety of bacterial systems[61,62]. Introduction of the strongly electronegative fluorine atom into the C-6 position of uracil decreases the pKa of the base and increases its susceptibility to nucleophilic reactions. The biological inactivity of 5a was attributed to the ease with which

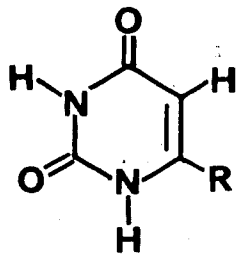

	R		R
a	F	e	$-CF_3$
b	Cl	f	$-CH_2F$
c	Br	g	-OH
d	I		

5

it undergoes hydrolysis to barbituric acid (5g), which is inactive in nucleic acid metabolism[63]. The biological activity of analogues 5c-f [64,65] was not reported but 5b exhibited moderate inhibition of microbial growth at high concentrations[66]. The 2,4-dimethoxy derivative of 5b was approximately 1000 fold more inhibitory in the same system.

Similar substituents in cytosine and thymine bases have also been examined. 6-Fluorocytosine (6a) was found to be weakly active against Candida albicans, Saccharomyces carlbergensis and Streptococcus faecalis[67]. The deamination of 6-fluorocytosine to the biologically inactive 6-fluorouracil derivative (5a), in a manner analogous to the inactivation of ara-C may account for its weak biological effects. 6-Chlorocytosine (6b) exhibited moderate antitumor activity in a C1498 myelogenous leukemia test system[68].

6-Fluorothymine (7a) was shown to inhibit the growth of influenza A PR8 in Ehrlich ascites tumor cells[69]. The activity of analogues 7b,c have not been reported[63,70].

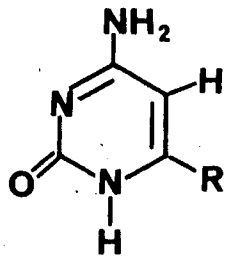

	R
a	-F
b	-Cl

6

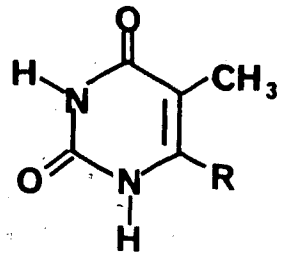

	R
a	-F
b	-Cl
c	-I

7

2. Pyrimidine Nucleosides with C-2' Halogenated Sugars

The biological activity of nucleoside analogues is a result of their structural and conformational similarities and dissimilarities to the natural enzyme substrates. The conformation of the analogues must be similar to the natural substrate or the resulting enzyme-substrate complex will not be ideal. The 2'-halo-2'-deoxyuridine analogues 8a-d in which the 2'-hydroxyl function has been replaced with a halogen atom in the ribose configuration, are considered conformational analogues of uridine (8e) rather than 2'-deoxyuridine (8f). The biological activity of these and related pyrimidine nucleoside analogues has been evaluated.

The 2'-halogenated ribosides of uracil (8a-c), thymine (9a-c) and 5-fluorouracil (10a-c) were originally synthesized as potential antimetabolites[71,72,73]. The 2'-iodo analogues 8d and 9d had been prepared earlier as intermediates in the conversion of pyrimidine nucleosides to deoxynucleosides and were not tested for biological

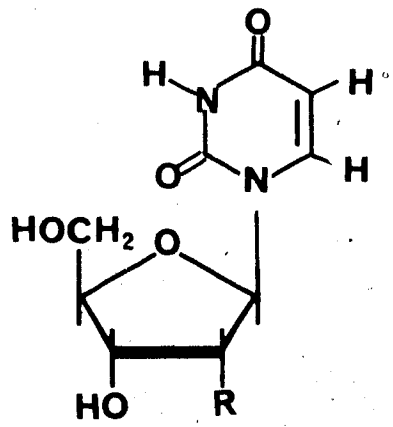

	R
a	F
b	Cl
c	Br
d	I
e	OH
f	H

8

activity[74]. The 2'-fluoro analogues 8a and 10a inhibited the growth of a uracil-requiring strain of Bacillus subtilis when grown in the presence of certain 5'-substituted nucleosides. The 2'-fluoro and 2'-chloro analogues of thymidine (10a,b) were not incorporated into mouse embryo cells[75]. The 5'-monophosphate of 8a was a substrate for thymidylate synthetase[76]. The difluoro analogue 10a was

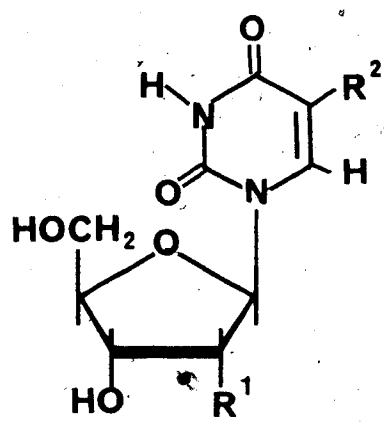

	R^1
a	F
b	Cl
c	Br
d	I

	R^2
9	CH_3
10	F
11	Br

phosphorylated by a crude enzyme extract from Ehrlich carcinoma cells and, as the 5'-monophosphate, inhibited thymidylate synthetase[77]. The diphosphate of 8a, 2'-FdUDP, was a substrate for Escherichia coli[78] polynucleotide phosphorylase, forming the homopolymer, poly 2'-FUdR. The fluoro polymer was a substrate for Micrococcus luteus RNA phosphodiesterase and pancreatic DNase II but was resistant to pancreatic RNase and DNase I. Poly 2'-FUdR also formed 1 : 1 complexes with polyadenylic acid but did not induce interferon[79]. The triphosphate of 8a was a substrate for Escherichia coli RNA polymerase and was incorporated into a polymer approximately 40% as efficiently as UTP[76]. The 2'-fluoro-2'-deoxycytidine derivative, 2'-FCdR (12a), was active against P815 and L5187 leukemia cell growth in vitro [82]. 2'-FdCDP was observed to be a substrate for Escherichia coli polynucleotide polymerase[78] and an inhibitor of ribonucleoside diphosphate reductase[80]. The latter enzyme was shown to catabolize 2'-FdCDP to fluoride ion, cytosine and a sugar pyrophosphate which in turn was metabolized to free pyrophosphate and a sugar. The enzyme was inactivated by 2'-FdCDP after approximately 100 turnovers of substrate[81].

2'-Chloro-2'-deoxyuridine (8b) was active against Bacillis subtilis growth [75] under similar conditions described for 8a and 12b and 13b were more potent inhibitors of P815 and L5187Y cell growth in vitro than the fluoro analogue (12a)[82]. The diphosphates of 8b and 12b were substrates of Micrococcus lysodeikticus polynucleotide phosphorylase[83,84]. The corresponding polymers were ineffective as inducers of interferon. This is in contrast with the 2'-fluoro- and

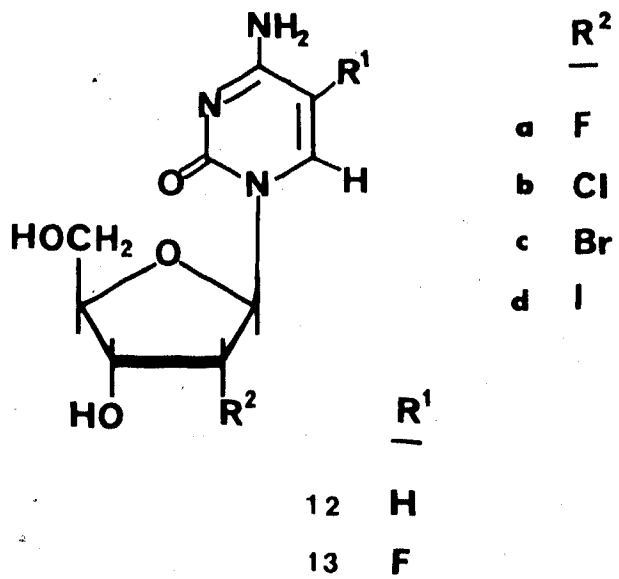

2'-chloro-2'-deoxyinosinic acid polymers which, when complexed with polycytidylic acid, exhibited interferon inducing activity. 2'-Chloro-2'-deoxycytidine-5'-diphosphate (12b), 2'-CldCDP and 2'-fluoro-2'-deoxycytidine-5'-diphosphate (12a), 2'-FdCDP, are classified as unreactive proinhibitors of Escherichia coli ribonucleoside diphosphate reductase. Inhibitors of this class are converted to active intermediates which react with the active site of the enzyme. 2'-Fluoro-2'-deoxycytidine-5'-diphosphate and 2'-CldCDP both seem to act in a similar manner. Inactivation of the enzyme results in a loss of titratable sulfhydryl groups which cannot be regenerated, suggesting irreversible inactivation of the enzyme active site [81]. The enzyme catalyzes the loss of free base and halide ion from the deoxyribose diphosphate sugar followed by cleavage of the diphosphate from the sugar. The halide ions are thought to be released via a free radical mechanism in which an hydrogen is abstracted from either the C-1' or C-3' positions. The authors speculate that the reactive intermediate could be analogous to structure 14. Structure 14 is a potent Michael acceptor which could be attacked by

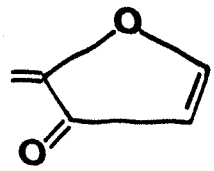

14

the sulfhydryl group of the enzyme and become covalently bound to the active site of the enzyme [80].

The biological activity of the 2'-bromo and 2'-iodo substituted deoxynucleosides (8c,d - 13c,d) has not been reported. However Fox et al. have suggested that the cytidine analogues (12c,d) and (13c,d) may be converted in vivo to the corresponding ara-C derivatives [85] and this hypothesis may also be valid for the uridine analogues as well. If this were the case, the biological activity of analogues (8c,d) and (10c,d) should parallel that of the corresponding ara-U and ara-5-fluorouracil derivatives. The 2'-bromo pyrimidine nucleosides may be substrates for the polynucleotide phosphorylase enzyme which is known to polymerize 2'-bromo-2'-deoxy-adenosine-5'-diphosphate [86].

E. Chemistry of Pyrimidine Nucleosides and Nucleobases

1. Chemistry of Pyrimidines

Pyrimidines, or 1,3-diazines (15), are six membered heterocyclic ring structures. The electron densities at the C-2, C-4 and C-6 positions of pyrimidine are qualitatively similar to the C-2, C-4 and C-6 positions of 1,3-dinitrobenzene (16) and pyridine (17) respectively. The low electron density at the C-2, C-4 and C-6 positions of pyrimidine is due to the combined inductive and resonance effects of the two ring

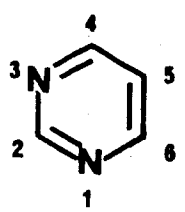

15

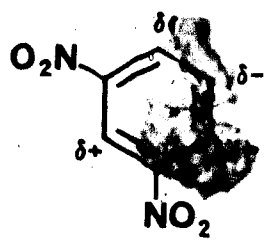

16

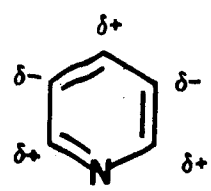

17

nitrogen atoms[87]. Nucleophilic substitution reactions on pyrimidine ring systems preferentially occur at the C-2, C-4 and C-6 positions. Theoretically, nucleophilic substitution at the C-2 position should be favoured relative to the C-4(6) position on the basis of resonance structures, however the converse is generally observed experimentally[88]. These reactions are subject to kinetic rather than thermodynamic control. The increased electrostatic repulsion, resulting from the effect of two nitrogen lone electron pairs upon the C-2 position

relative to the single nitrogen lone electron pair upon the C-4(6) position, is proposed as a plausible explanation for this observation[39].

The introduction of the keto functions of uracil (1a) and thymine (1c) or the amino function of cytosine (2) into the pyrimidine ring, enhance the ring stability significantly. Electron donating substituents also decrease the reactivity of pyrimidines with respect to subsequent introduction of nucleophiles, a property which is advantageous for selective syntheses[39]. The C-5 position of pyrimidine has a higher electron density than the other positions and is susceptible to electrophilic substitution when suitably activated by electron-donating substituents[87].

a. Synthesis of 6-Halogenated Pyrimidine Nucleobases

The synthesis of C-6 substituted pyrimidines can be approached via two general methods. The first method, called the principal synthesis, involves construction of the pyrimidine ring by condensation of two appropriately selected bifunctional, acyclic precursors. The second method involves manipulation of substituents present on a preformed pyrimidine nucleus. The principal synthesis is unsuitable for the synthesis of 2-, 4- or 6-halo pyrimidines[87]. Halogenation of the C-2, C-4 and C-6 positions has generally been accomplished via nucleophilic substitution reactions involving the preformed pyrimidine nucleus.

Most nucleophilic substitutions require the presence of a suitable leaving group. This is especially important for the synthesis of 6-substituted natural pyrimidine nucleobases because

the keto functions at C-2 and C-4 of uracil and thymine and the amino function at C-4 of cytosine deactivate the ring to nucleophilic attack. Therefore displacement reactions that occur at temperatures of 25°C or less for unsubstituted or activated pyrimidines require heating at reflux or pressure reaction conditions with deactivated pyrimidines (Scheme 3)[39].

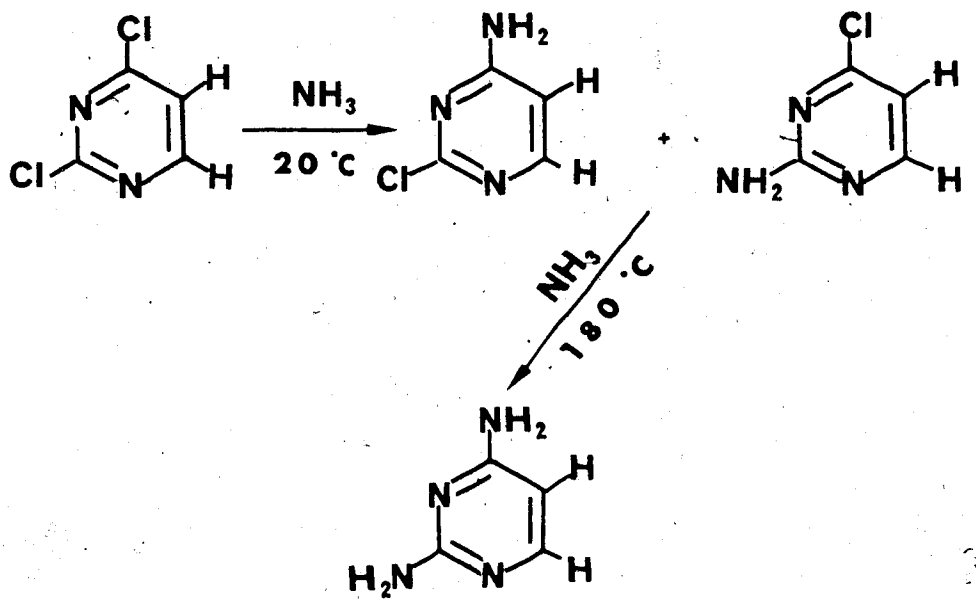

Scheme 3. Amination of 2,4-Dichloropyrimidine

The most common synthesis of 6-substituted pyrimidines is via the nucleophilic displacement of a 6-halo substituent. Thus bromo- and chloropyrimidines are readily prepared by the reaction of a phosphorous oxyhalide with the appropriate hydroxy pyrimidine (Scheme 4). The chloro compounds are the intermediates of choice

since chlorine is as reactive as bromine and iodide and is the most readily introduced halogen[87]. The fluoro- and iodopyrimidines have been most conveniently prepared by halide exchange with the chloro intermediate.

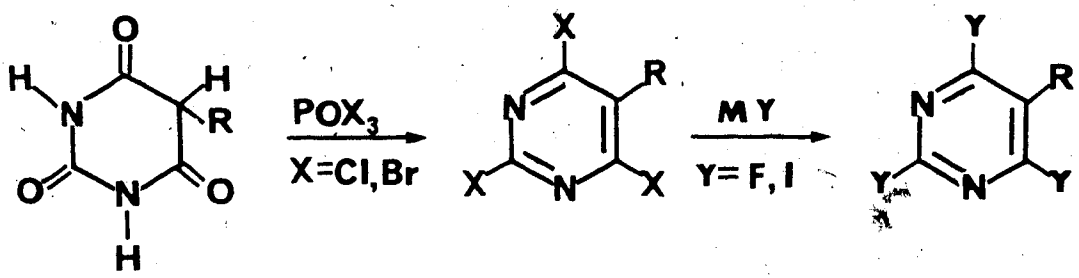

5 g R= H
h R= CH_3

18 a X= Cl
b X= Br

19 a Y= F
b Y= I

Scheme 4. Synthesis of 2,4,6-Trihalopyrimidines

The 6-chloro (5b) and 6-bromo (5c) analogues of uracil can be readily prepared from barbituric acid (5g) via the appropriate 2,4,6-trihalopyrimidine. Selective displacement of the C-2 and C-4 halide substituents of 18a,b (R = H) with methoxide anion, followed by demethylation using dilute mineral acid in acetic acid gave 6-chlorouracil (5b) and 6-bromouracil (5c)[64] respectively. Attempts to synthesize 6-iodouracil (5d) in a manner analogous to 5b or 5c resulted in the formation of barbituric acid (5g). Treatment of 6-chlorouracil (5b) directly with sodium iodide afforded 5d in good yield[64]. In contrast, the nucleophilicity of

fluoride anion was too low to allow the analogous fluorine for chlorine exchange with 6-chlorothymine (7b). The failure of this reaction was attributed to the presence of the C-2 and C-4 ketone functions which deactivate the ring to nucleophilic substitution[63]. The synthesis of 6-fluorothymine (7a) was successfully accomplished by the procedure reported for the syntheses of 6-fluorouracil (5a) and 6-fluorocytosine (6a)[63] or by the action of alkali on 2,4,6-trifluoro-5-methylpyrimidine (19a, $R = CH_3$)[69]. The C-6 fluorine substituent of 5a and 6a was too acid labile to be prepared by acidic cleavage of their benzyl ether derivatives, however, catalytic hydrogenation proved sufficiently mild to afford the desired fluoro pyrimidines 5a[62] and 6a[63].

The pKa and reactivity of pyrimidines are profoundly affected by the electronic character and position of functional substituents[39,87]. Halogen substitution, as expected, results in a decreased pKa compared with the parent, in the decreasing order F, Cl, Br and I[62]. This effect is much greater for C-6 substituents than for C-5 substituents. For example, introduction of the highly electronegative fluorine atom at C-5 of uracil decreases the pKa from 9.50 to 7.98. 6-Fluorouracil has a pKa of 4.03. Similar observations of a lower magnitude have been observed with the other halogen containing isomers. The electron-withdrawing effect of fluorine at the C-6 of pyrimidines significantly increases their susceptibility to acid catalyzed nucleophilic displacement reactions at this position. This

accounts for the difficulty in obtaining the 6-fluoro analogues of uracil (5a) and cytosine (6a) by acidic hydrolysis of the ether intermediate[62,67].

2. Modification of the Sugar Moiety of Pyrimidine Nucleosides

Synthetic procedures for the preparation of nucleosides with modified sugars can be divided into three major approaches. The first method employs a coupling reaction in which a derivatized base (TMS, -OEt) having the desired functionality and a sugar are coupled to form a nucleoside. In the second procedure the pyrimidine heterocycle is constructed using a preformed sugar analogue. The third approach involves the modification of a preformed natural or synthetic nucleoside[89]. Due to time constraints, the modification of preformed nucleosides provides the most suitable method for synthesizing radiopharmaceuticals. The coupling reactions require that the radioactive label be incorporated relatively early in the synthetic sequence before the nucleoside is actually formed. The condensation and deblocking procedures that must follow the labelling step are undesirable because they increase the total reaction time which is an important consideration with short-lived radionuclides, and further decrease the overall radiochemical yield. Synthesis of the pyrimidine ring of the desired nucleoside by condensation and cyclization reactions using the appropriate sugar as starting material, permits control over the stereochemistry of the product but requires several synthetic steps following the introduction of the label[90]. Modification of intact nucleosides offers important advantages

including retention of preexisting substituent configuration and stereochemistry at unaltered loci and the necessity for fewer reaction steps[89]. For these reasons the preformed nucleoside provides the best alternative as precursor for syntheses of short-lived radiolabelled analogues. A discussion of the major synthetic methods available for the introduction of substituents into the C-2' position of pyrimidine nucleosides follows. An excellent review covering chemical modification of the various positions on the ribose moiety of intact nucleosides has recently been published by Moffatt[91].

a. Synthesis of Pyrimidine 2,2'-Cyclonucleosides

The major methods of introducing substituents into the C-2' position of pyrimidine nucleosides can be divided into two categories: those reactions involving a 2,2'-cyclonucleoside directly and those reactions in which the 2,2'-cyclonucleoside is formed *in situ*.

2,2'-Cyclouridine (20) was first synthesized unintentionally in an attempt to deblock 3',5'-di-O-acetyl-2'-tosyluridine with methanolic ammonia to prepare the 2'-tosyluridine derivative[92]. The unexpected 2,2'-cyclouridine nucleoside was postulated to have arisen via intramolecular nucleophilic displacement of the tosyl function by the C-2 oxygen of the uracil base. This and similar methods[72] required numerous selective blocking and deblocking steps to prepare the 2,2'-cyclonucleoside from the starting riboside. A number of procedures were developed to circumvent these steps and provide a less cumbersome route to

the 2,2'-cyclo derivatives. The most convenient method for the synthesis of 2,2'-cyclouridine was reported by Hampton and Nichol[93]; this method has since proven useful in the synthesis of other 2,2'-cyclo pyrimidine nucleosides[89,91]. The reaction involves treatment of uridine with diphenylcarbonate and sodium bicarbonate in dimethylformamide or hexamethylphosphortriamide[94] to give 2,2'-cyclouridine in one step. The reaction is believed to proceed via an uridine 2',3'-cyclic carbonate intermediate (20,x = O). The pyrimidine C-2 oxygen preferentially attacks the C-2' position, rather than the C-3' position, to give the thermodynamically more stable 2,2'-cyclouridine derivative[95] (Scheme 5). 2,2'-Cyclouridine, prepared by treating uridine with either carbonyldiimidazole or thiocarbonyldiimidazole, is postulated to arise via a similar intermediate (20, x = O,S)[96].

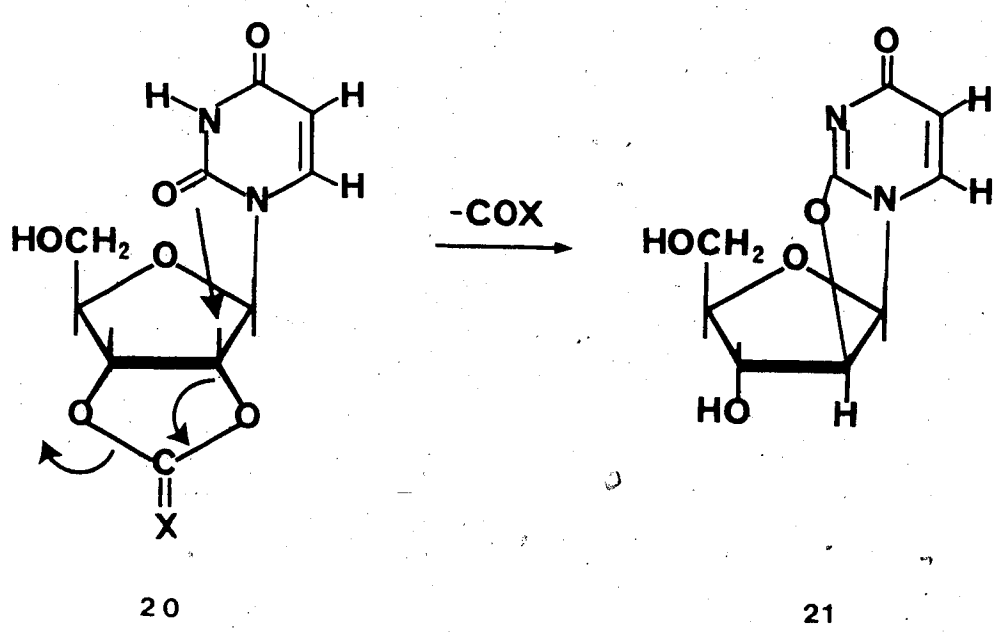

Scheme 5. Synthesis of 2,2'-Cyclouridine Via a 2',3'-Cyclic Carbonate Intermediate.

b. Reactions of 2,2'-Cyclonucleosides

The chemistry of 2'-substituted pyrimidine nucleosides and the chemistry of 2,2'-anhydro-1-β-D-arabinofuranosylpyrimidine nucleosides are inextricably related due to the propensity of the C-2 carbonyl to participate in intramolecular nucleophilic displacement reactions involving substituents on the sugar moiety[89]. Participation of the C-2 carbonyl of the pyrimidine heterocycle governs the stereochemistry of the substituents introduced into the C-2' position of intact pyrimidine nucleosides. Intramolecular nucleophilic displacement of a leaving group in the ribo configuration on the sugar by the C-2 carbonyl of the base occurs preferentially to substitution by an external nucleophile. Thus, only substitution with rentention of the ribo configuration at C-2' can occur with pyrimidine nucleosides in which the C-2 carbonyl is free to participate in the reaction.

The use of 2,2'-cyclopyrimidine nucleosides as precursors for the synthesis of 2'-substituted analogues originated with the synthesis of 2'-halo-2'-deoxy analogues of uridine, thymidine and 5-fluorouridine[71,72]. Fox et al.[72] noted that reaction of 2,2'-cyclouridine with aqueous 3.0 N hydrogen chloride gave two products identified as ara-U (23, R = H) and 2'-ClUdR (8b). When 2,2'-cyclouridine was reacted with an ethereal solution of anhydrous hydrogen chloride in the absence of water, 2'-ClUdR was obtained as the sole product in essentially quantitative yield. The reaction was successfully extended to include the 2'-fluoro, -bromo and -iodo analogues which can also be prepared

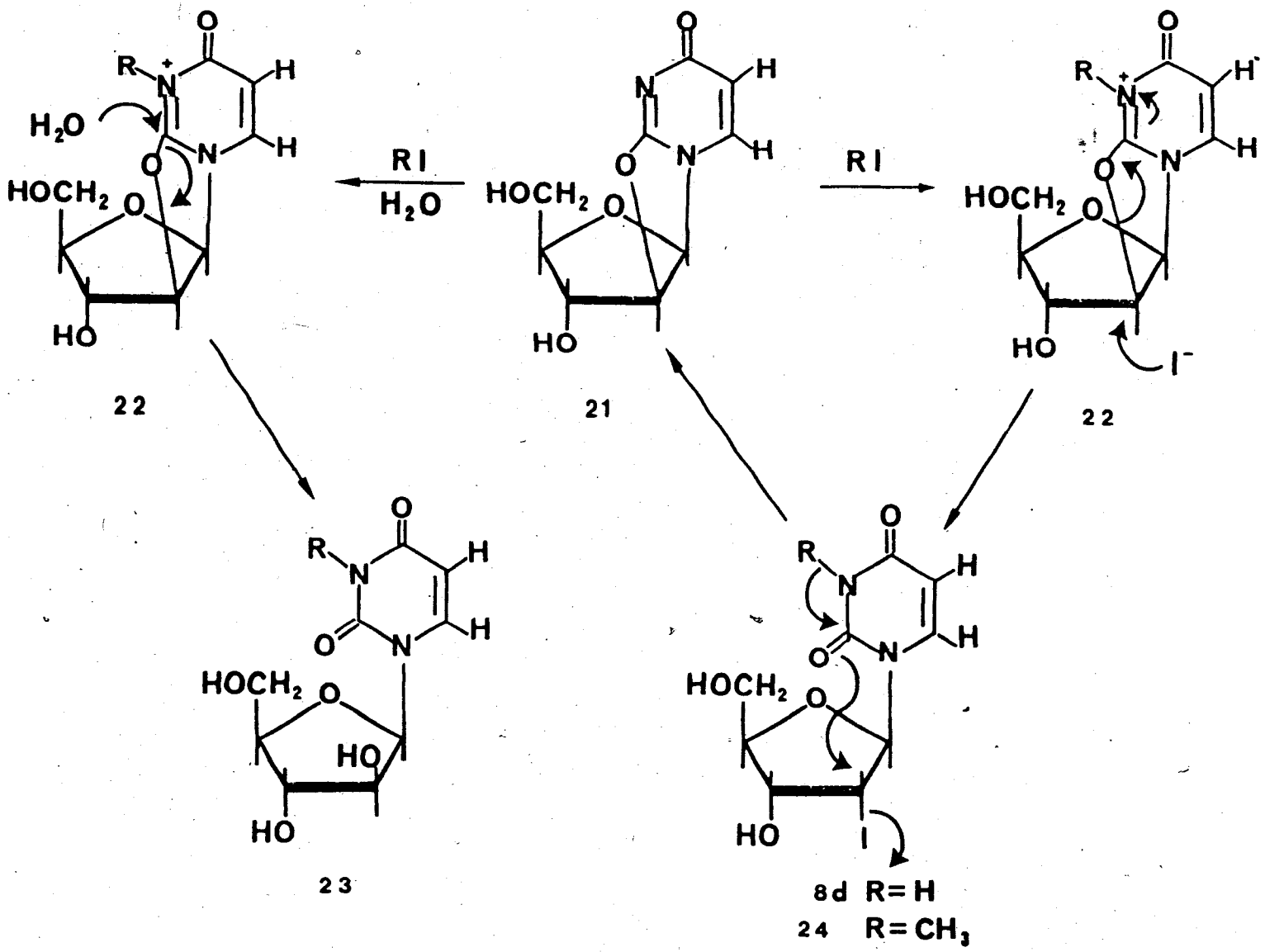

Scheme 6. Competitive Cleavage of the Anhydro Bond by Iodide and Water.

in good yield using this procedure. These reactions differ from the reaction of 2,2'-cyclouridine with sodium iodide reported by Brown et al.[97]. In the latter reaction, 2'-IUdR (8d) was obtained in low yield only after acetic acid was added. These findings prompted Fox et al. to postulate that protonation of the 2,2'-cyclo intermediate (22, R = H) was necessary to facilitate the cleavage of the anhydro bond (Scheme 6)[72,98]. Further evidence for this reaction mechanism was reported by Kikugawa et al.[99]. These authors synthesized N-3-methyl-2'-iodo-2'-deoxyuridine (24, R = $-CH_3$) by the reaction of methyl iodide with 2,2'-cyclouridine in dimethylformamide. Methylation (cf. protonation) occurred before cleavage of the 2,2'-anhydro bond to give the intermediate (22, R = $-CH_3$) if the reaction was stopped before it had gone to completion. This intermediate (22, R = $-CH_3$) liberated acid and was converted into the arabino analogue (23, R = $-CH_3$) in the presence of water. If the reaction was allowed to proceed in the absence of water, only the 2'-iodo nucleoside (24, R = $-CH_3$) was obtained. The observation that the stable crystalline hydrogen chloride or bromide salts of 2,2'-cyclouridine can be converted to the corresponding 2'-halogenated derivative simply upon heating lends further credence to the postulated reaction mechanism[72].

Other reagents for the introduction of halogens into the C-2' position of pyrimidine nucleosides, via cleavage of the 2,2'-anhydro bond, have also been proposed. The attempted synthesis of 2'-fluoro-2'-deoxycytidine (12a) (2'-FCdR) via the treatment of 2,2'-cyclocytidine with anhydrous hydrogen

fluoride was unsuccessful[100] and only low yields of 2'-FCdR were obtained by the decomposition of the hydrofluoride salt of 2,2'-cyclocytidine[90]. Instead, the synthesis of 2'-FCdR was achieved using a crown ether-anhydrous potassium fluoride complex in DMF. This procedure was only successful when the reaction mixture was vigorously dried by azeotropic distillation with benzene to remove all water.

The reaction of 2,2'-cyclonucleosides with nucleophiles does not always afford the desired 2'-substituted product. Nucleophilic substitution can also occur at the C-2 position of the pyrimidine heterocycle. This is exemplified by the reaction of aqueous hydrochloric acid with 2,2'-cyclouridine[71,72] in which both 2'-ClUdR and ara-U are produced. Nucleophilic attack of water at the C-2 position of the uracil ring competes with attack of chloride at the C-2' position of the sugar to give the aforementioned products.

F. Radiochemistry and Radionuclide Production

1. Radiochemistry

The successful synthesis of a radiolabelled molecule requires a consideration of the limitations imposed by the radionuclide, the basic chemical characteristics of the labelling reagents and the compound to be labelled. The main considerations introduced by the radionuclide are[32,101]:

1. the time required for synthesis and purification;
2. the specific activity required for the radiolabelled compound;
3. the requirement for small-scale procedures;
4. the limited number and availability of synthetic precursors; and
5. radiation protection for the personnel.

The major limiting factor in radioactive syntheses is the half-life of the radionuclide. For example, the use of short-lived radionuclides such as ^{34m}Cl ($T_{\frac{1}{2}} = 32$ min) and ^{18}F ($T_{\frac{1}{2}} = 109.7$ min)[33] stringently limits the time available for the synthetic and purification procedures, whereas the use of longer lived nuclides, including ^{123}I ($T_{\frac{1}{2}} = 13.2$ h) and ^{36}Cl ($T_{\frac{1}{2}} = 3 \times 10^5$ y)[33] imposes minimal time restraints. It should be recognized that after six half-lives have passed, less than 2% of the starting radioactivity remains, irrespective of the chemical yield[32]. Therefore, the two most important factors in the choice of reaction conditions are the rate of product formation and the rate of radioactive decay. For example, assuming first-order reaction kinetics, the relationship between these two constants is given by equation 1[101], where T_{max} is

$$T_{max} = (1/K_1) \ \ln(K_1/\lambda) + 1 \qquad \text{Equation 1}$$

the length of time required for optimum yield, K_1 is the rate of formation of the desired product (usually determined experimentally) and λ is the decay constant of the radionuclide. These factors may be better illustrated by Figure 2, which compares the absolute chemical yields of hypothetical reactions with the decay of the radionuclide[32,101]. Visual inspection of Figure 2 indicates that the initial rate of product formation is more important than the overall chemical yield. Equation 1 neglects the purification, separation and transfer steps that must also be performed. Those reactions requiring complex purification or workup of the final product may be less applicable than procedures which afford lower chemical yields but which require simple workup protocols.

In most instances a high specific activity radiopharmaceutical is desirable to minimize the possibility of eliciting an undesirable pharmacological response to the tracer or saturating the biological process being measured. The maximum specific activity theoretically possible is inversely proportional to the half-life of the radionuclide as shown by equation 2[102]:

$$-dN/dt = \lambda N = (\ln 2/T_{\frac{1}{2}})N \qquad \text{Equation 2}$$

where N is the number of atoms and λ is the decay constant of the radionuclide. This ideal, "carrier free" state is, in practice, virtually impossible to achieve due to isotopic dilution of the radioisotope, by other isotopes of the same element, present in the

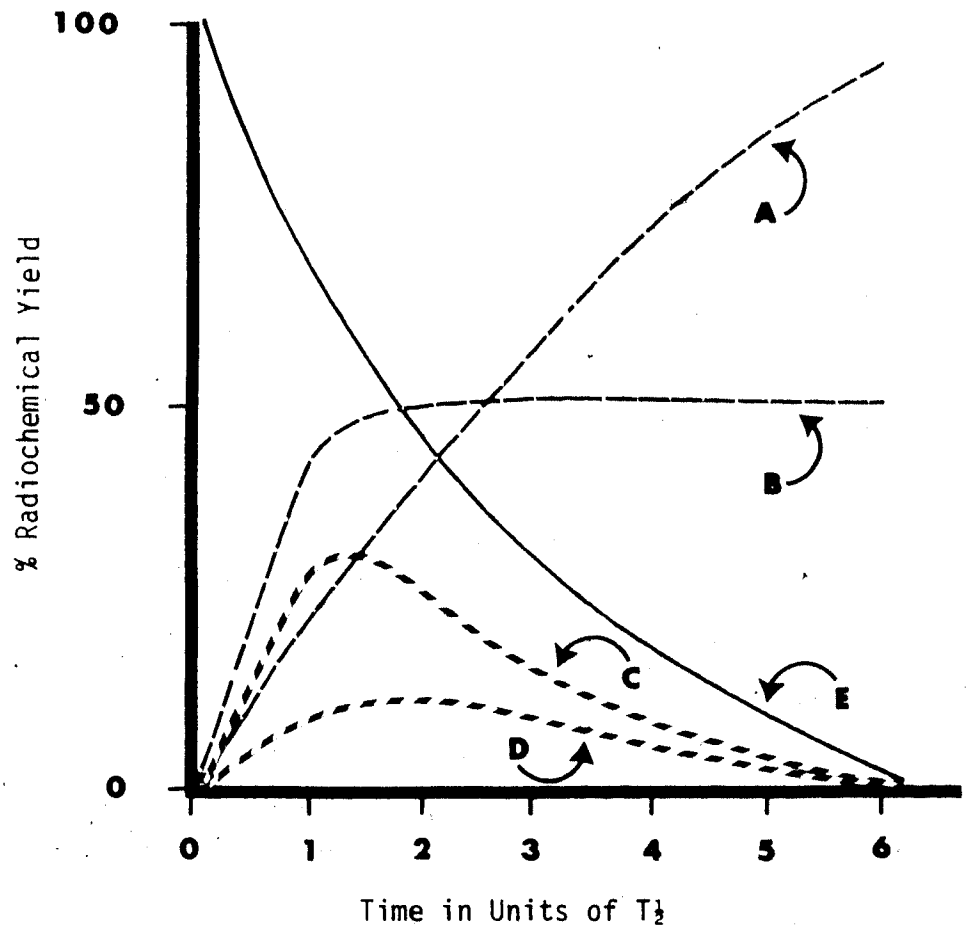

Curve A. High chemical yield reaction with slow reaction rate

Curve B. Intermediate chemical yield reaction with fast reaction rate

Curve C. Composite curve representing actual radiochemical yield from Curve B

Curve D. Composite curve representing actual radiochemical yield from Curve A

Curve E. Decay curve of the radionuclide

Figure 2. Effect of Reaction Kinetics (First Order) on Radiochemical Yield.

target material and reagents used during production[101]. The original terms, "carrier-free" and "carrier-added", neglect this problem of inadvertent dilution of the radionuclide and in this context a new term, "no-carrier-added", has been coined. The new definitions are as follows[103,104]:

1. Carrier-free (CF): The radionuclide is not contaminated with any other stable or radioactive nuclide of the same element.
2. No-carrier-added (NCA): The radionuclide has not been intentionally diluted with other stable or radioactive nuclides of the same element. The specific activity is very high and may be CF.
3. Carrier-added (CA): A known amount of stable or radioactive isotope has been added to the radionuclide of interest.
4. Carrier (C): A stable or radioactive isotope of the element in question.
5. The above definitions refer to a specific position or positions when applied to a given molecule.

In practice then, the highest specific activity that can be claimed is NCA which may approach CF status under rigorously controlled conditions. Radiochemical syntheses are usually conducted on as small a scale as possible, to reduce the amount of intentionally added carrier. This often introduces technical problems since it is difficult to handle and transfer reaction volumes smaller than 10-30 µl.

The specific activity of radiolabelled products to which carrier has been added during synthesis is dependent on the starting activity and the concentration of added carrier. If carrier must be added and

a high specific activity product is required, a high level of radioactivity must be used which may pose radiation protection problems. For shorter lived radionuclides, the problem is compounded by a constantly decreasing specific activity due to radionuclidic decay.

The availability of radiochemical precursors is another factor which must be considered when determining the labelling strategy. For example, reactor produced ^{18}F is available only as the anion while an accelerator can provide more novel anhydrous fluorinating reagents such as F_2, CF_3OF, NOF, SF_6 or SF_4[32]. Also, commercial sources of radioiodine often supply the radioisotope in aqueous solutions of sodium hydroxide, with or without added antioxidant. These additives may influence the selection of the reaction to be used.

2. Fluorine-18

Fluorine-18 ($T_{\frac{1}{2}} = 109.9$ min)[33] is the only radioisotope of fluorine that has a half-life of sufficient length to be of use as a radiopharmaceutical label. It decays primarily by β^+ emission (97%) and electron capture (3%) to the stable isotope ^{18}O. The β^+ ($E_{max} = 0.635$ MeV; $E_{ave} = 0.28$ MeV) emitted by ^{18}F has a maximum range of 0.7 mm in water[105] which is one of the shortest ranges of the medically relevant β^+ emitters (^{11}C, ^{13}N, ^{15}O, ^{34m}Cl, ^{52}Fe, ^{68}Ga, ^{77}Br and ^{81}Rb)[32,33]. These characteristics make ^{18}F a good candidate for PET. The range of the β^+ plays an important role in limiting the spatial resolution of the PET detection system. The coincident γ rays are emitted when the β^+ has reached thermal energy and has therefore travelled away

from its point of origin. Therefore the inherent spatial resolution of a particular β^+ emitting radiopharmaceutical is inversely proportional to the E_{max} and range of the β^+.

Early interest in ^{18}F production was focussed on developing an aqueous solution of fluoride-18 suitable for human use[106,107]. This could be accomplished in a nuclear reactor by irradiating an oxygen containing lithium salt with thermal neutrons, utilizing the $^{6}Li(n,t)\alpha$, $^{16}O(t,n)^{18}F$ nuclear reactions. The ^{18}F was recovered via various extraction[108,109,110] or distillation[111] techniques. Less complex recovery methods were required when a cyclotron was used to produce fluoride-18. The most common cyclotron production methods used helium-3 (^{3}He)[112] or helium 4 (^{4}He)[106] irradiation of a water target or ^{3}He, ^{4}He and deuteron (d)[112,114] bombardment of a neon target (Table II). The ^{18}F could be simply eluted from the target with sterile water or normal saline.

New synthetic intermediates and production methods for ^{18}F were necessary to exploit the potential of ^{18}F labelled radiopharmaceuticals. Reactor produced ^{18}F is generally available only as the fluoride anion because the quantitative oxidation of NCA ^{18}F is not practical[115]. Thus the chemistry of reactor ^{18}F has been limited to nucleophilic substitution and addition reactions using reagents such as anhydrous hydrogen fluoride[115], tetrafluoroborates[117], and metal fluorides[32]. New fluorinating reagents such as crown ether-potassium fluoride complexes[118] and tetraalkylammonium fluorides[119] have been prepared and their usefulness as nucleophilic fluorination reagents has been demonstrated[120,121]. Recently the preparation of XeF_2-^{18}F, an

TABLE II. Common Nuclear Reactions for Fluorine-18 Production[113,114]

Target Nucleus	Nuclear Reaction	Product	Q-value[1] MeV	Threshold Energy[2] MeV
^{16}O	α,pn	^{18}F	-18.544	23.180
^{16}O	α,2n	$^{18}Ne \xrightarrow{\beta^+} {}^{18}F$	-23.773	29.716
^{16}O	^{3}He,p	^{18}F	+2.003	0
^{16}O	^{3}He,n	$^{18}Ne \xrightarrow{\beta^+} {}^{18}F$	-3.196	3.795
^{16}O	^{3}H,n	^{18}F	+1.270	0
^{18}O	p,n	^{18}F	-2.437	-
^{18}O	^{3}He,t	^{18}F	-1.673	2.5
^{20}Ne	d,α	^{18}F	+2.796	0
^{20}Ne	^{3}He,αn	$^{18}Ne \xrightarrow{\beta^+} {}^{18}F$	-7.296	9.115
^{20}Ne	^{3}He,αp	^{18}F	-2.697	3.102

1. The Q-value of a nuclear reaction is the sum of the kinetic and radiant energies of the reactants minus the sum of the kinetic and radiant energies of the products[36].

2. The threshold energy is the energy limit for an incident particle or photon below which a particular endothermic reaction will not occur[36].

electrophilic fluorinating reagent, by exchange between XeF_2 and tetrabutylammonium fluoride-18 has been reported[122].

The cyclotron and van de Graaff charged particle accelerators provide the most convenient means for the production of electrophilic fluorinating reagents. The majority of these reagents, including CF_3OF[122], NOF, ClF and F_2[114] have been produced by addition of the appropriate carrier to the target gas prior to irradiation. The inert character of neon and ease of target gas handling have made the $^{20}Ne(d,\alpha)^{18}F$ reaction the production method of choice[124]. The production of anhydrous ^{18}F reaction intermediates by the irradiation of neon with ^3He and ^4He has also been investigated[114].

The production of anhydrous ^{18}F has not been limited to positively charged particle accelerators. Electron linear accelerators have also been used to produce the high energy photons necessary for γ induced nuclear reactions. No-carrier-added ^{18}F can be obtained via the $^{20}Ne(\gamma,2n)^{18}Ne \rightarrow ^{18}F$, $^{20}Ne(\gamma,pn)^{18}F$ and $^{23}Na(\gamma,\alpha n)^{18}F$ nuclear reactions. The ^{18}F can then be converted into reaction intermediates as described for cyclotron produced ^{18}F activity[125,126]. Carrier-added ^{18}F can be produced by direct irradiation of fluorine containing compounds using the $^{18}F(\gamma,n)^{18}F$ nuclear reactions[125].

The direct synthesis of ^{18}F labelled compounds <u>in situ</u> via either intramolecular conversion of ^{19}F to ^{18}F, or recoil labelling by extra-molecular generation of ^{18}F has also been investigated. The synthesis of ^{18}F labelled simple chlorofluorocarbons for pulmonary inhalation studies was accomplished in 10-30% radiochemical yields using recoil ^{18}F from the $^{20}Ne(d,\alpha)^{18}F$ reaction[127]. Direct activation of intra-molecular ^{19}F in CF_3Cl via the $^{19}F(p,pn)^{18}F$ reaction resulted in

radiochemical yields approximately one order of magnitude less than that observed with the recoil method[128].

When a position specific label is required, direct activation of a fluorinated precursor provides a higher radiochemical yield of the desired product than recoil labelling via extramolecularly generated ^{18}F[129]. Thus, the more promising approach is via the conversion of intramolecular ^{19}F to ^{18}F via the $^{19}F(n,2n)^{18}F$[129] or the $^{19}F(p,pn)^{18}F$[128] reactions. For example, the radiochemical yield of 5-[^{18}F]-fluorouracil was less than 1% when uracil was allowed to react with recoil ^{18}F atoms produced by the $^{20}Ne(d,\alpha)^{18}F$[14,130] nuclear reaction. In comparison, direct activation of 5-fluorouracil using the $^{19}F(n,2n)^{18}F$ reaction gave the ^{18}F labelled compound in 8% radiochemical yield[129].

3. Chlorine-34m

There are four radioisotopes of chlorine that have sufficiently long half-lives to be useful as tracers in biology and medicine. Chlorine-34m ($T_{\frac{1}{2}} = 32.0$ min)[33] is of particular interest in nuclear medicine because it is a short-lived positron emitting radionuclide. The decay spectrum of ^{34m}Cl is complex due to contributions from ^{34}Cl, the short-lived daughter radionuclide of ^{34m}Cl, and from the excited state of ^{34}S, the stable nuclide arising from ^{34}Cl decay. Chlorine-34m emits a high yield (47%) of 0.145 MeV photons in addition to two β^+'s (both 26 % abundance). The photon yield is increased a further 25 % by emmissions from decay of the excited state ^{34}S and the daughter ^{34}Cl, contributes a third β^+ (100 %) to the overall emission spectrum of ^{34m}Cl[131]. These properties make ^{34m}Cl and attractive radionuclide for

PET (coincident 0.511 MeV γ rays). Conventional single photon imaging (0.145 MeV γ rays) is complicated by the high background caused by the high energy annihilation photons.

Chlorine-34m may be produced by charged particle or fast neutron bombardment of the appropriate targets. High yields of low specific activity ^{34m}Cl can be obtained using either the $^{35}Cl(n,2n)^{34m}Cl$ or $^{35}Cl(p,pn)^{34m}Cl$ nuclear reactions. The specific activity of the ^{34m}Cl can be increased by separating it from the ^{35}Cl. This has been accomplished traditionally by modifications of the Szilard-Chalmers technique[132]. The long-lived chlorine radioisotope, ^{36}Cl, was prepared with high specific activity (555 MBq g^{-1} Cl) by Anbar and Neta[133] via the $^{35}Cl(n,\gamma)^{36}Cl$ reaction using chlorobenzene as target material. The inorganic chloride was recovered as $H^{36}Cl$ by distillation of the irradiated chlorobenzene in concentrated sulfuric acid. Machulla et al.[134] produced practically carrier-free ^{34m}Cl using a technique originally developed by Bell and Stoecklin[135] for the production of ^{36}Cl. The ^{34m}Cl was produced via the $^{35}Cl(p,pn)^{34m}Cl$ reaction using $K_2[ReCl_6]$ as the target material. The hexachloro complex of Re was chosen because of its radiation resistance at high doses, producing only free $^{36}Cl^-$ and $[ReCl_5{}^{36}Cl]^=$ after bombardment. In contrast, the organic chlorides decompose significantly at high radiation doses and complicate the separation techniques. The high specific activity of the ^{34m}Cl produced is attributed to the radiation stability of the $[ReCl_6]^=$ complex which is able to recombine very quickly with radiolytically produced free Cl^-. This effect accounts for the low radiochemical yields (15%) obtained after ion exchange chromatographic separation of the irradiation product[135].

Malcolme-Lawes[131] studied the effects of target composition on the yield of high specific activity ^{34m}Cl using the $^{35}Cl(n,2n)^{34m}Cl$ nuclear reaction. Various alkyl chlorides were irradiated in polyethylene ampoules after which the inorganic ^{34m}Cl was separated from organically bound ^{34m}Cl by extraction into 0.1 N aqueous NaOH. The highest yields of inorganic ^{34m}Cl were obtained when a mixture of chloroalkanes and nonhalogenated short chain alkanes were irradiated; this indicated that short chain chlorocarbons containing some hydrogen would be the most efficient target system for producing inorganic ^{34m}Cl. Brinkman and Visser[136] and Black and Morgan[137] conducted similar experiments in which glass ampoules were substituted for polyethylene. Qualitatively similar results to those of Malcolme-Lawes[131] were obtained where glass ampoules were used, however the absolute yield of inorganic chloride increased for each substrate studied.

Zatolokin et al.[138] compared the thick target yields of ^{34m}Cl produced by irradiation of natural isotopic abundance phosphorous, sulphur and chlorine targets with proton, deuteron, helium-3 or helium-4 (alpha) particles. The authors were interested in the technique as an analytical tool, rather than as a radiochlorine production method so no attempt was made to recover the ^{34m}Cl from the target materials. The highest yield of ^{34m}Cl was obtained by proton irradiation of chlorine, followed by alpha and proton irradiation of sulphur.

III. EXPERIMENTAL

A. Materials

1. Solvents and Reagents

The solvents used for both preparative and analytical chromatography were reagent grade and were glass distilled prior to use. Reagent grade dioxane and dimethylformamide were dried over calcium hydride at reflux temperature. Benzene was dried over sodium wire at reflux temperature. The dry solvents were stored in amber bottles over molecular sieves (3Å, Lindeman) or used immediately after distillation. Trifluoroacetic acid and trifluoroacetic anhydride (Aldrich) were used as supplied.

Sodium iodide, potassium iodide, sodium bicarbonate, sodium chloride, calcium chloride and potassium bromide were reagent grade. The inorganic salts were dried at 200°C and stored *in vacuo* at 80°C until use.

The samples of authentic nucleosides and organic reagents were analyzed by ^{1}H nmr and mp determination to confirm their identity and purity. Uracil and 2'-deoxyuridine were purchased from Nutritional Biochemicals. Uridine, 6-chloro-2,4-dimethoxypyrimidine, 2,2'-cyclocytidine hydrochloride and diphenylcarbonate were obtained from Aldrich. Authentic samples of 2'-fluoro-2'-deoxyuridine, 2'-fluoro-2'-deoxycytidine and 2'-chloro-2'-deoxyuridine were gifts from J.R. Mercer and 2'-bromo-2'-deoxyuridine was a gift from Y.W. Lee.

2. Radionuclides and Radiochemicals

The radiochemical purity of the commercial products was determined by the specific chromatographic techniques described by the manufacturer.

Chlorine-36 (^{36}Cl) was purchased (New England Nuclear) as an aqueous solution of hydrogen chloride (14.4 MBq ml^{-1}, 159 KBq mg^{-1} of chloride).

Iodine-125 (^{125}I) was purchased (Edmonton Radiopharmaceutical Center) as a no-carrier-added aqueous solution of 0.1 N sodium hydroxide (3.7 GBq ml^{-1}). The radionuclidic purity was confirmed by analysis of the gamma ray spectrum (Tracor Gamma Trac 2200) for additional gamma peaks. Only the singles peak at 27 KeV and the coincidence peak at 58 KeV, consistent with the expected ^{125}I spectrum[139], were observed.

6-[^{3}H]-Uridine (777 GBq $mmol^{-1}$, 37 MBq ml^{-1}) was purchased as an aqueous solution from Amersham Corporation (Oakville, Ontario). 2-[^{14}C]-Uridine was purchased from either Moravek Biochemicals (2.03 GBq $mmol^{-1}$, 1.85 MBq ml^{-1}) or Amersham Corporation (1.96 GBq $mmol^{-1}$, 1.85 MBq ml^{-1}). 6-[^{3}H]-2'-Deoxyuridine (925 GBq $mmol^{-1}$, 37 MBq ml^{-1}) was purchased from Amersham Corporation. 6-[^{3}H]-2'-Fluoro-2'-deoxyuridine (42.6 GBq $mmol^{-1}$) was obtained as a gift from J.R. Mercer or prepared as described in section III.C.2.a. Tritiated water was purchased from Amersham Corporation (4.33×10^{6} dpm g^{-1}).

B. Instrumental

1. Chemical Analysis

Melting points (mp) were determined with either a Büchi capillary apparatus or a Fisher-Johns hot plate apparatus and are uncorrected. Proton magnetic resonance (^{1}H nmr) spectra were recorded with deuterated dimethylsulfoxide as solvent and tetramethylsilane as internal standard using a Varian EM-360A spectrometer. Coupling constants are reported in Hertz (Hz). Mass spectra (ms) were measured with an AEI-MS-9 mass spectrometer. Exact mass measurements were used to determine elemental composition. Ultraviolet (uv) spectra and uv standard curves were obtained using a Unicam SP-1800 spectrometer.

2. Chromatographic Analysis

Reverse phase high performance liquid chromatography (rp-hplc) was performed using either a Hewlett-Packard or Tracor 994 solvent delivery system coupled to a Unicam variable wavelength uv spectrometer and a Waters μBondapak C-18 (3.9 mm x 300 mm) reverse phase column. Merck Lobar™ silica gel columns (25 mm x 270 mm or 37 mm x 400 mm) were used for normal phase liquid chromatography. For the Lobar system solvent was delivered under positive pressure (helium) and the effluent was monitored with a Unicam variable wavelength uv spectrometer. Column effluent radioactivity was monitored with either a Berthold BF 2025 flow detector or by collection of individual samples. The samples were analyzed by gamma spectroscopy (NaI(Tl) or Ge(Li)) or liquid scintillation counting (lsc).

Analytical thin layer chromatographic (tlc) separations were performed using precoated silica gel plates (Whatman MK-5 1 in x 3 in or Merck 50 mm x 75 mm) impregnated with shortwave uv indicator. Small scale preparative tlc was performed on prepoured silica gel plates (20 cm x 20 cm x 0.25 to 2.0 mm in thickness; Merck or Whatman). The chromatographic bands containing the components of interest were visualized with uv, removed from the plate and extracted with either methanol or the development solvent. The silica gel was removed from the solvent by either centrifugation or filtration.

Large scale preparative chromatographic separations were performed on an Hitachi centrifugal chromatograph (cc) coupled to a fixed wavelength uv (254 nm) detector. Thin layer chromatographic grade silica gel (Camag, Berlin, FRG) was used for the cc separations.

Paper chromatography was performed using Whatman number 1 chromatography paper (15 mm x 200 mm).

Radiochromatograms of γ emitting radionuclides were qualitatively analyzed with either a Berthold gas flow scanner or a custom built instrument using a collimated sodium iodide crystal (NaI(Tl)).

Quantitative analyses were obtained by triangulation of the peaks on the chromatogram trace or by dividing the chromatogram into individual sections and counting each sample directly. The radioactive components of chromatogram sections containing beta emitting nuclides were eluted by addition of 250 µl of water directly to the sample in a lsc vial. The samples were then dissolved in a water-compatible fluor, and counted by lsc.

To ensure reproducibility, and to avoid anomalous chromatographic behavior, all high specific activity samples were first diluted in

methanolic solutions of authentic standards before tlc analysis. Low specific activity samples requiring larger sample volumes (2-5 µl) for adequate count rates during subsequent analyses were applied as a row of spots rather than by reapplication over the original spot[140].

3. Gamma and Liquid Scintillation Spectroscopy

Gamma emitting samples containing more than 37 KBq were analyzed with a Capintec dose calibrator. The absolute activity of analytical samples was determined with a calibrated multi-channel spectrometer and Ge(Li) detector. Large numbers of samples were counted with either a Tracor TN-11 high resolution gamma spectrometer, a Tracor Gamma Trac 2200, or a Beckman 8000 automatic gamma spectrometer.

Beta emitting nuclides were counted with either a Berthold BF500, a Beckman LS9000, or a Tracor Mark III automatic liquid scintillation spectrometer. All samples were dark and temperature adapted for 24 hours before counting, unless otherwise stated.

Quench correction curves for lsc were prepared by accurately pipetting a known volume of calibrated standard of the appropriate radionuclide into a series of lsc vials containing unquenched fluor. The samples were counted to determine the precision of pipetting, and those samples deviating from the mean by more than 2.5% were rejected. The samples were then quenched by the addition of increasing volumes of solubilized tissue which was prepared following the same protocol used to prepare the unknown samples. Quenched background samples were also prepared with different volumes of solubilized tissue, omitting

the radioactive standard. The quenched samples were counted under the same conditions as the unknowns.

C. Methods

1. Radionuclide Production

a. Target Preparation

i. Gas Targets for Fluorine-18 and Chlorine-34m Production

The gas target jackets were machined from either copper or stainless steel and were fitted with liners prepared from either quartz, teflon, aluminum or stainless steel. The jackets and liners were rigorously cleaned using a series of aqueous and organic solvents before drying at 105°C for at least four hours. Valves were constructed from stainless steel or Monel™, and tubing was either teflon or stainless steel if contact with hydrogen fluoride or fluorine was intended. All components were cleaned and dried as above.

The target system was assembled while the components were still hot, and pressure tested for leaks with neon. The system was then dried *in vacuo* (< 0.1 Pa) at 50-80°C for at least 18 hours. The target system was then used directly without further treatment. In some cases the target was passivated (to decrease the surface reactivity) to fluorine by filling it to 150 kPa with anhydrous hydrogen fluoride (25-100%) in neon and heating at 110°C for 48 hours prior to use.

The target gas was separated from the vacuum of the cyclotron beam tube by a 22 μ Havar foil. The target

temperature was regulated with chilled recirculating methanol or water.

ii. Solid Targets for Fluorine-18, Chlorine-34m and Iodine-123 Production

Solid targets were prepared by compressing approximately 200 mg of the target material into a disk. The disk was mounted in a stainless steel target holder during irradiations. The target was isolated from the beam tube and the temperature was regulated as described above.

b. Production of Fluorine-18

i. $^{16}O(^{3}He,n)^{18}Ne \xrightarrow{\beta^+} {}^{18}F$

Fluorine-18 was produced, using the title reaction, by two methods. A solid target was prepared from tantalum pentoxide (Ta_2O_5) powder. The 28 MeV (incident energy) ^{3}He particles were attenuated to approximately 17 MeV with a 308 μ aluminum foil window. A stream of helium gas (300-500 ml min^{-1}) was swept across the solid target to carry the ^{18}Ne released from the target matrix into a series of traps containing anhydrous hydrogen fluoride in dioxane (5%) or 1.0 N aqueous sodium hydroxide. The trapped radioactivity was quantitatively and qualitatively analyzed with a Ge(Li) detector.

A second production method used a gas target system. The oxygen target gas was dried by passage through anhydrous calcium chloride before the target was filled. The target pressure was maintained at 200 kPa above atmospheric pressure and a flow rate of 300 ml min^{-1} of target gas was employed during irradiation. The target gas effluent was passed through two scrubber traps in series containing 1.0 N aqueous sodium hydroxide and 1% aqueous sodium iodide respectively. The trapped radioactivity was characterized as described above.

ii. $^{6}Li(n,^{3}H)\alpha$, $^{16}O(^{3}H,n)^{18}F$

Lithium carbonate (2 g) enriched to 95% ^{6}Li (Oakridge) was irradiated at a flux of 5×10^{12} n cm^{-2} s^{-1} at the Heidelberg Triga II reactor. The irradiated lithium carbonate, and carrier potassium fluoride, were transferred to a teflon container maintained at 200-250°C. Concentrated sulphuric acid was added slowly to the hot container. The hydrogen fluoride-18 evolved was carried in a stream of helium gas through heated teflon tubing to a teflon-lined reaction vessel where it was trapped in a solution of 2,2'-cyclouridine in dioxane. The accumulation of radioactivity in the reaction vessel was monitored with a survey meter and collection was terminated when no further increase was apparent. The activity collected was quantitated in a dose calibrator and analyzed qualitatively with a Ge(Li) detector.

iii. $^{20}Ne(d,\alpha)^{18}F$

Sodium fluoride-18, produced via the $^{20}Ne(d,\alpha)^{18}F$ reaction, was prepared routinely as an aqueous solution in normal saline or distilled water intended for clinical use. The target system consisted of a quartz liner which was filled with enough normal saline or water to cover the liner surface. The linter was rotated on its longitudinal axis during the irradiation. This design enabled the ^{18}F

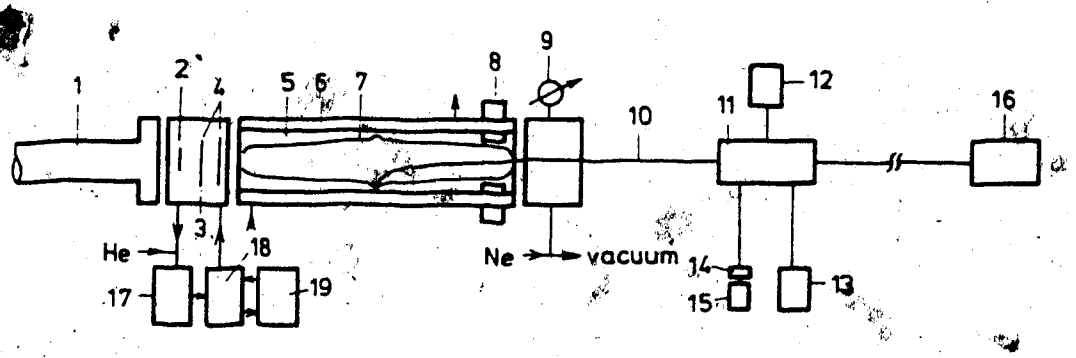

Figure 3. Target System for Routine Production of ^{18}F for Clinical Use[142].
1) Beam pipe; 2) collimator; 3) heat exchanger for foils; 4) foils; 5) target; 6) water cooling; 7) quartz tube; 8) magnetic rotation system; 9) pressure gauge; 10) solvent solution; 11) remotely operated valve; 12) isotonic saline solution; 13) injection pump; 14) millipore filter; 15) evacuated sterile vessel; 16) electronic control; 17) pump for heat exchanger; 18) heat exchanger; 19) thermostat.

to be washed from the walls during the irradiation and removed from the target immediately after bombardment (Figure 3)[141,142].

Figure 4 illustrates the gas target and recovery system that was developed for the production of anhydrous hydrogen

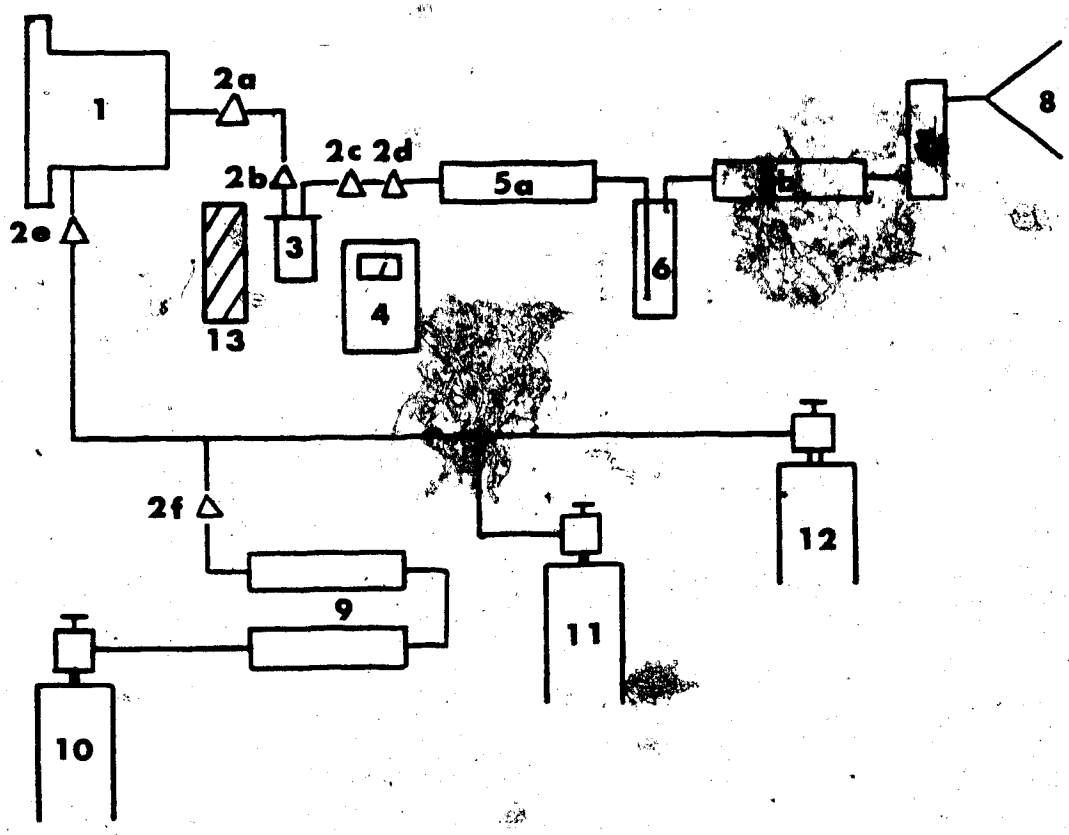

Figure 4. Recovery System for Anhydrous Hydrogen Fluoride-18. 1) target; 2a-f) two-way valves; 3) ^{18}F trap and reaction vessel; 4) survey meter; 5a,b) silica-gel traps; 6) aqueous NaOH scrubber; 7) rotameter; 8) waste gas bag; 9) Ne target gas drying columns; 10) Ne (99.99% pure); 11) anhydrous hydrogen fluoride (HF, 99.9%); 12) anhydrous HF in Ne; 13) lead shielding for (4).

fluoride-18. The system was constructed from stainless steel and teflon which are resistant to anhydrous hydrogen fluoride and elemental fluorine. This construction also allowed the target to be dried *in vacuo* by flaming with a bunsen burner when necessary. The reaction vessel (3) which also served as the first collection flask, could be isolated by valves (2a,b,c and d) from the system, and removed to a hot cell for further processing without altering the integrity of the target or exposing personnel to airborne ^{18}F. The target gases (200-400 kPa above atmospheric pressure) could be vented into the reaction vessel (3) containing a suspension of 2,2'-cyclouridine in dioxane and a secondary series of traps (5a,b and 6), through a gas flow rotameter (7) and into a waste gas storage bag (8). The collection vessel was monitored for recovered ^{18}F with a shielded survey detector (4). Pure neon (10) or neon containing carrier anhydrous hydrogen fluoride (1-10% v/v) (12) was passed through the target, into the collection system, until no increase in the collection vessel (3) radiation field was noted.

The recovered radioactivity was analyzed quantitatively in a dose calibrator and qualitatively with a Ge(Li) detector.

c. Production of Chlorine-34m

i. $^{35}Cl(p,pn)^{34m}Cl$

A solid target was prepared from natural abundance magnesium chloride ($^{35}Cl = 75.77\%$)[33] and irradiated with 22 MeV protons. The target was cooled with methanol (-20°C) and isolated from the cyclotron beam tube vacuum with a 22 μ Havar foil window.

After irradiation, the pellet of magnesium chloride was crushed and quantitatively recovered in methanol for further chemical workup, as described in section III.C.2.d. Aliquots of the irradiated target were analyzed with a Ge(Li) detector to quantitate and characterize the product.

ii. $^{34}S(p,n)^{34m}Cl$ and $^{34}S(d,2n)^{34m}Cl$

The target system (Figure 5) consisted of a glass lined cylinder (2), separated from the beam tube vacuum with a 22 μ Havar foil, connected by teflon tubing to an anion exchange column (5). After irradiation, the hydrogen sulfide was passed through the anion exchange resin, where the ^{34m}Cl was trapped. The flow rate (50 ml min^{-1}) was monitored with a gas flow rotameter (6) located after the anion exchange resin. The closed system was completed with an evacuated waste gas collection bag (7) to trap the effluent hydrogen sulfide. The ion exchange resin

could be isolated by Quick Connectors™ (4a,b) and removed from the collection system. In this way, volatile radioactivity was retained within the target and the trapping system.

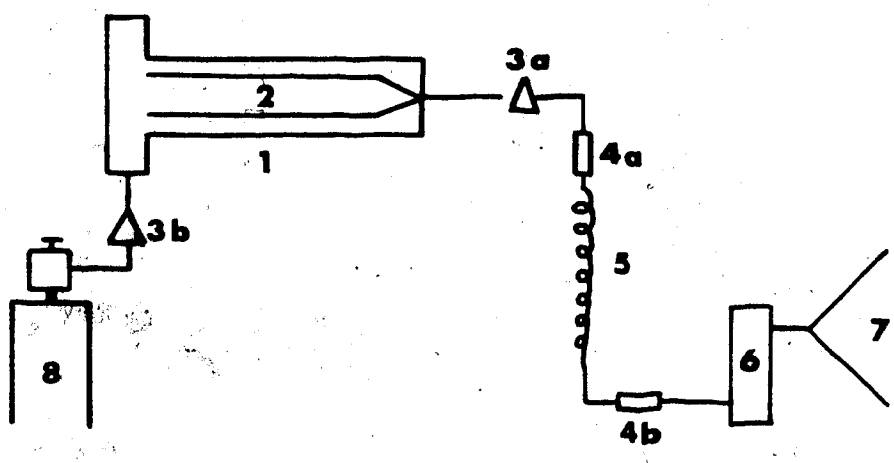

Figure 5. Target System for ^{34m}Cl Production.
1) target; 2) glass liner; 3a,b) two-way valves; 4a,b) quick connectors™; 5) anion exchange resin; 6) gas flow rotameter; 7) waste gas bag; 8) hydrogen sulfide cylinder.

The trapping system consisted of an anion exchange column connected via a stainless steel needle valve to the glass sleeve. The Dowex 21-K anion exchange resin (4.5 mEq g^{-1} dry weight) was prepared by exchange with 1.0 N aqueous hydrochloric or acetic acid and washed with distilled water. The resin was washed with absolute ethanol and dried *in vacuo* over silica gel-phosphorous pentoxide at ambient temperature.

The ion exchange column was packed in teflon tubing under vacuum to a uniform density of 4.7 mg dry resin per cm of tubing. An aliquot of the irradiation product was characterized with a Ge(Li) detector.

d. Production of Bromine-82

Bromine-82 labelled compounds were prepared as described by Lee *et al.*[143] by neutron activation. The precursors contained natural abundance bromine (^{81}Br=49.31%)[33] and were irradiated at a neutron flux of 10^{12} n cm^{-2} s^{-1} for up to four hours at the University of Alberta Slowpoke Facility (UASF).

The total amount of ^{82}Br and contaminating $^{80m}Br/^{80}Br$ arising from competing nuclear reactions was calculated from the formula:

$$A = N\sigma_{\gamma}\phi(1-e^{-\lambda t_{irr}}) \qquad \text{Equation 3}$$

where N is the mass of the irradiated isotope in terms of Avogadros number, σ_{γ} is the thermal neutron cross section (n,γ reaction) of the irradiated isotope in barns, ϕ is the neutron flux in n cm^{-2} s^{-1}, λ is the decay constant of the radionuclide produced and t_{irr} is the length of time of irradiation of the sample.

The presence of ^{80m}Br and ^{80}Br contamination was monitored by analysis of the gamma ray spectrum (Tracor Gamma-Trac 2200) of the product.

e. Production of Iodine-123

Iodine-123 (^{123}I) was prepared as described by F. Helus *et al.*[144] with minor modifications. The ^{123}I, produced by the $^{124}Te(p,2n)^{123}I$ nuclear reaction, was sublimed from the tellurium oxide (86.71% enriched ^{124}Te, Oak Ridge, USA) at 750°C and collected in a stream of oxygen (10 ml min^{-1}) on a liquid nitrogen cooled cold finger of either quartz, copper or gold. The ^{123}I was removed from the cold finger by halide exchange with a methanolic solution of either sodium iodide or sodium chloride. The major radionuclidic impurities, determined with a Ge(Li) detector, were ^{121}I (0.84%) and ^{124}I (1.23%) calculated to the end of irradiation.

2. Synthesis

The procedures employed for the synthesis of the 2[redacted]2'-deoxyuridine analogues were modifications of the methods reported by Codington[72], Cushley[18] and Thelander[81]. Synthesis of 2'-fluoro-2'-deoxycytidine was accomplished by the method of Mengel and Guschlbauer[100]. 2,2'-Cyclouridine was prepared by the method of Hampton and Nichol[63]. The 6-halouracil analogues were synthesized as described by Horwitz and Tomson[64].

a. 2'-Fluoro-2'-deoxyuridine (2'-FUdR)

i. Reaction of Anhydrous Hydrogen Fluoride with 2,2'-Cyclouridine

Anhydrous hydrogen fluoride (6.8 mmol) diluted with neon was passed through a suspension of 2,2'-cyclouridine (31.5 mg,

0.139 mmol) in anhydrous dioxane (22 ml) in a teflon-lined stainless steel reaction vessel. The reaction mixture was heated at 175°C (oil bath temperature) for 140 minutes. An aliquot (0.9 ml) was diluted with distilled water and titrated with 0.1 N sodium hydroxide to determine the unreacted hydrogen fluoride concentration. The remaining solution was treated with aqueous calcium carbonate until the evolution of gas had ceased and was then filtered. The solvent was removed in vacuo at 40°C, and the residue was purified by preparative silica gel tlc (20 x 20 cm x 1.0 mm in thickness) using chloroform-ethanol (4:1 v/v) as the development solvent. The uv band corresponding to authentic 2'-fluoro-2'-deoxyuridine (2'-FUdR) ($R_f = 0.54$) was eluted with absolute ethanol to yield the title compound (15.6 mg, 46%). ^{1}H nmr (DMSO-d_6) δ: 3.45 [3H, m, $C_{4'}$-H and $C_{5'}$-H], 4.14 [1H, m($J_{3',F} = 24$), $C_{3'}$-H], 5.02 [1H, d($J_{2',F} = 52$) of m, $C_{2'}$-H], 5.66 [1H, d($J_{5,6} = 8$), C_5-H], 5.89 [1H, d($J_{1',F} = 18$) of d($J_{1',2'} = 2$), $C_{1'}$-H], 7.88 [1H, d($J_{5,6} = 8$), C_6-H].

ii. Reaction of Anhydrous Hydrogen Fluoride-18 with 2,2'-Cyclouridine

The hydrogen fluoride-18, generated as described in section III.C.1, was trapped on-line in a suspension of 2,2'-cyclouridine in dioxane. A teflon-lined stainless steel vessel served as both the reaction vessel and the trap. An aliquot of the reaction solution was diluted with water and titrated with 0.1 N sodium hydroxide to determine the amount

of unreacted hydrogen fluoride. The remaining reaction volume was treated with an aqueous suspension of calcium or barium carbonate. The supernatant was filtered and the solvent was removed *in vacuo*. The residue was redissolved in water and passed through a minicolumn of either lanthanium fluoride on DEAE cellulose (5% w/w) or aluminum oxide to remove the free fluoride-18. The identity and radiochemical yield of the product was determined by silica gel tlc, rp-hplc or preparative silica gel column chromatography (Merck B column).

iii. Reaction of Anhydrous Hydrogen Fluoride with 6-[^{3}H]-2,2'-Cyclouridine

A methanolic solution of 6-[^{3}H]-2,2'-cyclouridine (3.07 MBq, 4.9 μmol) was evaporated to dryness in a teflon vial under a stream of nitrogen, then dried *in vacuo* (< 0.13 kPa) at ambient temperature for 24 hours. The residue was dissolved in anhydrous dioxane (1.3 ml) and the solution was saturated with anhydrous hydrogen fluoride which was bubbled into the solution through a rubber septum. The rubber septum was replaced with a teflon cap and the sealed vial was placed in a stainless steel reaction vessel containing 1.0 ml dioxane, to equilibrate internal and external pressure, and heated at 110°C for 15 hours. The straw colored reaction mixture was treated with aqueous calcium carbonate until the evolution of carbon dioxide had ceased. The suspension was filtered and the solvent removed *in vacuo*. The residue was purified by

preparative silica gel tlc using chloroform-ethanol (4:1 v/v) as the development solvent. The chromatographic band migrating with authentic 2'-FUdR was eluted and rechromatographed using chloroform-dioxane-methanol (8:6:3 v/v) as the development solvent. The band co-chromatographing with standard 2'-FUdR was eluted with methanol to give 6-[^{3}H]-2'-fluoro-2'-deoxyuridine in 19.2% (0.59 MBq) radiochemical yield. The specific activity was calculated to be 21.67 MBq mmol^{-1}.

b. 2'-Fluoro-2'-deoxycytidine (2'-FCdR)

i. Reaction of Potassium Fluoride with 2,2'-Cyclocytidine Hydrochloride in the Presence of Dicyclohexyl-18-Crown-6

Potassium fluoride (496 mg, 8.55 mmol) was dried *in vacuo* at 160°C for 12 hours and 2,2'-cyclocytidine hydrochloride (140 mg, 0.532 mmol) was dried *in vacuo* (< 0.1 Pa) at ambient temperature for 72 hours. Dicyclohexyl-18-crown-6 (202 mg, 0.543 mmol), anhydrous benzene (20 ml) and anhydrous dimethylformamide (20 ml) were added to the dry potassium fluoride under a helium atmosphere, and the solution heated at 130°C. When the benzene azeotrope had been collected (80 min), dry 2,2'-cyclocytidine hydrochloride was added and the reaction mixture was heated under reflux for 5.5 hours. The solvent was removed *in vacuo* and the residual oil adsorbed onto a slurry of silica gel and chloroform. This material was added to a slurry-packed silica gel column and eluted with a

stepwise solvent gradient from chloroform (250 ml) to chloroform-methanol (3:2 v/v). Fractions 15, 16 and 17 (15 ml) were combined to give 2'-fluoro-2'-deoxycytidine in 52.7% (69 mg, 0.281 mmol) chemical yield. ^{1}H nmr (DMSO-d_6) δ: 3.60 [3H, m, $C_{5'}$-H and $C_{4'}$-H], 4.14 [1H, m($J_{3',F} \cong 20$), $C_{3'}$-H], 4.90 [1H, d($J_{2',F} = 54$) of d($J_{2',3'} = 4$) of d($J_{2',1'} = 2$), $C_{2'}$-H], 5.20 [1H, q($J_{5'\text{-OH},5'\text{-H}} = 4$), $C_{5'}$-OH, exchanges with deuterium oxide], 5.62 [1H, d($J_{3'\text{-OH},3'\text{-H}} = 6$), $C_{3'}$-OH, exchanges with deuterium oxide], 5.82 [1H, d($J_{5,6} = 8$), C_5-H], 5.89 [1H, d($J_{1',F} = 18$) of d($J_{1',2'} = 2$), $C_{1'}$-H], 7.21 and 7.38 [2H, C_4-NH_2 exchanges with deuterium oxide], 7.92 [1H, d($J_{5,6} = 8$), C_6-H].

c. 6-Chlorouracil

i. Demethylation of 2,4-Dimethoxy-6-chloropyrimidine

A solution of 2,4-dimethoxy-6-chloropyrimidine (5.89 g, 33.7 mmol) in glacial acetic acid (450 ml) and 2.0 N hydrochloric acid (65 ml) was heated under reflux for 45 minutes. Removal of the solvent *in vacuo* at 45°C afforded a yellowish solid which was recrystallized twice from water to give 6-chlorouracil as fluffy white crystals, mp 295-298°C (dec), lit. 298-300°C (dec)[64] (3.587 g, 72%). ^{1}H nmr (DMSO-d_6) δ: 5.73 [1H, s, C_5-H], 11.24 [1H, s, N_1-H exchanges with deuterium oxide], 12.00 [1H, s, N_3-H exchanges with deuterium oxide]; exact mass calculated for $C_4H_3N_2O_2{}^{35}Cl$: 145.98825; found (high resolution ms): 145.98736.

ii. Calcium Chloride Exchange of 6-Iodouracil

Anhydrous calcium chloride (2.76 mg, 0.025 mmol) and 6-iodouracil (17.7 mg, 0.074 mmol) were suspended in dry dimethylformamide (50 µl) in a sealed glass pressure vial. The suspension was heated at 140°C with gentle intermittent agitation until the mixture became homogeneous. The solution gradually changed color and formed a red-brown precipitate after 60 minutes. The yield of 6-chlorouracil, determined by quantitative rp-hplc (water-methanol 49:1 v/v), was 77.4% (5.69 mg, 0.039 mmol). Product identity was established by cochromatography with authentic 6-chlorouracil on silica gel tlc using chloroform-ethanol (4:1 v/v) as development solvent and rp-hplc (as above).

iii. Calcium Chloride-36 Exchange of 6-Iodouracil

Calcium hydroxide (13.26 mg, 0.179 mmol) was titrated directly in the reaction vial with an aqueous solution of [^{36}Cl]-hydrogen chloride (1.88 MBq, 0.323 mmol). The vial was sealed, agitated until the calcium hydroxide had dissolved and the water was then removed *in vacuo* at 85°C. 6-Iodouracil (79.2 mg, 0.333 mmol) and dry dimethylformamide (200 µl) were added to the anhydrous calcium chloride-36. The suspension was heated at 152°C for 30 minutes, at which time analytical tlc (silica gel) using chloroform-ethanol (4:1 v/v) indicated that 77% of the ^{36}Cl activity was associated with the 6-chlorouracil standard. The residual activity remained near the

solvent front. 6-[^{36}Cl]-Chlorouracil was separated from unreacted 6-iodouracil and calcium chloride-36 by preparative cc (5 mm silica gel disk) with a solvent gradient elution from 100% chloroform to chloroform-ethanol (3:2 v/v). Fractions 25 through 35 (50 ml) were combined and the solvent was removed *in vacuo*. The residue was redissolved in water and passed through a AgCl-cellulose column to remove chloride-36 contamination, which gave a final radiochemical yield of 31.6% (0.59 MBq).

d. 2'-Chloro-2'-deoxyuridine (2'-ClUdR)

i. Reaction of Sodium Chloride with 2,2'-Cyclouridine

Sodium chloride (2.63 g, 44.58 mmol), 2,2'-cyclouridine (1.02 g, 4.50 mmol) and trifluoroacetic acid (5.0 ml, 66.6 mmol) were stirred in dry dimethylformamide (15 ml) at 130°C for 20 minutes. The reaction mixture supernatant was poured into cold diethylether (75 ml) giving a white precipitate which was recrystallized from methanol to yield 624 mg (2.38 mmol, 52.9%) of 2'-chloro-2'-deoxyuridine (2'-ClUdR), mp 206-207°C, lit. 207-212[72]. The reaction mixture residue was dissolved in methanol and the products were separated by preparative cc (5 mm silica gel disk) using a solvent gradient from chloroform (100%) to chloroform-methanol (2:1 v/v). Fractions 12, 13 and 14 (50 ml) contained 2'-ClUdR (^{1}H nmr and tlc), fractions 16, 17 and 18 contained ara-U (identical

by ^1H nmr and tlc with an authentic sample) and fractions 20 through 26 contained 2,2'-cyclouridine (tlc). ^1H nmr (DMSO-d_6) δ: 3.62 [2H, s(broad), $C_{5'}$-H], 3.96 [1H, m, $C_{4'}$-H], 4.18 [1H, m, collapses to a triplet after deuterium oxide exchange ($J_{2',3'} = J_{3',4'} = 5$), $C_{3'}$-H], 4.53 [1H, t($J_{1',2'} = J_{2',3'} = 5$), $C_{2'}$-H], 5.22 [1H, broad s, $C_{5'}$-OH, exchanges with deuterium oxide], 5.65 [1H, d($J_{5,6} = 8$), C_5-H], 5.86 [1H, d($J_{3'\text{-OH},3'} = 5$), $C_{3'}$-OH, exchanges with deuterium oxide], 5.99 [1H, d($J_{1',2'} = 6$), $C_{1'}$-H], 7.92 [1H, d($J_{5,6} = 8$), C_6-H]; exact mass calculated for $C_9H_{11}N_2O_5{}^{35}Cl$: 262.0358; found (high resolution ms): 262.0367; exact mass calculated for $C_9H_{11}N_2O_5{}^{37}Cl$: 264.0327; found (high resolution ms): 264.0363.

ii. Reaction of Sodium Chloride-36 with 2,2'-Cyclouridine

An aqueous solution of hydrogen chloride-36 (3.18 MBq, 20.52 mg, 0.56 mmol) was titrated with aqueous 10.0 N sodium hydroxide (55 µl, 0.55 mmol) directly in a glass pressure vial. The water was removed *in vacuo* at ambient temperature and the contents were dried *in vacuo* at 170°C for 2 hours. A solution of 2,2'-cyclouridine (123 mg, 0.54 mmol) in anhydrous dimethylformamide (5.0 ml) and trifluoroacetic acid (50 µl, 0.65 mmol) was added and the reaction was heated at 163°C for 30 minutes. The solvent was removed *in vacuo* and the reaction mixture was purified by preparative cc using a solvent gradient of increasing proportions of methanol in chloroform. Fractions

24 through 28 (50 ml) afforded the desired 2'-[^{36}Cl]-ClUdR in 29.8% (43.0 mg, 0.164 mmol) chemical yield and 29.4% (0.93 MBq) radiochemical yield as determined by rp-hplc (methanol-water 1:19 v/v). The theoretical specific activity was 5.66 MBq mmol^{-1}; the observed specific activity was 5.46 MBq mmol^{-1}. The product was identified by cochromatography with an authentic sample by silica gel tlc using chloroform-dioxane-methanol (8:6:3 v/v) and chloroform-ethanol (4:1 v/v) and rp-hplc (methanol-water 1:19 v/v).

iii. Reaction of Magnesium Chloride-34m with 2,2'-Cyclouridine

A suspension of magnesium chloride-34m (∿ 2.10 mmol, 19.26 MBq) in methanol was evaporated to dryness at 160°C under a stream of helium. A solution of 2,2'-cyclouridine (12.6 mg, 0.056 mmol) in anhydrous dimethylformamide (3 ml) and trifluoroacetic acid (325 µl, 4.2 mmol) was added to the magnesium chloride-34m and the suspension was heated at 160°C for 15 minutes. The reaction mixture was eluted with methanol from a mini column of aluminum oxide prior to purification by preparative silica gel tlc using chloroform-ethanol (2:1 v/v) as the development solvent. The product which cochromatographed with authentic 2'-ClUdR was recovered in 55.8% chemical yield (8.19 mg, 0.031 mmol) as estimated from rp-hplc. The ^{1}H nmr spectrum and tlc R_f values were identical with an authentic sample.

The 2'-[^{34m}Cl]-ClUdR was recovered in 2.7% (0.52 MBq) radiochemical yield (calculated at the end of irradiation).

iv. Reaction of Dowex 21-K Chloride with 2,2'-Cyclouridine

Dowex 21-K anion exchange resin (33.9 mg, 0.152 mmol of chloride anion) and 2,2'-cyclouridine (32.5 mg, 0.144 mmol) were suspended in anhydrous dimethylformamide (3.0 ml). Trifluoroacetic acid (15 µl, 0.20 mmol) was added and the reaction was stirred at 160°C for 60 minutes. Reaction progress was monitored by rp-hplc analysis of aliquots (20 µl) taken during the course of the reaction. The final product was purified by preparative tlc with chloroform-ethanol (4:1 v/v) as development solvent. The ^{1}H nmr spectrum and tlc R_f values were identical with an authentic sample.

v. Reaction of Dowex 21-K Chloride-34m with 2,2'-Cyclouridine

Approximately 3 cm (equivalent to 0.063 mmol chloride) of the ion exchange trapping column labelled with 19.07 MBq of ^{34m}Cl was added to a solution of 2,2'-cyclouridine (13.0 mg, 0.058 mmol) in anhydrous dimethylformamide (1.2 ml). Trifluoroacetic acid (0.026 mmol) was added to the suspension and the reaction mixture was stirred at 140°C for 15 minutes. The progress of the reaction was monitored by silica gel radio-tlc with chloroform-ethanol

(2:1 v/v) as the development solvent. The radiochemical yield was calculated to be 22.2% (4.26 MBq) with a specific activity of 0.304 GBq $mmol^{-1}$ (calculated at the end of irradiation).

vi. Reaction of Calcium Chloride with 6-[^{3}H]-2,2'-Cyclouridine

A methanolic solution of 6-[^{3}H]-2,2'-cyclouridine (2.87 MBq) was evaporated to dryness directly in a glass pressure reaction vial under a stream of nitrogen gas at ambient temperature. Anhydrous calcium chloride (1.9 mg, 17.0 μmol) was added, and the vessel was sealed and dried *in vacuo* (< 0.13 kPa) for 18 hours at ambient temperature. Anhydrous dimethylformamide (0.5 ml) was added and the suspension was heated at 150°C for approximately 2 min to effect solution. After the suspension cooled to ambient temperature, trifluoroacetic acid (5 μl, 65 μmol) was added and the reaction mixture was heated at 150°C for 15 minutes. The reaction mixture was purified directly by preparative silica gel tlc with chloroform-ethanol (4:1 v/v) as the development solvent. The faint uv absorbing band which corresponded to an authentic standard was extracted to give 1.52 MBq of 6-[^{3}H]-2'-ClUdR (53.2% radiochemical yield). The specific activity was determined by a combination of rp-hplc and lsc to be 11.1 GBq $mmol^{-1}$.

e. 2'-Bromo-2'-deoxyuridine (2'-BrUdR)

i. Reaction of Potassium Bromide with 6-[^{3}H]-2,2'-Cyclouridine

A methanolic solution of 6-[^{3}H]-2,2'-cyclouridine (2.74 MBq) was evaporated to dryness directly in a glass pressure reaction vial under a stream of nitrogen gas at ambient temperature. Anhydrous potassium bromide (4.40 mg, 0.037 mmol) was added to the vessel which was sealed and dried *in vacuo* (< 0.13 kPa) for 18 hours at ambient temperature. Dry dimethylformamide (0.5 ml) was added to the reaction and the suspension was heated for approximately 3 minutes to effect solution. The suspension was cooled to room temperature, trifluoroacetic acid (5 µl, 0.065 mmol) was added, and the reaction mixture was heated at 150°C for 30 minutes. The reaction mixture was purified directly by preparative tlc with chloroform-ethanol (4:1 v/v) as the development solvent. Extraction of the very faint uv absorbing band which corresponded to authentic standard gave 6-[^{3}H]-2'-BrUdR in 26.6% radiochemical yield (0.73 MBq).

f. 2'-Iodo-2'-deoxyuridine (2'-IUdR)

i. Reaction of Sodium Iodide with 2,2'-Cyclouridine

Sodium iodide (3.08 g, 20.53 mmol) and 2,2'-cyclouridine (0.445 g, 1.97 mmol) were suspended with vigorous stirring in dry dioxane. Trifluoroacetic acid (1.0 ml, 12.9 mmol) was

added and the suspension heated at reflux for 25 minutes at which time most of the solids had dissolved leaving a yellow solution. The dioxane from the reaction supernatant was removed *in vacuo* and the residue was recrystallized from absolute ethanol to give 2'-IUdR (0.366 g, 52%), mp 152-154°C (dec); lit. 145-147°C (dec)[145]. ^{1}H nmr (DMSO-d_6) δ: 3.58 [2H, m, C_5'-H], 3.90 [2H, m, C_3'-H and C_4'-H], 4.47 [1H, d($J_{2',3'}$ = 3) of d($J_{1',2'}$ = 8), C_2'-H], 5.15 [1H, t($J_{5',5'\text{-OH}}$ = 5), C_5'-OH, exchanges with deuterium oxide], 5.68 [1H, d($J_{5,6}$ = 8), C_5-H], 5.98 [1H, d($J_{3',3'\text{-OH}}$ = 5, C_3'-OH, exchanges with deuterium oxide], 6.20 [1H, d($J_{1',2'}$ = 8), C_1'-H], 7.85 [1H, d($J_{5,6}$ = 8), C_6-H].

ii. Reaction of Hydrogen Iodide with 2,2'-Cyclouridine

2,2'-Cyclouridine (64.2 mg, 0.28 mmol) was suspended in dioxane (25 ml) and hydrogen iodide gas was bubbled directly into the reaction mixture (5 ml min^{-1} for 20 minutes; 4.5 mmol). The reaction vessel was sealed and heated at 100°C for 60 minutes. The solvent was removed *in vacuo* at 30°C and the residue was chromatographed on two silica gel plates (20 cm x 20 cm x 0.5 mm). The two major products were identified by tlc as unreacted 2,2'-cyclouridine (R_f = 0.15) and 2'-IUdR (R_f = 0.55). The 2'-IUdR was eluted from the silica gel in 29.9% chemical yield (30.2 mg). The ^{1}H nmr spectrum and tlc R_f values were identical with an authentic sample.

iii. Reaction of Sodium Iodide-125 with 2,2'-Cyclouridine

Sodium iodide (5.2 mg, 0.035 mmol) and 2,2'-cyclouridine (16.6 mg, 0.073 mmol) were added to an aqueous solution of iodine-125 (98.0 MBq) in 0.1 N sodium hydroxide (0.030 mmol) and dried *in vacuo* (< 0.13 kPa) at ambient temperature for 24 hours. Dry dioxane (2.0 ml) was added and the suspension was heated at 150°C to effect solution. The solution was cooled to room temperature, trifluoroacetic acid (10 µl, 0.13 mmol) was added and the reaction mixture heated at 148°C for 16 minutes. The light yellow supernatant was removed and the residue was washed with dioxane (1.0 ml). The two fractions were combined and purified by preparative tlc using chloroform-ethanol (4:1 v/v) as the development solvent. The uv absorbing band which cochromatographed with authentic 2'-IUdR was extracted with methanol to give 2'-[^{125}I]-IUdR in 47% (45.9 MBq) radiochemical yield. The specific activity was determined by rp-hplc and gamma spectroscopy to be 2.72 GBq mmol^{-1}.

iv. Reaction of Sodium Iodide-123 with 2,2'-Cyclouridine

A methanolic solution of sodium iodide-123 (0.45 GBq, 0.0014 mmol) was evaporated to dryness directly in a glass pressure vial at 135°C under a stream of nitrogen gas. Dioxane (1.0 ml), 2,2'-cyclouridine (0.6 mg, 0.0026 mmol) and

trifluoroacetic acid (2 µl, 0.026 mmol) were added to the dry sodium iodide-123 and stirred at 135°C for 15 minutes. The light yellow supernatant which contained 90% of the radioactivity was purified directly via silica gel tlc with chloroform-ethanol (4:1 v/v) as development solvent. The uv band which corresponded to authentic 2'-IUdR was extracted with methanol to give 2'-[^{123}I]-IUdR in 83.1% (0.37 GBq) radiochemical yield. Radiochromatographic analysis with rp-hplc and silica gel tlc confirmed the identity and radiochemical yield (80.0%) of the product. The specific activity was calculated to be 0.63 TBq mmol^{-1}.

v. Reaction of NCA Sodium Iodide-123 with 2,2'-Cyclouridine

Iodine-123 (0.46 GBq) was recovered from the gold foil by non-isotopic exchange with methanolic sodium chloride (0.0062 mmol) without added carrier iodide and evaporated to dryness directly in a glass pressure vial by heating under a stream of nitrogen gas. Dioxane (1.0 ml), 2,2'-cyclouridine (0.8 mg, 0.0035 mmol) and trifluoroacetic acid (2 µl, 0.026 mmol) were added to the ^{123}I and the suspension was heated at 135°C with stirring for 15 minutes. Aliquots of the reaction were diluted with carrier 2'-IUdR and analyzed radiochromatographically. Silica gel tlc (chloroform-ethanol 4:1 v/v) and rp-hplc (water-methanol 9:1 v/v) indicated the radiochemical yield of 2'-[^{123}I]-IUdR to be 20.8% and 21.3% respectively.

vi. Reaction of Sodium Iodide with 2-[^{14}C]-2,2'-Cyclouridine

Sodium iodide (0.304 mg, 0.002 mmol) and 2-[^{14}C]-2,2'-cyclouridine (0.130 MBq) were dried *in vacuo* (< 0.13 kPa) at 80°C for 4 hours and then at ambient temperature for 12 hours. Dioxane (200 µl) was added and the resulting suspension was stirred at 140°C to effect solution, and allowed to cool to ambient temperature. Trifluoroacetic acid (5 µl, 0.065 mmol) was added and the solution stirred at 136°C for 15 minutes. The 2-[^{14}C]-2'-IUdR was isolated directly, by preparative silica gel tlc with chloroform-ethanol (4:1 v/v) as development solvent, in 28.7% (0.037 MBq) radiochemical yield. A radiochemical purity of 97.8% was determined by radio-tlc with chloroform-dioxane-methanol (8:6:3 v/v) as development solvent.

g. 6-Iodouracil

i. Sodium Iodide Exchange of 6-Chlorouracil

Sodium iodide (7.972 g, 53.15 mmol) and 6-chlorouracil (0.989 g, 6.75 mmol) were stirred in dimethylformamide (8.0 ml) under a nitrogen atmosphere for 75 minutes at 145°C. The dark red suspension, which solidified upon cooling, was transferred in aqueous methanol and the solvent removed *in vacuo* at 60°C. The residue was stirred with hot water (8.0 ml) and the supernatant was removed to yield 0.144 g of a yellow water-insoluble solid. Another 0.843 g of a similar

yellow solid precipitated from the aqueous supernatant, after it cooled to room temperature to give a combined product weight of 0.987 g (4.14 mmol, 61.4%), mp 272-275°C (dec). A second recrystallization from absolute ethanol gave pale green to colorless needles in 34.3% yield (0.551 g, 2.32 mmol); mp 278-279°C (dec) lit: 279-280°C (dec)[64]: ^{1}H nmr (DMSO-d_6) δ: 5.82 [(1H, s, C_5-H], 10.35 [1H, broad s, N_3-H, exchanges with deuterium oxide]; exact mass calculated for $C_4H_3N_2O_2I$: 237.9230; found (high resolution ms) 237.9238.

ii. Sodium Iodide-123 Exchange of 6-Chlorouracil

Sodium iodide-123 (0.36 GBq, 0.0007 mmol) in methanol (0.5 ml) was evaporated in a stepwise manner directly in a 0.2 ml glass pressure reaction vial at 150°C under a stream of nitrogen. Sodium iodide (12.0 mg, 0.081 mmol), 6-chlorouracil (19.3 mg, 0.131 mmol) and dimethylformamide (25 μl) were added to the sodium iodide-123 and heated at 150°C for 113 minutes. The reaction mixture was dissolved in methanol and purified by preparative tlc (chloroform-ethanol 2:1 v/v). The uv absorbing band which cochromatographed with authentic 6-iodouracil was recovered in 44.4% (0.16 GBq) radiochemical yield. Quantitative and qualitative rp-hplc (water-methanol 9:1 v/v) analysis of the crude reaction product indicated a radiochemical yield of 45.5% of 6-[^{123}I]-iodouracil.

h. 2,2'-Cyclouridine (2,2'-CUR)

i. Reaction of Diphenylcarbonate with Uridine

Uridine (1.99 g, 8.14 mmol), diphenylcarbonate (2.81 g, 13.0 mmol) and sodium bicarbonate (0.05 g, 0.57 mmol) were dissolved in dry dimethylformamide (4.0 ml) and stirred at 140°C for 25 minutes. The reaction mixture was poured onto ice cold diethyl ether (20 ml), to yield a yellowish semisolid precipitate which was recrystallized from hot methanol to give 2,2'-cyclouridine (1.36 g, 73.7%) as an off white powder, mp 238-239°C. A second recrystallization from hot methanol gave the product as colorless, needle-like crystals (0.804 g, 43.7%) mp 242.5-244.5°C; lit 238-244°C[18]; 246-248°C[93]), ^{1}H nmr (DMSO-d_6) δ: 3.26 [2H, m(collapses to a d($J_{4',5'}$ = 5.5) after deuterium oxide exchange) $C_{5'}$-H], 4.11 [1H, t($J_{4',5'}$ = 5), $C_{4'}$-H], 4.43 [1H, d($J_{3',3'\text{-OH}}$ = 3), collapses to a singlet after deuterium exchange, $C_{3'}$-H], 4.99 [1H, t($J_{5'\text{-OH},5'}$ = 5) exchanges with deuterium oxide, $C_{5'}$-OH], 5.24 [1H, d($J_{1',2'}$ = 6), $C_{2'}$-H], 5.86 [1H, d($J_{5,6}$ = 8), C_5-H], 5.92 [1H, d($J_{3'\text{-OH},3'}$ = 4) exchanges with deuterium oxide, $C_{3'}$-OH], 6.34 [1H, d($J_{1',2'}$ = 6), $C_{1'}$-H], 7.87 [1H, d($J_{5,6}$ = 8), C_6-H].

ii. Reaction of Diphenylcarbonate with 6-[^{3}H]-Uridine

Uridine (2.0 mg, 0.0082 mmol), diphenylcarbonate (4.85 mg, 0.025 mmol) and sodium bicarbonate (∿ 0.05 mg) were mixed with

an aqueous solution of 6-[^{3}H]-uridine (7.98 MBq). The water was removed under a stream of nitrogen gas at room temperature and the reactants were dried in vacuo at 40°C for 9 hours. The dried reactants were dissolved in dimethylformamide (0.3 ml) and heated at 153°C for 15 minutes. The solvent was removed under a stream of nitrogen gas at ambient temperature and the product used without further purification. The product was identified as 6-[^{3}H]-2,2'-cyclouridine by radiochromatographic analysis on silica gel tlc (chloroform-ethanol 1:1 v/v). The radiochemical yield was 83.7% (6.68 MBq).

iii. Effect of Reaction Time on Yield of 6-[^{3}H]-2,2'-Cyclouridine

Uridine (14.5 mg, 0.06 mmol), diphenylcarbonate (18.5 mg, 0.10 mmol) and sodium bicarbonate (catalytic amount) were added to an aqueous solution of 6-[^{3}H]-uridine (0.25 MBq) and dried in vacuo for 2 hours at ambient temperature and then for a further 16 hours at 80°C. Anhydrous dimethylformamide (0.5 ml) was added to the reactants and the reaction mixture was stirred at room temperature until dissolution was complete. The solution was heated at 152°C for 30 minutes. Samples (10 µl) were removed at 5 minute intervals for tlc analysis (duplicate). A 3 µl aliquot of each sample was plated directly onto silica gel tlc plates. The remaining 7 µl aliquot was added to a methanolic solution of uracil, uridine and 2,2'-cyclouridine and applied to the tlc plates. All tlc chromatograms were

developed with chloroform-ethanol (1:1 v/v) as the development solvent. The standards were located by uv visualization. The appropriate sections were analyzed by lsc and the fraction of the total radioactivity associated with each compound was calculated.

i. Arabinouridine (Ara-U)

i. Reaction of Sodium Hydroxide with 2,2'-Cyclouridine

A solution of 2,2'-cyclouridine (68.4 mg, 0.28 mmol) in 1.0 N aqueous sodium hydroxide (1.0 mmol) was heated at 148°C for 5 minutes with stirring. The reaction products were separated by cc using chloroform-methanol (4:1 v/v) as the development solvent. Fractions 6 through 9 (50 ml) gave arabinouridine (15.4 mg, 22.6%). ^{1}H nmr (DMSO-d_6) δ: 3.58 [2H, m, $C_{5'}$-H], 3.72 [2H, m, $C_{3'}$-H and $C_{4'}$-H], 3.93 [2H, m, collapses to q after exchange with deuterium oxide ($J_{1',2'} = J_{2',3'} = 4$) $C_{2'}$-H and $C_{2'}$-OH], 5.00 [1H, broad s, C_5-OH, exchanges with deuterium oxide], 5.54 (2H, d($J_{5,6} = 8$), C_5-H, broad s, $C_{3'}$-OH, exchanges with deuterium oxide], 5.95 [1H, d($J_{1',2'} = 4$), $C_{1'}$-H], 7.58 [1H, d($J_{5,6} = 8$), C_6-H], 11.30 [1H, broad s, N_3-H, exchanges with deuterium oxide].

3. Tissue Distribution

6-Iodouracil and the 2'-halo-2'-deoxyuridine analogues were designed to be used for tumor delineation and determination of the proliferative potential of a tumor mass using non-invasive gamma-camera imaging techniques. The tissue distribution studies were designed to determine whether or not the radiohalogenated analogues synthesized have the characteristics of a useful tumor delineating agent. Three distribution parameters were considered important:

1. the degree of tumor specificity (tumor specific activity relative to other tissues);
2. the absolute concentration of radioactivity in the tumor (number of photons available for detection); and
3. the ratio between the radioactivity in the tumor and in the blood and between the tumor and the surrounding tissue (the degree of contrast between the tumor and background radiation)[146].

These parameters were determined as a function of time after injection of the radiolabelled analogues. The chemical identity of the radioactivity in the tumor and background tissues was not determined because the gamma-camera cannot distinguish between the initial chemical form of the injected radioactivity and any metabolites which retain the radioactive label[10].

a. Animal Tumor Models

i. Lewis Lung Carcinoma

The Lewis lung tumor model has been used for screening of chemotherapeutic agents by the U.S. National Cancer Institute [147]. The Lewis lung carcinoma originated spontaneously as a carcinoma of the lung in a C57BL mouse. It is a rapidly growing tumor of the epidermoid carcinoma type. A solid tumor is formed after subpannicular transplantation of a small piece of the tumor [148].

The Lewis lung carcinoma tumor model used in these studies was donated by Dr. A.R.P. Paterson of the McEachern Laboratory, University of Alberta. The tumor line was maintained in young adult (20-25 g) male, BDF_1 hybrid mice as a solid tumor [148]. A donor mouse bearing the solid tumor was sacrificed by cervical dislocation and the tumor mass was excised and submerged in sterile physiological saline. A fragment of the tumor was inserted subpannicularly in the pectoral region of an anesthetized (diethyl ether) mouse with a trochar [148a]. Tumors were re-transplanted in a ten to twelve day cycle for maintenance and eight to ten days in advance for tissue distribution studies.

ii. Walker 256 Carcinoma

The Walker 256 carcinoma originated spontaneously as a mammary adenocarcinoma in a female rat. It is a hardy tumor and can be maintained in a variety of rat strains as a solid tumor [149]. The Walker 256 tumor model has been used to screen a number of experimental tumor imaging agents [12,150].

The Walker 256 carcinosarcoma tumor model was maintained by the Central Animal Laboratory of the German Cancer Research Center in Heidelberg. Young, male, Wistar rats (200-250 g), inoculated either subpannicularly in the upper dorsal region or intramuscularly in the right hind muscle group were obtained directly from the animal center. Approximately 10^7 cells were transplanted for each tumor, five to seven days before use.

b. Tissue Samples

Thirty seconds before expiration of the time interval, each animal (rat or mouse) was anesthetized with ether, exsanguinated by cardiac puncture, then sacrificed by cervical dislocation. The tissues of interest were excised in their entirety, blotted free of blood and weighed. The whole organ or aliquots thereof were prepared for analysis as described specifically for each analogue tested. The muscle tissue samples consisted of specimens from the front and rear muscle groups of the hind leg contralateral to the tumor bearing leg. The femur from the same leg

was taken as the bone sample. Thyroid uptake of radioiodide was blocked by administering 1% potassium iodide in the drinking water 48 hours prior to injection of radioiodide labelled compounds[151], unless otherwise stated. Skin samples were obtained from the back of the animal to decrease the possibility of urinary contamination during handling.

c. 6-[^{3}H]-2'-Fluoro-2'-deoxyuridine

The 6-[^{3}H]-2'-fluoro-2'-deoxyuridine (42.6 GBq mmol^{-1}) was generously prepared for this study by J.R. Mercer. Five male Wistar rats bearing Walker 256 carcinomas were used for each time period. Each rat was injected with 0.15 MBq (3.5 pmol) of 6-[^{3}H]-2'-FUdR in 0.4 ml normal saline intravenously via a tail vein. Aliquots of each tissue (approximately 100 mg) were accurately weighed directly in glass lsc vials and immersed in Soluene-350™ tissue solubilizer (2.0 ml). Each sample was heated at 50°C in a water bath until a clear solution, free from particulate matter, was obtained. Upon cooling to ambient temperature, the samples were dissolved in 15 ml of a liquid scintillation cocktail consisting of diphenyloxazole (4.0 g l^{-1}) and p-bis-[2-(5-phenyl-oxazolyl)]benzene (50 mg l^{-1}) in toluene (TPP). Blood samples were digested in 2.0 ml Soluene-350™-isopropanol (1:1 v/v) at 50°C, then decolorized with 30% hydrogen peroxide (0.2 ml). The solubilized sample was then dissolved in 15 ml of a mixture of Instagel™-isopropanol (9:1 v/v) liquid scintillation cocktail.

The standards for the tissue sample quench correction curve were prepared using a tritiated water standard dissolved in Soluene-350™ and added to the TPP fluor. Each standard was quenched with a blood and liver homogenate (1:1 w/w) solubilized in Soluene-350™. The standard curve for the blood samples was prepared with tritiated water in Instagel™-isopropanol (9:1 v/v). The standards were quenched with whole blood solubilized in Soluene-350™ and decolorized with 30% hydrogen peroxide.

The samples and standards were counted with a Berthold BF 5000/300 HP9825 liquid scintillation spectrometer. Counting efficiency and background correction calculations were determined automatically.

d. 2'-[^{36}Cl]-Chloro-2'-deoxyuridine

2'-[^{36}Cl]-Chloro-2'-deoxyuridine (5.66 MBq mmol^{-1}) was purified by preparative cc as described elsewhere (III.C.2.d) and stored as a solution in sterile normal saline (77.3 kBq ml^{-1}). Analytical tlc and rp-hplc indicated a minimum radiochemical purity of 97.6 and 99.5% respectively at the time of use.

Six BDF_1 mice bearing Lewis lung carcinomas were used at each time interval studied. Each mouse was injected intravenously with 7.78 kBq of 2'-[^{36}Cl]-ClUdR (1.37 μmol) in 0.1 ml normal saline.

The excised tissues were weighed directly in glass lsc vials. The entire heart, lungs, spleen, kidney, testis, tibia and femur were wetted with distilled water (0.2 ml), immersed in NCS™ (1.5-2.0 ml) tissue solubilizer and heated at 50°C until a clear solution was obtained. Aliquots (approximately 100 mg) of liver, tumor and muscle were treated as described above. The samples were cooled to ambient temperature, dissolved in Riafluor™ liquid scintillation fluor (15 ml) and neutralized with a mixture of 4% aqueous $SnCl_2$ and acetic acid (1:1 v/v) to decrease chemiluminescence.

Blood samples (approximately 100 mg) were lysed with distilled water (0.2 ml), digested in NCS™ (1.0 ml) at 50°C for 1 hour and decolorized with 30% hydrogen peroxide (0.2 ml). The blood samples were then treated as described for the tissue samples.

Urine samples were collected by excising the intact bladder and transferring it and the contents to an lsc vial. Aliquots (5 μl) of urine were analyzed directly by tlc (chloroform-ethanol, 2:1 v/v). The plates were visualized under uv, the radioactivity cochromatographing with authentic 2'-ClUdR was isolated, and the remainder of the chromatogram was divided into 1 cm sections. The distribution of radioactivity on the plate was determined as described in section III.B.2. The urine remaining was diluted with distilled water (0.2 ml) and counted directly in Riafluor™ (15 ml).

The standards required for the quench correction curve were prepared with aqueous sodium chloride-36 dissolved in Riafluor™ and were quenched with blood solubilized in NCS™. The counting

efficiency of an unquenched sample of ^{36}Cl was assumed to be approximately 100%[152,153] and the quenched samples were normalized to the unquenched sample count rate. The samples were counted with a Beckman LS9000 liquid scintillation spectrometer, which determined the counting efficiency and background correction automatically.

e. 2'-[^{123}I]-Iodo-2'-deoxyuridine

i. Tissue Distribution

2'-[^{123}I]-Iodo-2'-deoxyuridine was purified prior to use by preparative tlc (silica gel) using chloroform-ethanol (4:1 v/v) to remove organic impurities. An aqueous solution of the purified product was passed through a AgCl/cellulose (5% w/w) column to remove any free iodide-123 remaining. Analytical micro tlc (silica gel) with chloroform-ethanol (4:1 v/v) as development solvent indicated a radiochemical purity greater than 99.0%.

Three male Wistar rats bearing Walker 256 tumors inoculated intramuscularly in the right hind leg muscle group were used for each time period studied. Each rat was injected with 1.48 MBq of 2'-[^{123}I]-IUdR (0.63 TBq mmol^{-1}; 2.35 pmol at time of injection) via the tail vein. The tissue samples were weighed directly in plastic gamma counting tubes. The samples were counted on a Tracor TN-11™ high resolution gamma ray spectrometer programmed to correct for background and decay.

ii. Whole Body Excretion

Three rats were injected with 1.67 MBq of 2'-[^{123}I]-IUdR intravenously. The urine and whole body elimination profile of 2'-[^{123}I]-IUdR was monitored by determining the whole body radioactivity remaining, after the rats were induced to micturate, at various time intervals following injection. The whole body radioactivity was measured at the designated time intervals with a Capintec™ dose calibrator. A measurement obtained 30 seconds after injection was set as time zero and all subsequent measurements were normalized to this time and activity. Aliquots of the urine collected after micturition were diluted with non-radioactive 2'-IUdR and analyzed directly by micro tlc (silica gel) with chloroform-ethanol (2:1 v/v) as the development solvent. The chromatograms were visualized under uv light and scanned for qualitative distribution of radioactivity with a Berthold chromatogram scanner. The appropriate sections of the chromatograms were collected and quantitatively analyzed by gamma spectrometry with a NaI(Tl) well detector.

f. 6-[^{123}I]-Iodouracil

6-[^{123}I]-Iodouracil was purified the evening before use by preparative silica gel tlc using chloroform-ethanol (4:1 v/v) as the development solvent, then refrigerated in a dry state until use. The product was dissolved in water and passed through a AgCl/DEAE cellulose column immediately prior to use. Analytical

tlc (chloroform-ethanol 2:1 or 4:1 v/v) indicated a radiochemical purity greater than 99%.

Each rat, bearing a Walker 256 tumor, was injected with 1.85 MBq of 6-[^{123}I]-iodouracil (2.54 GBq mmol^{-1} at the time of injection). The tissue samples were prepared and analyzed as described for the 2'-[^{123}I]-IUdR study with the exception that prior to anesthesia, micturition was induced and the urine collected on glass plates. The urine was applied directly to minicolumns of AgCl/cellulose (2 cm in 1 ml tuberculin syringe) and eluted with distilled water (0.5 ml) to remove free iodide-123. The eluate, after the addition of carrier 6-iodouracil, was analyzed directly by tlc (silica gel) with chloroform-ethanol (2:1 v/v) as the development solvent. The plates were visualized under uv light to locate the 6-iodouracil standard. Those plates containing sufficient activity were scanned with the chromatogram scanner to determine the qualitative radioactivity distribution profile. The chromatograms were then divided into sections and the radioactivity in each section measured by gamma spectroscopy (NaI(Tl) well crystal). The radioactivity on AgCl/cellulose columns and in the remaining column eluate was measured in a similar manner.

g. Co-administration of 6-[^{123}I]-Iodouracil and 6-Chlorouracil

6-[^{123}I]-Iodouracil (8.02 GBq mmol^{-1} at time of injection) was purified as described in section III.C.3.e to remove organic impurities other than 6-chlorouracil. Analytical radio-tlc

(ethylacetate-ethanol, 4:1 v/v and chloroform-ethanol, 4:1 v/v) indicated a radiochemical purity of greater than 99%. The relative concentrations of 6-iodouracil and 6-chlorouracil in the injection solution were determined by quantitative rp-hplc (water-methanol, 9:1 v/v).

Three rats bearing Walker 256 tumors were studied at each time interval. Each rat was injected with 0.09 μmol 6-[^{123}I]-iodouracil (0.74 MBq) and 0.03 μmol 6-chlorouracil in 0.5 ml normal saline. Tissue samples were prepared and analyzed as described for 2'-[^{123}I]-IUdR.

h. Whole Body Excretion of Sodium Iodide-123

Sodium iodide-123 was obtained as described (III.C.1.e) with the exception that an aqueous solution of 0.1 N sodium hydroxide was used to recover the ^{123}I without added carrier. For whole body elimination studies, 1.67 MBq of sodium iodide-123 in normal saline was injected intravenously into three normal male Wistar rats. The time zero measurements were made 30 seconds after injection as described for 2'-[^{123}I]-IUdR and the remaining measurements were taken after micturition was induced.

4. Whole Body Imaging

a. 2'-[^{123}I]-Iodo-2'-deoxyuridine

Non-invasive, qualitative tissue distribution studies were performed with a Searle HP gamma camera fitted with a pinhole

collimator. The rats were initially anesthetized with ether and positioned under the gamma camera. Rats bearing subpannicular Walker 256 tumors in the upper dorsal region were positioned to present a dorsal view, thereby elevating the tumor, while rats bearing intramuscular tumors in the hind leg were imaged from the dorsal aspect with the legs spread apart and the tumor somewhat isolated from the body. During the imaging procedure, the rats were maintained under nitrous oxide/halothane/oxygen anesthesia and body temperature was kept constant with an electric heating pad.

A continuous dynamic image was recorded on magnetic tape for the initial 30 to 60 minutes post injection. Static images were recorded (10^5 counts image^{-1}) at longer time periods on both Polaroid film and magnetic tape. The camera was activated just prior to intravenous injection of the 2'-[^{123}I]-IUdR (12.0-14.8 MBq; 23.5 pmol).

b. <u>6-[^{123}I]-Iodouracil</u>

Non-invasive distribution studies with 6-[^{123}I]-iodouracil were performed essentially as described for 2'-[^{123}I]-IUdR. Dynamic and static images were recorded after intravenous injection of 17.04 MBq of 6-[^{123}I]-iodouracil (7.2 μmol) in Wistar rats bearing Walker 256 carcinomas.

c. Sodium Iodide-123

The no carrier added ^{123}I was obtained as a sterile normal saline solution from Dr. Sinn of the Radiopharmacology Department of the German Cancer Research Center.

The qualitative whole body distribution of sodium iodide-123 was determined in one normal male Wistar rat and two rats bearing a Walker 256 carcinoma in either the right hind leg (intramuscular) or the upper dorsal region (subpannicular). The animals were anesthetized and positioned for imaging as described for 2'-[^{123}I]-IUdR. A dynamic image was recorded during the initial 45 minutes following intravenous injection of sodium iodide-123 (26.3-28.5 MBq) and static images (10^5 counts image^{-1}) were obtained thereafter.

IV. RESULTS AND DISCUSSION

A. Radionuclide Production

Most radionuclides can be produced by more than one nuclear reaction. The ultimate use of the product is an important consideration in selecting the production methodology. The yield, specific activity and radionuclidic purity required of the product, the complexity of the chemistry required to synthesize the product and the half-life of the radionuclide must be balanced against the availability of particle type and particle energy required by the nuclear reaction, the cost of the target material and handling and recovery of the radionuclide[154].

All of the radionuclides used in this study, with the exception of ^{18}F and ^{34m}Cl, were routinely available in a chemical form directly applicable to the synthesis of the radiohalogenated nucleosides and pyrimidines. The preparation of the short-lived radionuclides, ^{82}Br and ^{123}I, required only minor modification of routine procedures as described in the experimental section (III.C.1) whereas ^{36}Cl and ^{125}I were available commercially. It was therefore necessary to examine the feasibility of a number of different nuclear reactions for the production and recovery of ^{18}F and ^{34m}Cl.

1. Fluorine-18

Aqueous fluoride-18 was routinely prepared as a solution in normal saline intended for clinical use. The nucleophilicity of ^{18}F anion produced in this way is greatly reduced due to hydration of the fluoride anion and the formation of strong hydrogen bonds in protic solvents[32]. Therefore aqueous solutions of ^{18}F were unsuitable for the chemical applications described in this thesis. The conversion of the aqueous

^{18}F anion, produced in this manner, to anhydrous hydrogen fluoride by distillation from hot concentrated sulphuric acid was largely unsuccessful. Although hydrogen fluoride-18 was recovered after distillation in moderate yield (Table III), the product was not suitable for fluorination of 2,2'-cyclouridine. The best radiochemical yield was obtained when ^{18}F

Table III. Recovery of ^{18}F Via Distillation Techniques.

Nuclear Reaction	Target Material	Recovery Methods	Recovery[1] (%)
$^{20}Ne(d,\alpha)^{18}F$	Neon gas	Recovered in normal saline and distilled directly from concentrated sulphuric acid	54.7
$^{20}Ne(d,\alpha)^{18}F$	Neon gas	Recovered in water, diluted with potassium fluoride, dried and distilled from sulphuric acid	32.2 ± 12.4
$^{6}Li(n,^{3}H)^{4}He$, $^{16}O(^{3}H,n)^{18}F$	Li_2CO_3 (95% ^{6}Li)	Anhydrous Li_2CO_3 distilled directly from 95% sulphuric acid	2.1 ± 0.7

1. Yield calculated as the % recovered in the distillate from the total activity added to the sulphuric acid.

was recovered from the target in normal saline and distilled directly from hot sulphuric acid. The ^{18}F recovered, however, was not anhydrous and contained large concentrations of chloride ion. The recovery of ^{18}F in distilled water rather than normal saline, followed by the evaporation of water in the presence of carrier potassium fluoride, did not completely eliminate the problem of contamination by either

water or chloride. This conclusion was based upon the presence of ara-U and 2'-ClUdR peaks in the rp-hplc trace of the final reaction product. The presence of chloride contamination was most likely due to incomplete removal of the sodium chloride from the target. Recovery of anhydrous hydrogen fluoride-18 from aqueous ^{18}F was inefficient and time consuming.

A second method employed reactor produced ^{18}F via the $^{6}Li(n,^{3}H)^{4}He$, $^{16}O(^{3}H,n)^{18}F$ nuclear reactions. Lithium carbonate was irradiated as an anhydrous salt and the ^{18}F produced was distilled directly from hot sulphuric acid in a stream of helium carrier gas. The recovery of ^{18}F with this method was also inefficient and unsatisfactory (Table III). Similar results have been reported concerning the distillation of ^{18}F from sulphuric acid. Nozaki et al.[116] reported that it was necessary to vigorously agitate the sulphuric acid solution with 3-5 g min^{-1} of steam in order to remove the ^{18}F. The ^{18}F was subsequently trapped on an anion exchange resin. The resin was dried and the ^{18}F was eluted with carrier anhydrous hydrogen fluoride. The method produced a product which had a low specific activity and was not completely anhydrous. Others[117,121] also found it necessary to use aqueous sulphuric acid and high flow rates of an agitating gas to remove the ^{18}F during the distillation. In these instances the recovered ^{18}F required drying before subsequent use. Gnade et al.[118] recently reported a method whereby ^{18}F could be recovered as anhydrous hydrogen fluoride via distillation from sulphuric acid. The method was complex because it required the separation of the ^{18}F from the irradiated lithium carbonate before the distillation step. Azeotropic sulphuric acid (98%) was necessary to prevent the co-distillation of water with the hydrogen fluoride.

In view of these results, recovery of ^{18}F as anhydrous hydrogen fluoride-18 by distillation was discontinued in favor of a faster and more efficient method requiring less sample handling. The feasibility of recovering ^{18}F as anhydrous hydrogen fluoride directly from the cyclotron target after irradiation was therefore investigated. The ^{18}F species produced during such irradiations is known to be highly reactive and to bind tenaciously to the target surface[118,155]. Fluorine-18 can be produced directly or via a parent-daughter system in which ^{18}Ne ($T_{\frac{1}{2}} = 1.7$ sec)[33] decays to ^{18}F[113,114]. The ^{18}Ne should be more readily removed from a target than ^{18}F, since it is chemically inert. Both of these production methods were investigated.

Initially the irradiation of ^{16}O (natural isotopic abundance) containing targets with ^{3}He particles was investigated (Table IV). Fluorine-18 was produced directly via the $^{16}O(^{3}He,p)^{18}F$ and $^{18}O(^{3}He,^{3}H)^{18}F$ reactions and indirectly via the $^{16}O(^{3}He,n)^{18}Ne \xrightarrow{\beta^+} {}^{18}F$ reaction[121]. No detectable amount of ^{18}F was removed from the target during the irradiation of a continuous flow of oxygen gas and only a trace of ^{18}F was recovered using a solid tantalum pentoxide target swept with helium gas. In spite of the fact that flow rates up to 500 ml min^{-1} of target gas were used, the major radionuclides removed, without the addition of carrier hydrogen fluoride, were β^+ emitters which had half-lives of 125.7 ± 2.0 s and 20.4 ± 0.4 min. These half-lives corresponded well with those of ^{15}O ($T_{\frac{1}{2}} = 124$ sec) and ^{11}C ($T_{\frac{1}{2}} = 20.3$ min) respectively[33], which were possible contaminants produced via the $^{16}O(^{3}He,\alpha)^{15}O$ and $^{16}O(^{3}He,2\alpha)^{11}C$ nuclear reactions (Table V)[112].

TABLE IV. Recovery of ^{18}F Via Gas Flow Techniques.

Nuclear Reaction	Target Material	Recovery Methods	Recovery[1] (%)
$^{16}O(^{3}He,n)^{18}Ne$ $^{16}O(^{3}He,p)^{18}F$	O_2 gas	Continuous flow of O_2 during the irradiation	trace
$^{16}O(^{3}He,^{3}H)^{18}F$	Ta_2O_5	Helium swept over the Ta_2O_5 during the irradiation	trace
$^{20}Ne(d,\alpha)^{18}F$	Neon gas	Target[2] passivated at 110°C with anhydrous HF (100%) for 48 hr	
		a. Anhydrous HF (46 mg) was passed through the target after irradiation	51.8
		b. Anhydrous HF (16 mg) was passed through the target during and after irradiation	28.8
$^{20}Ne(d,\alpha)^{18}F$	Neon gas	Target[2] passivated at 110°C with F_2 (25% in neon) for 48 hr	
		a. Anhydrous HF (12 mg) was passed through the target during and after irradiation	59.5
$^{20}Ne(d,\alpha)^{18}F$	Neon gas	Target[3] not passivated	
		a. Anhydrous HF (2 mg) was passed through the target after irradiation	37.0
		b. Anhydrous HF (7.2 mg) was passed through the target after irradiation	31.5
		c. Anhydrous HF (53 mg) was passed through the target after irradiation	69.3

1. Yields normalized to the recovery obtained routinely for clinical use using the rotating quartz liner (0.63 GBq μA^{-1} h^{-1}).

2. Stainless steel target with stainless steel liner and 15 ml volume.

3. Stainless steel unlined target with 100 ml volume.

TABLE V. Possible Interfering Nuclear Reactions with the $^{16}O(^{3}He,n)^{18}Ne$ and $^{20}Ne(d,\alpha)^{18}F$ Reactions[113,157]

Target Nucleus	Reaction	Product Nucleus	Decay Mode	$T_{\frac{1}{2}}$	Q Value
^{16}O	$^{3}He,\alpha$	^{15}O	β^{+}	123.6 s	4.823
^{16}O	$^{3}He,2\alpha$	^{11}C	β^{+}	20.3 min	- 5.3
^{16}O	$^{3}He,\alpha pn$	^{13}N	β^{+}	9.96 min	-12.9
^{18}O	$^{3}He,2n$	^{19}Ne	β^{+}	18 s	- 3.75
^{18}O	$^{3}He,^{6}Li$	^{15}O	β^{+}	123.6 s	- 6.31
^{18}O	$^{3}He,^{10}Be$	^{11}C	β^{+}	20.3 min	- 9.11
^{18}O	$^{3}He,^{8}Li$	^{13}N	β^{+}	9.96 min	-12.41
^{20}Ne	d,n	^{21}Na	β^{+},γ	22.8 s	
^{22}Ne	d,2n	^{22}Na	β^{+},γ	2.60 yr	

The inability to remove more than trace amounts of ^{18}F from the target may be explained in part by the fact that only 5% of the total yield of ^{18}F produced by ^{3}He irradiation of oxygen is derived from the decay of ^{18}Ne to ^{18}F[156]. Furthermore, the very short half-life of ^{18}Ne may have required higher flow rates than those used in order to remove an appreciable fraction of the ^{18}Ne produced before it decayed to ^{18}F[157]. These high flow rates were not conducive to trapping the ^{18}F in on-line, small volume liquid traps. Others[116] have also found that ^{18}F produced during the irradiation of oxygen gas with ^{3}He or ^{4}He particles remained in the target until carrier anhydrous hydrogen fluoride was added to the target.

The $^{20}Ne(d,\alpha)^{18}F$ reaction was selected for further investigation because it would afford the highest radiochemical yield, with the exception of the $^{18}O(p,n)^{18}F$ reaction[124]. In addition the neon would act as a chemically inert carrier which would aid in the recovery of ^{18}F from the target.

The recovery values given in Table IV are normalized to the yield (0.63 GBq μA^{-1} h^{-1}) recovered from the rotating target during the routine production of ^{18}F under optimum conditions. The facilities necessary to passivate the targets, as suggested by Lambrecht et al.[114] were not available. However targets which were treated with either elemental fluorine (150 kPa of 25% fluorine in neon) or anhydrous hydrogen fluoride (100 kPa of 100% anhydrous hydrogen fluoride) at 110°C did produce higher recoveries than non-treated targets. The data, however, are not directly comparable between treated and non-treated targets because the operating parameters varied from experiment to experiment.

The ^{18}F recovered was analyzed by γ-spectroscopy with a Ge(Li) detector. Analysis of the 0.511 MeV annihilation γ-line indicated the mean half-life was 111.2 ± 3.5 minutes, which compares favourably with the published value of 109.9 minutes[4] for ^{18}F. Sodium-21, produced by low energy deuterons via the $^{20}Ne(d,n)^{21}Na$ reaction[142], was not detected since it would have decayed prior to analysis due to its short half-life ($T_{\frac{1}{2}}$ = 22.8 s) [33]. The 1.27 MeV gamma line of ^{22}Na, produced via the $^{22}Ne(d,2n)^{22}Na$ reaction, was also absent from the spectrum (Table V). No gamma lines, other than 0.511 MeV annihilation γ's, were observed.

2. Chlorine-34m

Several different approaches to the production of ^{34m}Cl and its recovery from the target system were investigated. The feasibility of using the $^{35}Cl(p,pn)^{34m}Cl$ nuclear reaction was investigated because this reaction is known to produce ^{34m}Cl in high yield[34]. Accordingly, a solid disk of magnesium chloride (natural isotopic abundance, 75.55% ^{35}Cl)[33] was irradiated with 22 MeV protons, producing ^{34m}Cl in good yield. Unfortunately the large mass of magnesium chloride (200 mg) required for a solid target diluted the specific activity of the final product to an unacceptable level (96.2 kBq mg^{-1} magnesium chloride). Various methods[131-135] of separating ^{34m}Cl from the target material to increase the final specific activity to a more acceptable level were considered. In view of the 32 minute half-life of ^{34m}Cl, the relatively long and complex separation techniques and low overall radiochemical yields obtained, these procedures did not represent an attractive solution to the problem.

A more attractive alternative seemed to be the $^{34}S(p,n)^{34m}Cl$ and $^{34}S(d,2n)^{34m}Cl$ nuclear reactions, in which ^{34m}Cl is produced directly by nuclear transformation, without added carrier. These reactions produce ^{34m}Cl in appreciable yields using natural isotopic abundance (4.21% ^{34}S)[33] sulfur containing targets. Therefore, an expensive isotopically enriched target was not required for the developmental work. The target and recovery system (Figure 7, III.c.ii) developed for the production of ^{34m}Cl was conceptually similar to the system used for ^{18}F production. Hydrogen sulfide was chosen as the target

material because it is a gas and could be readily handled with the existing techniques.

The data in Table VI compare the radiochemical yields of ^{34m}Cl obtained under various experimental conditions. The recovery values (MBq μA^{-1} h^{-1}) were determined by quantitative analysis[158] of the 0.145 and 1.17 MeV γ-lines characteristic of ^{34m}Cl with a Ge(Li) detector. The 0.511 MeV annihilation γ-line was not included in the analysis as this line contains contributions from both ^{34m}Cl and ^{34}Cl as well as other possible positron emitting contaminants. Equation 4 was used to correct for the decay which had occurred during the irradiation, in order that the various irradiations could be compared.

$$Y = \frac{\lambda . A}{I(1-e^{-\lambda t})} \qquad \text{Equation 4}$$

In equation 4 Y is the thick target yield in dps μA^{-1} h^{-1}, A is the activity of the radionuclide, in dps, determined at the end of irradiation, I is the irradiation current in μA, t is the length of time of the irradiation and λ is the decay constant of the radionuclide. The theoretical yield for each reaction was calculated from the results reported by Zatolokin et al.[138]. The variations in the percentage of ^{34m}Cl recovered, using different production parameters, are best explained by changes in the target gas pressure and the precipitation of elemental sulfur during irradiation. An increase in the hydrogen sulfide pressure inside the target would be expected to enhance ^{34m}Cl production by

TABLE VI. Radiochemical Yields of ^{34m}Cl

Target[1] Material	Nuclear Reaction	Target Pressure (kPa)	Resin Counter-ion	Beam Intensity (μA)	Time of Irradiation (min)	Theoretical[2] Yield (%)	Activity Recovered (MBq μA^{-1} h^{-1})
H_2S	$^{34}S(p,n)^{34m}Cl$	400	Cl^-	4	30	14.4	13.0
		150	Cl^-	1	10	3.8	3.42
		150	OAc^-	1	10	3.4	3.03
H_2S	$^{34}S(d,2n)^{34m}Cl$	400	Cl^-	4.5	30		0.54
		200	Cl^-	1.5	10		0.23

1. Target material was of natural isotopic abundance; 4.21% ^{34}S[33].

2. Theoretical yield was calculated from the data reported by Zatolokin et al.[138].

increasing the effective cross-section and the stopping power of the target. The absolute yield of ^{34m}Cl would increase until the target could stop all of the proton beam, within the energy range covering the reaction cross-section (thick target). The thick target pressure of hydrogen sulfide for this target system was estimated at 700 kPa for 22 MeV protons and 200 kPa for 12 MeV deuterons[159]. The higher target pressure also allowed a larger proportion of the target volume to be removed during recovery of the target gas. During the recovery of ^{34m}Cl from the target, the residual hydrogen sulfide remaining in the target after atmospheric pressure was reached was not removed. The hydrogen sulfide was oxidized to elemental sulfur during irradiation and it was necessary to release the target gas slowly from the target or the precipitated sulfur particles would block the Quick Connectors™ and ion exchange column in the recovery system. Addition of a carrier gas was found to aggravate the problem. Therefore the target was allowed to reach equilibrium with atmospheric pressure and the remaining radioactivity was not recovered. The precipitation of elemental sulfur during irradiation also resulted in a concommitant reduction of hydrogen sulfide pressure in the target, thereby reducing the effective cross-section of the target. The recovery of ^{34m}Cl may have been further complicated by the formation of sulfur chlorides during the irradiation, which would have co-precipitated with the elemental sulfur[160].

The reaction products were analyzed and the radiochemical purity determined with a Ge(Li) detector. The spectra obtained for the $^{34}S(p,n)^{34m}Cl$ and $^{34}S(d,2n)^{34m}Cl$ reaction products were free from gamma lines which were not attributable to ^{34m}Cl or ^{34}Cl. The only interfering gamma line detected in the $^{35}Cl(p,pn)^{34m}Cl$ reaction

product spectrum was observed at 1.367 MeV. This gamma line corresponded to ^{24}Na arising from the $^{25}Mg(p,2p)^{24}Na$[161] or the $^{26}Mg(p,^{3}He)^{24}Na$[162] nuclear reactions which could occur at the proton energies used.

The half-lives of the reaction products were determined with either a Ge(Li) detector or a dose calibrator. Data collected with a Ge(Li) detector required long counting times and were corrected for decay occurring during the counting period with equation 5[163]:

$$T = {}^{1}/_{\lambda} \ln \frac{\lambda(t_2 - t_1)}{1-e^{-\lambda(t_2-t_1)}} \qquad \text{Equation 5}$$

where T is the corrected time for the observed counts, λ is the decay constant of the radionuclide and $t_2 - t_1$ is the counting time of the sample. A comparison of the half-life values determined for the product of each nuclear reaction is given in Table VII. These experimental values agree closely with the accepted half-life of 32.0 minutes[33].

TABLE VII. Observed Half-Lives for ^{34m}Cl

Target[1] Material	Nuclear Reaction	Analytical Method	Observed Half-Life (min)
$MgCl_2$	$^{35}Cl(p,pn)^{34m}Cl$	Ge(Li)	32.1
H_2S	$^{34}S(p,n)^{34m}Cl$	Ge(Li)	32.4
		Dose Calibrator	31.7
H_2S	$^{34}S(d,2n)^{34m}Cl$	Ge(Li)	34.5

1. Target material was of natural isotopic abundance, 75.77% ^{35}Cl and 4.21% ^{34}S[33].

3. Bromine-82

Bromine-82 ($T_{\frac{1}{2}} = 35.3$ h) labelled 2'-BrUdR was prepared as described by Lee et al.[143,164] by direct neutron activation of the brominated precursor (III.C.1.d). This labelling technique was complicated by Szilard-Chalmers cleavage and thermal and radiolytic decomposition of the product. The free bromide-82 formed via the Szilard-Chalmers process during irradiation was efficiently removed by elution of an aqueous solution of the product through a mini-column of AgCl impregnated cellulose. The thermal and radiolytic decomposition products were readily separated from 2'-[^{82}Br]-BrUdR by rp-hplc which was also used to simultaneously determine the relative specific activity of the product. The specific activity varied with the time and intensity of neutron irradiation of the sample. The radiochemical purity of the final 2'-[^{82}Br]-BrUdR was greater than 99%.

The radionuclidic purity of the product was monitored with a Tracor 2200 gamma spectrometer and multichannel analyzer. Neutron activation of natural isotopic abundance Br produced four bromine radioisotopes concommitantly. The ^{79}Br(n,γ) nuclear reaction produced ^{80}Br ($T_{\frac{1}{2}} = 17.7$ min) and ^{80m}Br ($T_{\frac{1}{2}} = 4.42$ h) while ^{82}Br and ^{82m}Br ($T_{\frac{1}{2}} = 6.05$ min) arose from the ^{81}Br(n,γ)^{82}Br/^{82m}Br reaction[33]. Analysis of the irradiated product, after allowing sufficient time for the total decay of ^{80m}Br, revealed no γ-peaks not attributable to ^{82}Br.

B. Synthesis of 6-Halouracil Analogues

Nucleophilic displacement of a halogen atom provides a facile route to C-2, C-4 and C-6 substituted pyrimidines[39,87]. Chlorine, bromine and iodine are displaced in aromatic nucleophilic substitution reactions with approximately equal facility. The usual order of reactivity is Cl > Br > I, which is opposite the normal order observed in nucleophilic substitutions. This reversed order of reactivity is explained by the fact that the formation of the intermediate-complex during the reaction is the rate-limiting step and this process is promoted by groups with strong -I (electron withdrawing) effects[165]. Therefore 6-chlorouracil (5b) and 6-iodouracil (5d) were selected as precursors for the synthesis of 6-[^{123}I]-iodouracil and 6-[^{36}Cl]-chlorouracil respectively (Scheme 7). The stable starting materials were synthesized according to the procedures reported by Horwitz and Tomson[64]. Details of the stable syntheses and reaction products will not be discussed in detail except where they are relevant to the labelling reactions.

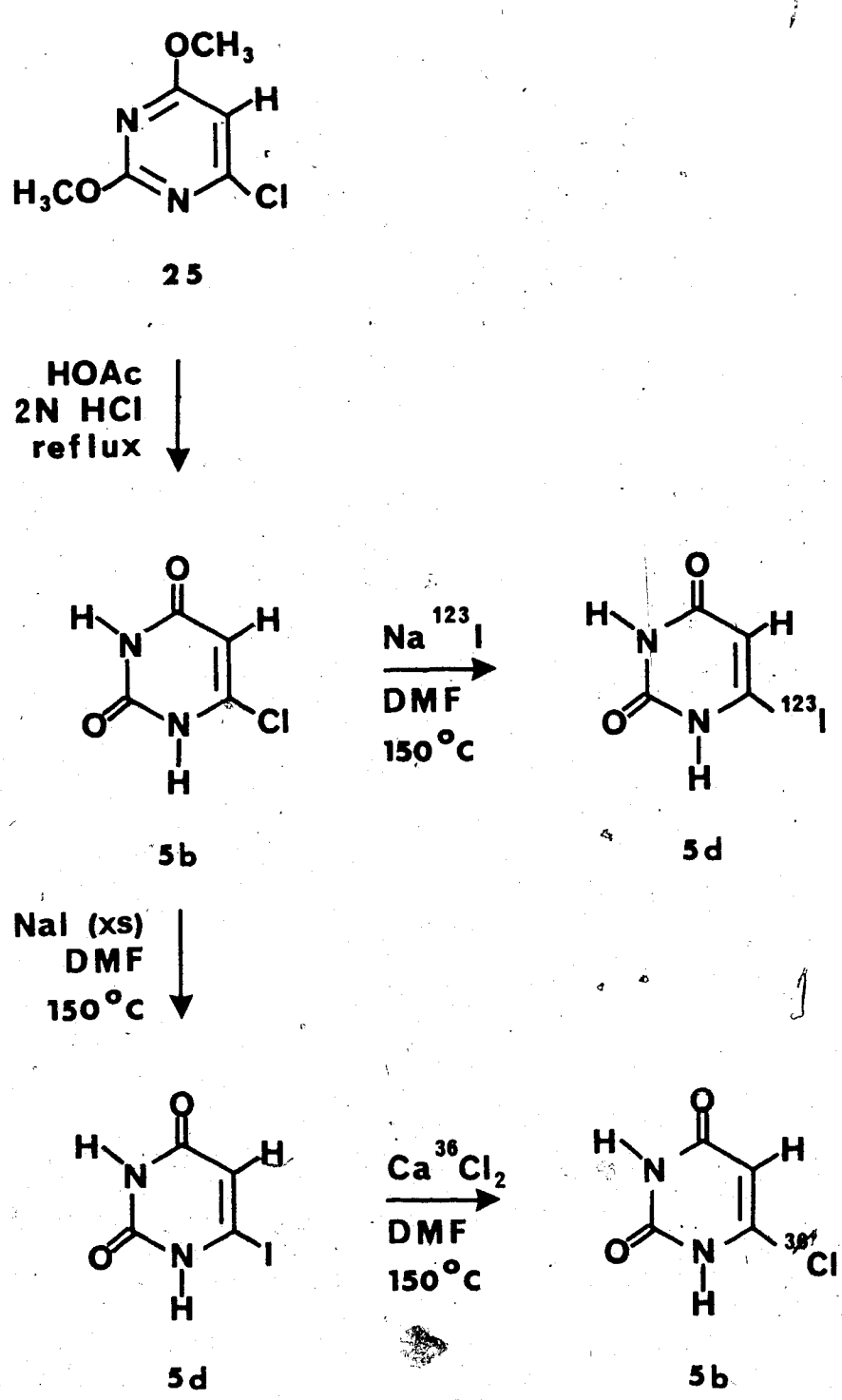

Scheme 7. Synthesis of 6-[^{123}I]-iodouracil and 6-[^{36}Cl]-chlorouracil.

1. 6-[^{36}Cl]-Chlorouracil (5b)

6-Iodouracil (5d) was selected as the precursor for the synthesis of 6-[^{36}Cl]-chlorouracil (5b) rather than 6-bromouracil (5c) since 6-chlorouracil was more readily separated from 6-iodouracil than from 6-bromouracil. Initial attempts to synthesize 5b by the reaction of equimolar amounts of sodium chloride and 5d in dimethylformamide yielded only trace quantities of 5b. This was probably due to the low solubility of sodium chloride in dimethylformamide. Halogen-halogen exchange reactions reach an equilibrium which can be shifted in the direction of the product by using an excess of the desired halide. This was not acceptable, as a molar excess of carrier nucleophile would have resulted in an inherent reduction in the radiochemical yield and specific activity of the product. The use of a chloride salt which is more soluble in the reaction solvent than the iodide salt would provide another method for shifting the equilibrium in the desired direction. With this in mind, equimolar quantities of anhydrous ferric chloride were reacted with 6-iodouracil. Unfortunately, this reaction gave a complex mixture of reaction products from which it was difficult to separate the desired 6-chlorouracil. The complex reaction mixture probably resulted from side reactions due to the oxidizing potential of ferric chloride[166]. On the other hand, reaction of anhydrous calcium chloride with 5d in dimethylformamide afforded 6-chlorouracil in greater than 60% chemical yield. This procedure was therefore used to prepare 6-[^{36}Cl]-chlorouracil.

A preliminary experiment (Table VIII) indicated than an optimum radiochemical yield was obtained within 30 minutes using equimolar

quantities of reactants. Calcium chloride-36 was prepared quantitatively by the titration of calcium hydroxide with an aqueous solution of hydrogen chloride-36 and evaporated to dryness *in vacuo* at 85°C. The anhydrous calcium chloride-36 was allowed to react with 6-iodouracil in dimethylformamide for 30 minutes to give the ^{36}Cl labelled 5b in 77% radiochemical yield. The identity of the product as 6-[^{36}Cl]-chlorouracil was established by co-chromatography with an authentic sample on silica gel tlc and rp-hplc. The 6-[^{36}Cl]-chlorouracil was readily separated from 6-iodouracil using preparative-cc (silica gel).

2. 6-[^{123}I]-Iodouracil (5d)

The synthesis of 6-[^{123}I]-iodouracil (5d) required a modification of the preparative procedure in order to obtain an acceptable specific activity and radiochemical yield. Preliminary experiments indicated

TABLE VIII. Radiochemical Synthesis of 6-[^{36}Cl]-Chlorouracil: Reaction Conditions and Radiochemical Yields.

$Ca^{36}Cl_2$ [μmol]	6-IU [μmol]	Ratio (Cl^-/6-iodouracil)	Temperature °C	Time min	Radiochemical Yield %
38	67	1.1	150°	30	73.1
				60	65.7
				90	54.2
179	333	1.1	152°	31	77.1

the reaction was concentration dependent with respect to iodide (Table IX). The lowest practical concentration of iodide was found to be 2.5 to 3.0 μmol of iodide per μl of dimethylformamide. Reactions using dioxane as solvent were not suitable, possibly due to the low solubility of sodium iodide and 6-chlorouracil. The data from the last experiment in Table IX also suggested that 5d was degraded at high temperatures with time.

The optimum solvent volume for the synthesis of 6-[^{123}I]-iodouracil was approximately 25 μl (Table X). Solvent volumes less than this were difficult to manipulate. Larger volumes unnecessarily diluted the final specific activity of the product due to the increased amount of carrier iodide required to keep the iodide:solvent volume ratio in the optimum range. 6-[^{123}I]-Iodouracil (5d), prepared by the reaction of sodium iodide-123 with 6-chlorouracil (5b) under the conditions outlined in Table X, was separated from unreacted 5b and iodide-123 by preparative-tlc. The relative mobilities of 5d and 5b were very similar and in some experiments it was not possible to remove all of the starting material 5b. The chemical purity of the radioiodinated product 5d was determined by monitoring the uv absorption profile of the radio-rp-hplc eluent. Contamination levels of less than 1% of 6-chlorouracil in the 6-[^{123}I]-iodouracil product (on a molar basis) were readily detected (Figure 6). The radiochemical purity of 5d was determined by radio-tlc which was more efficient than radio-rp-hplc for detecting low levels of radioactive contaminants. The radiochemical purity of 6-[^{123}I]-iodouracil after preparative-tlc was greater than 95%. The residual radioactive impurity which was free iodide-123 was readily removed from

TABLE IX. Synthesis of 6-Iodouracil: Reaction Conditions and Chemical Yields.

NaI µmol	6-ClU µmol	Molar Ratio (I^-/6-Chlorouracil)	Molar Concentration (µmol I^-/µl)	Solvent[1] Volume µl	Reaction Temp °C	Reaction Time min	Chemical[2] Yield %
9.3	11.0	0.84	0.009	1000[3]	160	61	trace
65.3	34.2	1.91	0.065	1000	180	120	trace
159.3	13.7	11.63	0.159	1000	195	56	trace
433	34.2	12.66	0.216	2000	180	60	trace
68.7	67.1	1.02	0.687	100	170	120	20.1
						165	22.0
253	68.5	3.69	2.53	100	160	30	24.2
						60	31.7
855	298	2.87	2.85	300	165	60	63.4
						120	83.5
						180	83.4
74.7	74.6	1.00	2.99	25	180	30	59.0
						60	63.0
						90	53.8
						120	44.4

1. Anhydrous dimethylformamide as solvent.
2. Chemical yields calculated from rp-hplc analysis.
3. Dioxane used as solvent.

TABLE X. Synthesis of 6-[^{123}I]-Iodouracil: Reaction Conditions and Radiochemical Yields.

NaI µmol	6-ClU µmol	Molar Ratio (I^-/6-Chlorouracil)	Molar Concentration (µmol I^-/µl)	Solvent[1] Volume µl	Reaction Temp °C	Reaction Time min	Radiochemical Yield %
56.7	16.4	3.5	2.3	25	140-150	90	2.5
32.1	27.4	1.2	3.2	10	165	65	26.2
81.4	132	0.6	3.3	25	150	113	45.5
79.3	85.6	0.9	3.2	25	150-160	120	51.1
62.1	62.3	1.0	2.5	25	150-160	118	55.4

1. Anhydrous dimethylformamide as solvent.

the final product by a AgCl impregnated DEAE-cellulose column. The final radiochemical purity of the product was greater than 99%. The purified 6-[^{123}I]-iodouracil was quite stable on storage at 4°C as a dry film on the surface of a sealed glass flask. It exhibited only 3% decomposition to free iodide-123 in a twelve hour period.

Solvent: Methanol:Water 9:1 v/v; 1.5 ml min^{-1}; uv detection (254 nm); radioactivity detection (plastic scintillator); chart speed 1 cm min^{-1}; Sil-1-X® C-18 reverse phase column (30 cm x 3.9 mm id).

Trace A: Radioactive detector trace. Peak 1. Iodide-123 in column void volume (4.2% with respect to total ^{123}I activity). Peak 2. 6-[^{123}I]-IU (95.8% radiochemical purity).

Trace B: Ultraviolet detector trace. Peak 1. Column void volume. Peak 2. 6-ClU contaminant (0.7% with respect to 6-IU). Peak 3. 6-IU (99.3% chemical purity).

Figure 6. Radio-rp-hplc Trace of 6-[^{123}I]-Iodouracil After Preparative-tlc.

C. Synthesis of 2'-Halo-2'-deoxyuridine Analogues

Uridine analogues, modified at the C-2' sugar position, are readily prepared by reaction of 2,2'-cyclouridine (21) with the appropriate nucleophile under anhydrous conditions (see II.D.2). The presence of water in the reaction mixture reduces the yield of the desired C-2' sugar substituted product, due to a competing reaction in which water cleaves the 2,2'-anhydro bond by nucleophilic attack at the C-2 of the uracil ring to afford ara-U (23, R = H). Nucleophilic attack at the C-2 of uracil is kinetically favored with respect to attack at the C-2' sugar position because it requires a lower activation energy. When the nucleophile introduced into the C-2 position of uracil is a good leaving group, the reaction is readily reversible *via* attack of the C-2' *arabino* hydroxyl at the C-2 position to reform the 2,2'-cyclonucleoside. When the C-2 substituent is an hydroxyl function, the thermodynamically stable uracil ring is formed, due to tautomerism to the 2,4-diketopyrimidine ring system, and reformation of the cyclonucleoside is not favoured. On the other hand, Sn2 nucleophilic displacement at the C-2' sugar terminus, which requires a higher activation energy, affords a thermodynamically more stable product than attack at the C-2 position. This is due to the formation of the stable uracil ring system and an sp^3 alkyl-nucleophile bond. This latter product is more resistant to recyclization than the C-2 substituted product due to the higher activation energy barrier for the reverse process[167]. Cleavage of the 2,2'-anhydro bond by nucleophilic attack at the C-2' sugar position is facilitated in acidic media, probably due to protonation of the N-3 of the uracil ring[99] (Scheme 6, section E.2.b).

The synthesis and structural characterization of the 2'-halo-2'-deoxyuridine derivatives, first synthesized by Fox et al.[18,71] via reaction of anhydrous hydrogen halides with 2,2'-cyclouridine (21), have been discussed in the literature section. The radiohalogenated analogues (8a-d) were prepared by modification of these reported methods (Scheme 8). The stable analogues were first synthesized, via the modified methods subsequently used to prepare the radiolabelled analogues, to provide evidence for the structures assigned the radiolabelled analogues. This work will not be discussed except where the details are relevant to the radiosyntheses described.

1. 2,2'-Cyclouridine (21)

The synthesis of 2,2'-cyclouridine must be conducted under anhydrous conditions to prevent the desired product from reacting further with water to produce ara-U (23, R = H). In preparative scale reactions, trace quantities of moisture in the reaction mixture have little noticeable effect on the direction in which the reaction will proceed. On the other hand, traces of impurities in small scale reactions can significantly alter the outcome. In preliminary experiments designed to optimize the reaction conditions for the small scale synthesis of 6-[^{3}H]-2,2'-cyclouridine from 6-[^{3}H]-uridine, radiochemical yields as low as 5% were obtained. The dimethylformamide used as the solvent in the reaction was stored over 3 Å molecular sieves to remove traces of moisture inadvertently introduced during storage. When freshly distilled dimethylformamide was employed rather than dimethylformamide stored over molecular sieves the radiochemical yield

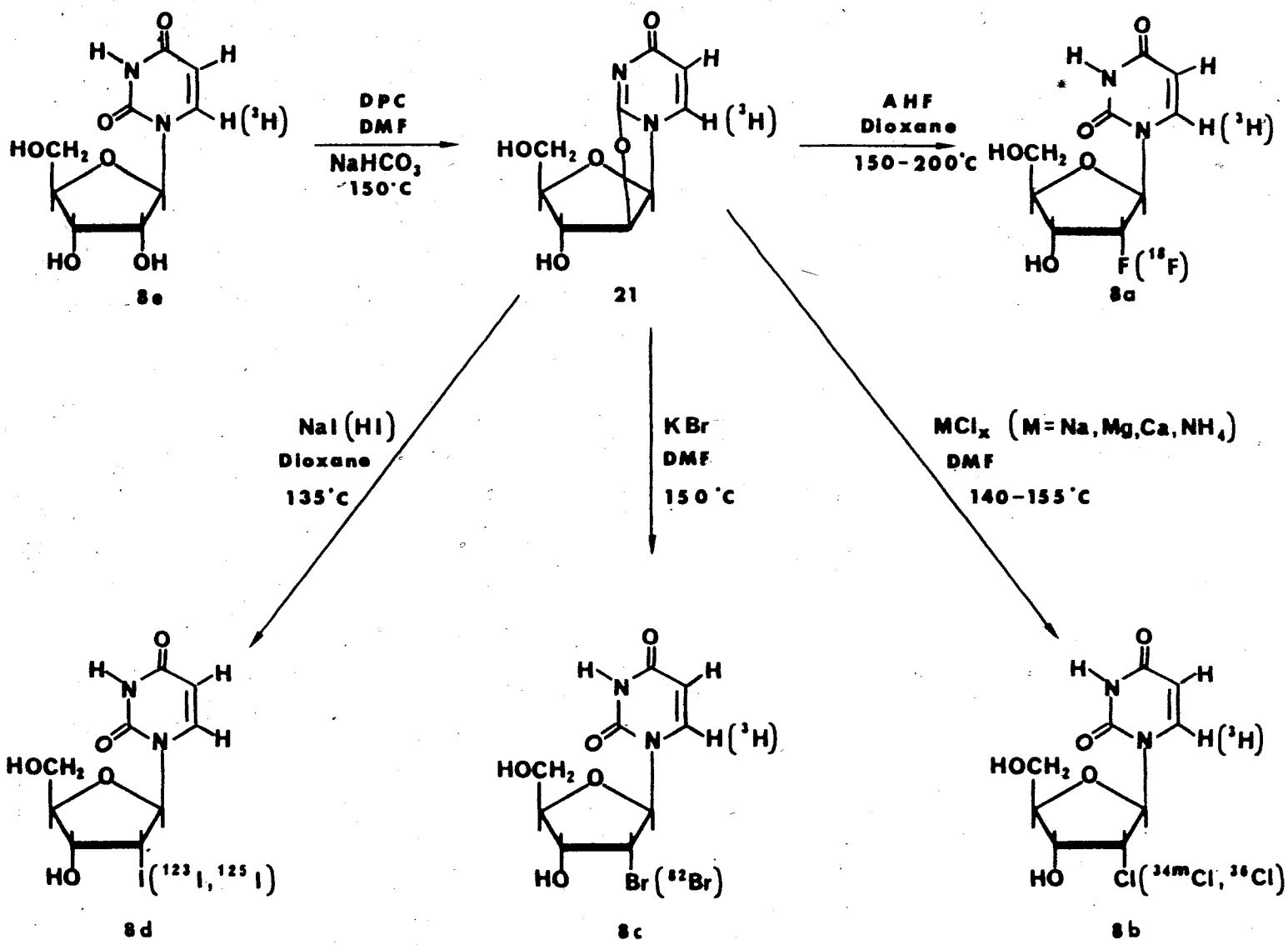

Scheme 8. Synthesis of Radiolabelled 2'-Halo-2'-deoxyuridine Analogues.

was greater than 80%. The low initial yields may have been caused by traces of aluminum-silicate powder from the molecular sieves (silica gel has been reported to catalyze rearrangement reactions[168] and cleave ethers[169]) or other impurities inadvertently added during use or formed during storage of the solvent. The reaction proceeded rapidly at 152°C, reaching a maximum radiochemical yield within 10-15 minutes (Figure 7) when freshly distilled solvent was used. Thus the preparative synthesis of 6-[^{3}H]-2,2'-cyclouridine was accomplished in 83.7% radiochemical yield within 16 minutes at 153°C (III.C.2.h).

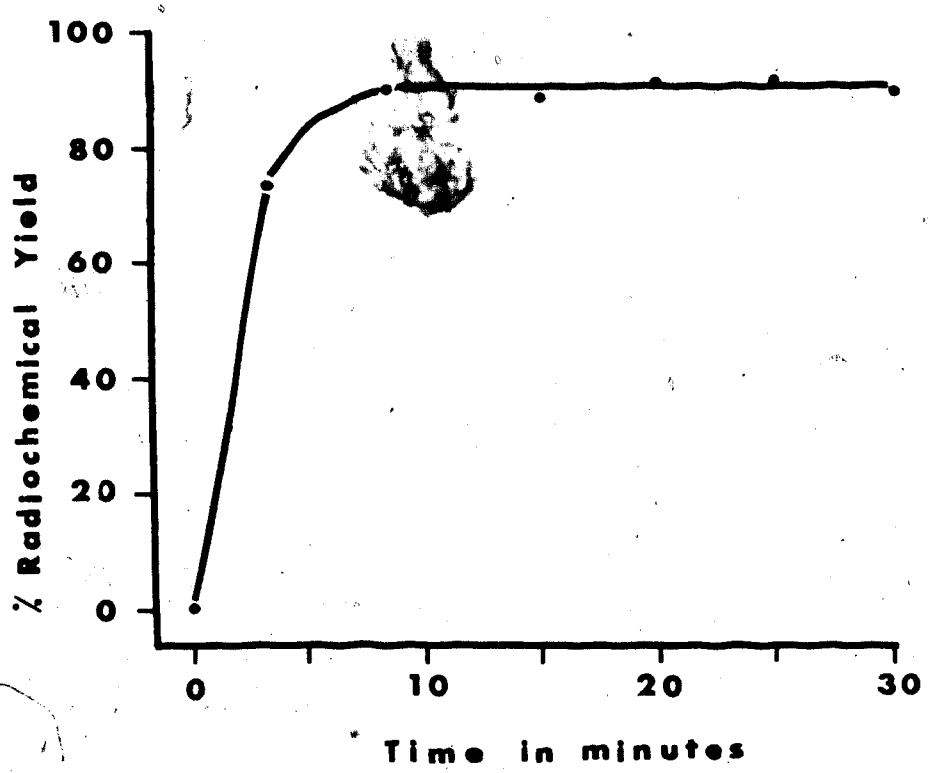

Figure 7. Radiochemical Yield of 6-[^{3}H]-2,2'-Cyclouridine as a Function of Reaction Time.

2. 2'-Fluoro-2'-deoxyuridine (8a)

Two methods for the synthesis of 2'-FUdR (8a) were investigated. The procedure reported by Codington et al.[71] required reaction of 2,2'-cyclouridine (21) with an excess of anhydrous hydrogen fluoride in dioxane for 18 hours at 110°C. These reaction conditions were modified by increasing the reaction temperature and decreasing the reaction time to compensate for the short half-life of ^{18}F ($T_{\frac{1}{2}}$ = 109.7 minutes)[33]. Optimum chemical yields of 2'-FUdR, determined previously in our laboratory by J. Mercer[170], were obtained using ten equivalents of anhydrous hydrogen fluoride. Reactions using fewer equivalents of anhydrous hydrogen fluoride afforded significantly lower chemical yields of 2'-FUdR. Under these circumstances, a ten-fold excess of fluoride anion would afford a maximum theoretical radiochemical yield of 10% of the starting ^{18}F activity. When the chemical yield is considered, the overall radiochemical yield would be approximately 3%. The absolute and relative radiochemical yields of 2'-[^{18}F]-FUdR synthesized using anhydrous hydrogen fluoride-18 (see III.C.2.a) are given in Table XI. The concentration of anhydrous hydrogen fluoride trapped in the reaction vessel after the recovery of ^{18}F from the target was difficult to control. The actual concentration present during reaction was determined by standard acid-base titration of an aliquot of the reaction mixture with sodium hydroxide to a phenolphthalein end point. The radiochemical synthesis proceeded poorly, affording 2'-[^{18}]-FUdR in trace quantities only. The relatively harsh conditions necessary to force the fluorination reaction also resulted in the degradative formation of uracil and other unidentified products which were less

TABLE XI. Synthesis of 2'-[^{18}F]-Fluoro-2'-deoxyuridine: Reaction Conditions and Radiochemical Yields using Anhydrous Hydrogen Fluoride-18.

2,2'-CUR µmol	Anhydrous Hydrogen Fluoride µmol	Molar Ratio F^-/2,2'-CUR	Reaction Time min	Reaction Temp °C	Radiochemical Yield %[1] (%)[2]
21	100	4.8	65	160	0.15 (0.72)
49	360	7.8	60	160-210	0.09 (0.70)
22	1029	47	92	180	0.16 (7.4)
54	2640	49	61	185	0.40 (19.0)
4.4	230	52	32	180	0.13 (6.8)

1. Absolute radiochemical yield recovered after purification by preparative silica gel column or thin layer chromatography, calculated back to end of irradiation.
2. Relative radiochemical yield calculated on the theoretical maximum ^{18}F which could be incorporated due to the excess of fluoride anion, calculated back to end of irradiation.

polar than the desired product (8a) or starting material (21). The presence of ara-U (23, R = H) in some of the reactions indicated that moisture was not always completely excluded from the ^{18}F target-recovery system.

While the developmental work for the synthesis of 2'-[^{18}F]-FUdR was in progress, Mengel and Guschlbauer[100] published the synthesis of 2'-Fluoro-2'-deoxycytidine (12a, 2'-FCdR) via the reaction of a potassium fluoride-crown ether complex with 2,2'-cyclocytidine hydrochloride. The direct application of this method to the synthesis of 2'-FUdR from 2,2'-cyclouridine was unsuccessful. Under similar

conditions, 2'-FCdR was obtained from 2,2'-cyclocytidine hydrochloride in good yield (see III.C.2.b). This indicated that the reported procedure had been properly reproduced and that the synthesis of 2'-FUdR required different reaction conditions. Upon the addition of trifluoroacetic acid to the crown ether-potassium fluoride reaction, to facilitate cleavage of the 2,2'-anhydro bond, small quantities of a product with similar chromatographic R_f values (silica gel-tlc and rp-hplc) to 2'-FUdR were detected. The quantity of product recovered was too small to allow more rigorous structural determination of the unlabelled product. Preliminary syntheses with potassium fluoride-18 indicated that low levels of ^{18}F were associated with the product, suggesting that 2'-[^{18}F]-FUdR may have been synthesized using this method. These results warrant further investigation into the synthesis of 2'-[^{18}F]-FUdR using the potassium fluoride-crown ether reagent.

The low absolute radiochemical yields and the short physical half-life of ^{18}F precluded the use of 2'-[^{18}F]-FUdR directly for further biological studies. Therefore the 6-[^{3}H]-2'-FUdR analogue was synthesized (see III.C.2.a) as an alternate radiolabelled analogue of 2'-FUdR. 6-[^{3}H]-2'-Fluoro-2'-deoxyuridine was prepared, using the reaction conditions determined by J. Mercer[170], via the reaction of excess anhydrous hydrogen fluoride with 6-[^{3}H]-2,2'-cyclouridine at 110°C for 15 hours. A lower reaction temperature than that used in the ^{18}F syntheses was employed to decrease the number and amount of thermal degradation products formed at high temperatures. An unidentified ^{3}H-containing contaminant having a similar but slightly less polar R_f value than 6-[^{3}H]-2'-FUdR required sequential purification

by silica gel tlc using two different solvent systems before an acceptable radiochemical purity (98.9%) was obtained.

3. 2'-Chloro-2'-deoxyuridine (8b)

The procedure reported for the synthesis of 2'-ClUdR (8b) was reinvestigated to determine if a practical chemical yield could be obtained within a time period compatible with ^{34m}Cl ($T_{\frac{1}{2}}$ = 32.0 minutes)[33] and to evaluate nucleophilic chlorinating reagents other than anhydrous hydrogen chloride. Preliminary experiments on a small scale (1-5 mg) indicated that the reaction of 2,2'-cyclouridine with an excess of chloride anion (ammonium, calcium, magnesium and sodium salts) afforded 2'-ClUdR in nearly quantitative yield, as determined by the disappearance of 2,2'-cyclouridine from the reaction mixture monitored by chromatographic analysis using rp-hplc. Sequential analysis of the reaction of ammonium chloride with 2,2'-cyclouridine was used to determine the optimum reaction time. The reaction proceeded rapidly in both dioxane and dimethylformamide, with only a trace of 2,2'-cyclouridine remaining after 15 minutes at 150°C. Dimethylformamide, rather than dioxane, was chosen as the solvent for further syntheses, due to its superior solvating properties.

Reaction of magnesium chloride-34m, produced by proton irradiation of a solid magnesium chloride target (see III.C.1.c) with 2,2'-cyclouridine afforded 2'-ClUdR as the major product in near quantitative yield, but low radiochemical yield (1-3%). The low radiochemical yield was due to the large amount of material necessary to prepare the solid target, therefore resulting in a large excess of non-radioactive

chloride anion in the reaction mixture. The identity of the product was confirmed by comparison of tlc, rp-hplc and ^{1}H nmr data with an authentic sample.

An alternative method for producing ^{34m}Cl using the $^{34}S(p,n)^{34m}Cl$ and $^{34}S(d,2n)^{34m}Cl$ reactions provided ^{34m}Cl having very high specific activity (NCA). Chlorine-34m produced by irradiation of hydrogen sulfide gas could be readily separated from the target gas using an anion exchange resin (III.C.1.c). Preliminary experiments in which equimolar quantities of the chloride form of Dowex 21-K anion exchange resin and 2,2'-cyclouridine (21) were heated in dimethylformamide and trifluoroacetic acid indicated that a maximum chemical yield of 2'-ClUdR was obtained within 10 minutes at 160°C. Longer reaction times resulted in decomposition of the product to ara-U. These results were also observed during the reaction of Dowex 21-K-^{34m}Cl with 21 in dimethylformamide at 155°C (Table XII). A maximum radiochemical yield (34.5%) was obtained within 5 minutes. When the reaction temperature was decreased to 140°C, a small increase in radiochemical yield from 31 to 36% at 10 minutes was obtained. The presence of ara-U in the reaction product was most likely due to incomplete drying of the Dowex 21-K anion exchange resin. The resin proved to be a facile chlorinating reagent and facilitated purification of the 2'-[^{34m}Cl]-ClUdR by retaining the majority of unreacted chloride-34m.

2'-[^{36}Cl]-Chloro-2'-deoxyuridine rather than 2'-[^{34m}Cl]-ClUdR was used in the biological studies, as the long half-life of ^{36}Cl ($T_{\frac{1}{2}} = 3 \times 10^{5}$ y)[33] was more convenient than the short half-life of ^{34m}Cl for sample manipulation and analysis. The 2'-[^{36}Cl]-ClUdR was prepared via

TABLE XII. Synthesis of 2'-[^{34m}Cl]-Chloro-2'-deoxyuridine: Reaction Conditions and Radiochemical Yields.

Dimethyl-formamide Volume ml	Chloride[1] µmol	2,2'-Cyclo-uridine µmol	Temperature °C	Time Min	Radiochemical Yield (%)[2]
1.2	63.5	57.5	155	5	35
				10	31
				15	22
3.0	63.5	57.5	140	10	36

1. Dowex 21-K anion exchange resin.
2. Decay corrected to EOB.

the reaction of 2,2'-cyclouridine with sodium chloride-36, and recovered in 29% radiochemical yield after preparative-cc purification. The final specific activity (5.46 MBq mmol^{-1}) of the product was equal to the specific activity of the starting material, indicating that no dilution with extraneous chloride had occurred during the reaction and purification procedures.

The tritiated analogue 6-[^{3}H]-2'-ClUdR with a higher specific activity (11.1 GBQ mmol^{-1}) than 2'[^{36}Cl]-ClUdR was prepared via the reaction of anhydrous calcium chloride with 6-[^{3}H]-2,2'-cyclouridine. 6-[^{3}H]-2'-Chloro-2'-deoxyuridine was obtained in 53.2% radiochemical yield after preparative-tlc purification.

4. 2'-Bromo-2'-deoxyuridine (8c)

6-[^{3}H]-2'-Bromo-2'-deoxyuridine was prepared as an alternative tracer for 2'-[^{82}Br]-BrUdR via reaction of potassium bromide with 6-[^{3}H]-2,2'-cyclouridine. The product was purified by preparative-tlc. In contrast to 6-[^{3}H]-2'-ClUdR (8b), 6-[^{3}H]-2'-BrUdR (8c) was not stable when stored at 4°C. Both tritiated nucleoside analogues 8b and 8c were prepared from the same sample of 6-[^{3}H]-2,2'-cyclouridine and were stored under similar conditions. 6-[^{3}H]-2'-Chloro-2'-deoxyuridine was still 98% radiochemically pure after storage as a solid under refrigeration for seven days. On the other hand, 6-[^{3}H]-2'-BrUdR was only 85.3% radiochemically pure after storage under identical conditions for the same time period. The major radioactive impurity corresponded closely with the retention time of ara-U (23, R = H) as determined by rp-hplc analysis. This suggested that the tritium label was stable. The instability of 6-[^{3}H]-2'-BrUdR may be explained by intramolecular nucleophilic attack of the C-2 oxygen of uracil at the C-2' sugar terminus to displace bromide anion which is a good leaving group. 6-[^{3}H]-Arabinouridine (23, R = H) could then arise from nucleophilic attack by water at the C-2 of the uracil moiety to cleave the 2,2'-anhydro linkage in a manner similar to the mechanism proposed by Watanabe et al.[85]. Recent studies with cytidine analogues which have good leaving groups in the ribo-, arabino- and xylofuranosyl configurations indicated that these positions may undergo intramolecular nucleophilic displacement reactions in vivo that eventually lead to the unsubstituted arabinofuranosyl nucleosides as shown in Scheme 9. The relative stability of the 6-[^{3}H]-2'-ClUdR analogue may be explained

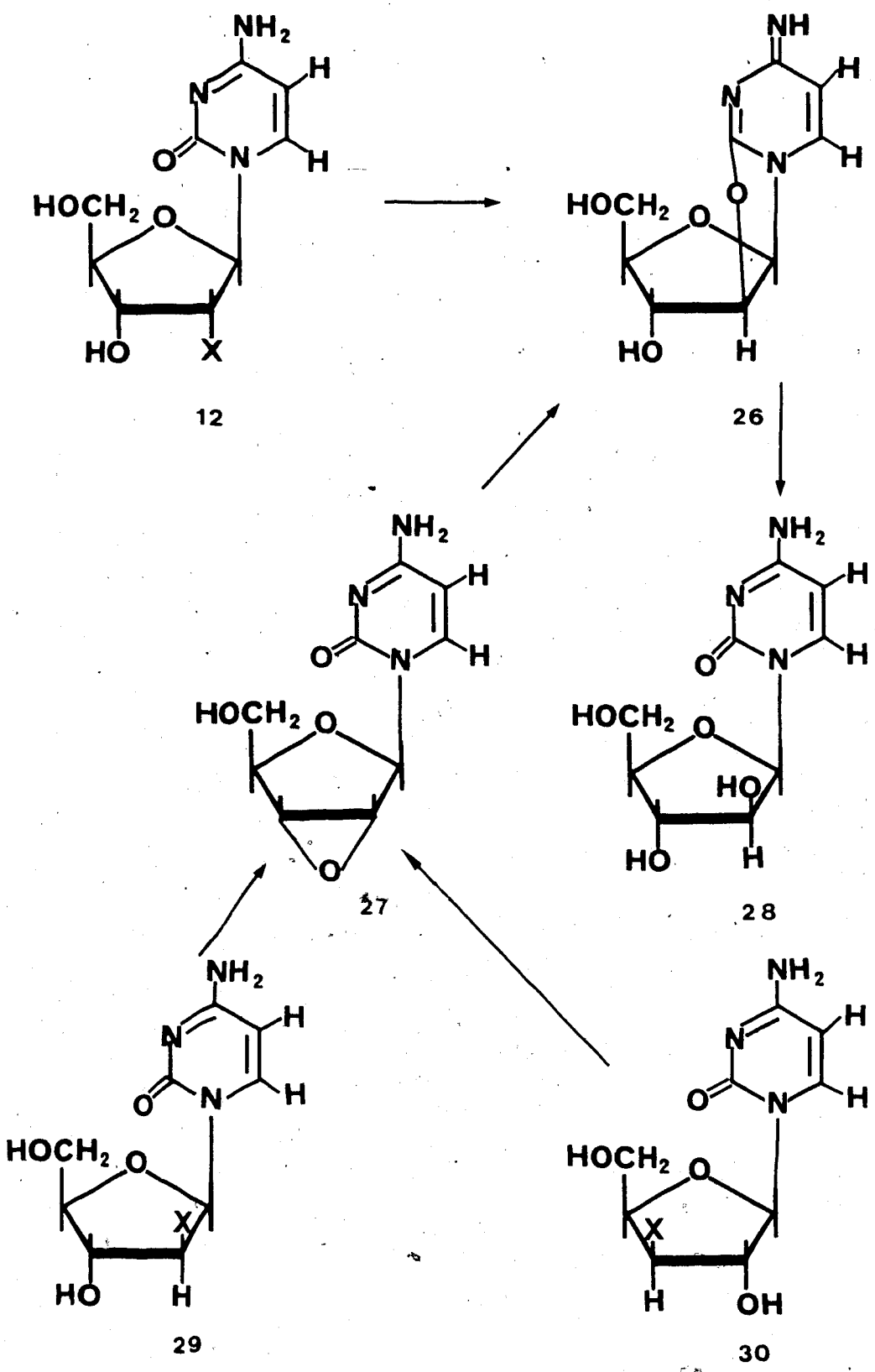

Scheme 9. Intramolecular Conversion of Modified Cytosine Nucleosides to Ara-C[85].

by the poorer leaving ability of chloride in comparison with bromide. Watanabe et al.[85] also noted that the conversion of 3'-iodoxylocytosine (30, x = I) was converted to ara-C (29, x = OH) at a slower rate than 3'-bromoxylocytosine (30, x = Br). This was attributed to differences between the furanose conformations of the C-3' substituted nucleosides in which the 3'-iodo-sugar assumed a conformation less favourable to nucleophilic displacement by the 2'-hydroxyl function. Therefore, following a similar line of reasoning, the differences in stability of 8b and 8c may also be due to differences in the preferred conformations assumed by the C-2' substituted analogues. The conformation of the 2'-bromo analogue could facilitate the displacement of the bromine atom by the uracil C-2 oxygen whereas the 2'-chloro sugar conformation could be less favourable to displacement of the chlorine atom.

5. 2'-Iodo-2'-deoxyuridine (8d)

Recovery of ^{123}I anion, for the synthesis of 2'-[^{123}I]-IUdR (8d), from the cold-finger trapping surface (see III.C.1.e) was independent of the construction material of the cold-finger. The radiochemical yield of 2'-[^{123}I]-IUdR was also independent of the trapping surface of the source of ^{123}I but was influenced by the exchange solvent used to remove the ^{123}I from the cold-finger. The radiochemical yield of 2'-[^{123}I]-IUdR rapidly reached a maximum, then slowly decreased when an aqueous exchange solvent was used (Table XIII). When a methanolic exchange solution was employed the radiochemical yield and rate of reaction were similar to that observed with an aqueous source of ^{123}I. However, the yield did not decrease with reaction time but rather

TABLE XIII. Synthesis of 2'-[^{123}I]-Iodo-2'-deoxyuridine: Reaction Conditions and Radiochemical Yields.

^{123}I Trapping Material	Exchange Solvent	Carrier Iodide µmol	2,2'-Cyclo-uridine µmol	Dioxane Volume ml	Reaction Temp °C	Reaction Time min	Radiochemical Yield % (%)[1]
copper	water	10.0	9.0	0.5	120	15	58 (64)
						30	49 (54)
						60	37 (41)
gold	methanol	6.3	4.9	2.3	135	15	45 (58)
						32	47 (60)
						43	48 (62)
gold	methanol	1.4	4.4	1.0	135	15	71
		1.4	5.8	1.0	140	20	57
		1.4	2.6	1.0	135	25	84
gold	methanol	1.4	2.6	1.0	135	30	77[2]
		NCA[3]	3.5		133	15	21[2]
quartz	water	1.4	4.0	1.0	110-135	20	5
		NCA[4]	2.6		162	20	5
quartz	methanol	1.3	4.4		125-150	15	65
		1.3	4.4		125-150	15	73

1. Yield calculated on maximum theoretical radiochemical yield possible with excess iodide in reaction.
2. The ^{123}I was from the same source for both reactions.
3. Used 3.1 µmol sodium chloride as non-isotopic carrier.
4. Used 150 µmol sodium chloride as non-isotopic carrier.

increased slowly. The addition of a small amount of carrier iodide influenced the direction and yield of the reaction. In no-carrier-added (NCA) reactions, in which sodium chloride was used as a non-isotopic exchange carrier, the radiochemical yields were lower than observed in carrier-added syntheses using the same ^{123}I source. In addition, the number of radioactive side-products was greater in reactions using no-added-carrier iodide (Figure 8). Limited shelf-life studies in normal saline at 20°C and 37°C indicated that 2'-[^{123}I]-IUdR was stable *in vitro*, exhibiting minimal loss of iodide-123 within 21 hours. The *in vitro* stability of 2'-[^{123}I]-IUdR was unexpected in view of the facile intramolecular displacement of good leaving groups in the C-2' position by the C-2 oxygen of the pyrimidine ring. The stability of 2'-IUdR was also unusual in view of the instability of 2'-BrUdR, since iodide is a better leaving group than bromide. The unexpected stability of 2'-[^{123}I]-IUdR could be due to the 2'-iodo-sugar adopting a conformation in which the displacement of the C-2' substituent is less favoured than in the conformation adopted by the 2'-bromo analogue, as discussed in section IV.C.d.

The synthesis of 2'-[^{125}I]-IUdR was complicated by the presence of sodium hydroxide in the ^{125}I solution (iodination grade). The synthesis proceeded smoothly when a two-fold excess of 2,2'-cyclouridine and trifluoroacetic acid (based on the sodium hydroxide concentration) was used, providing 2'-[^{125}I]-IUdR in moderate yield (III.C.2.f).

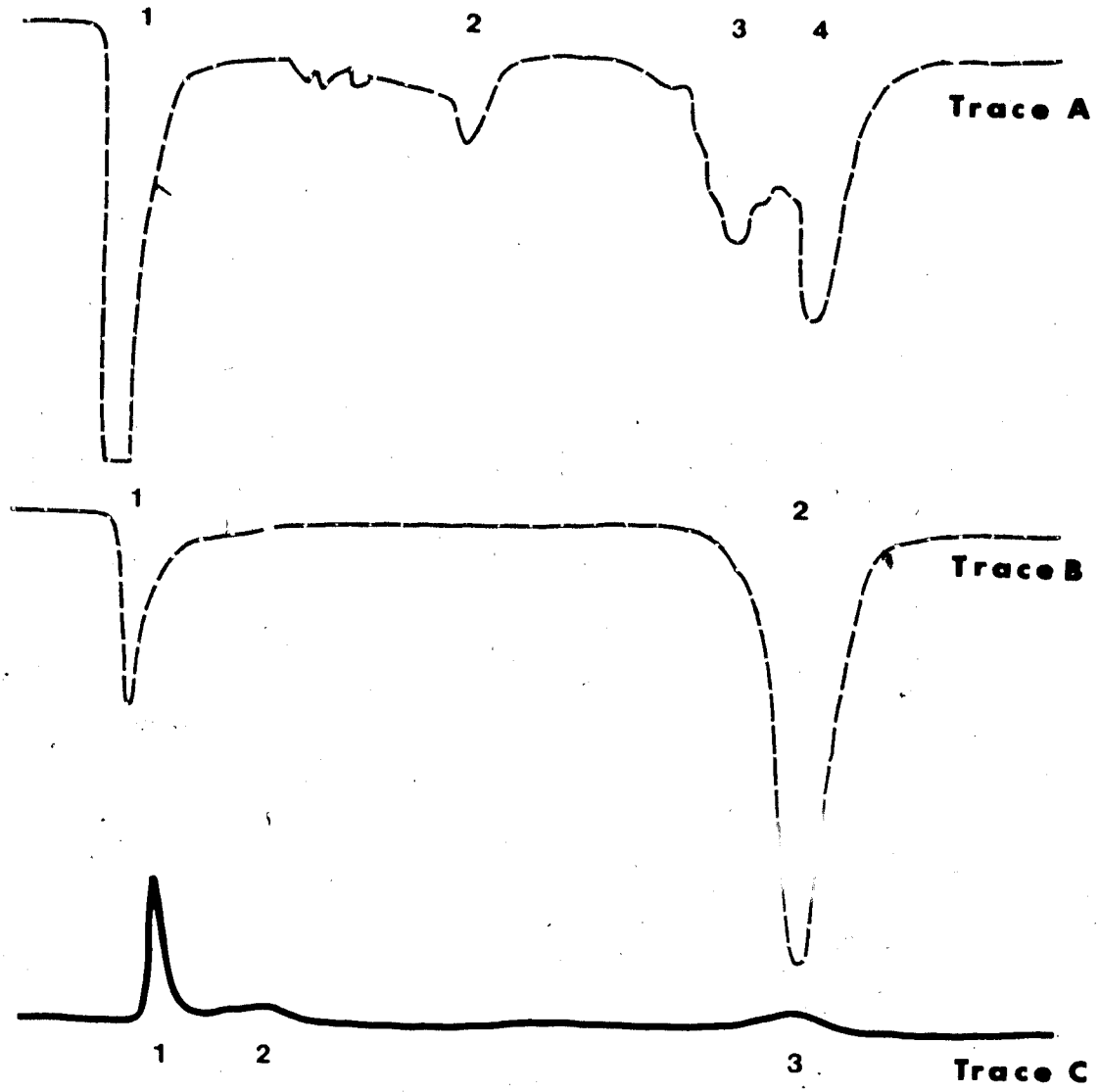

Solvent: Methanol:Water 9:1 v/v; 2.0 ml min^{-1}; uv detection (254 nm); radioactivity detection (plastic scintillator); chart speed 1 cm min^{-1}; Sil-1-X® C-18 reverse phase column (30 cm x 3.9 mm id).

Trace A: Radioactive trace of no carrier added reaction. Peak 1. Iodide-123 (column void volume). Peaks 2 & 3. Unidentified radiochemical contaminants. Peak 4. 2'-[^{123}I]-IUdR.

Trace B: Radioactive trace of carrier added reaction. Peak 1. Iodide-123 (column void volume). Peak 2. 2'-[^{123}I]-IUdR.

Trace C: Ultraviolet detection of carrier added reaction. Peak 1. Column void volume. Peak 2. 2,2'-Cyclouridine. Peak 3. 2'-IUdR.

Figure 8. Radio-rp-hplc Trace of 2'-[^{123}I]-Iodo-2'-deoxyuridine Prepared With and Without Added Carrier Iodide.

D. Biological Evaluation

The biological evaluation of the radiohalogenated nucleobases and nucleosides synthesized as tumor probes has been limited to *in vivo* tissue distribution studies in murine tumor models. The ideal situation would allow research and diagnosis with new radioactive tumor-diagnostic agents to be done with the human model. Although transplantable tumors in rats and mice are obviously not identical to spontaneous tumors in man, studies using tumor models provide important biological information not obtainable by other methods.

The metabolism of the radiohalogenated pyrimidines tested was not investigated because the gammma camera can not distinguish between radioactivity emitted by the original radiotracer and radioactivity emitted by metabolites of the tracer. No rigorous attempt was made to identify the radiolabelled metabolites by conventional methods once the animal had been injected. The initial tissue distribution studies were evaluated on the basis of whether or not these new radiolabelled agents would be useful for the non-invasive delineation of a tumor mass. Therefore, the overall distribution of the radiolabel, as viewed externally by a gamma-camera, was the criterion used in the evaluation. The important aspects of these studies were to determine if the radiolabelled analogues would:

1. demonstrate high tumor to background ratios and therefore enable visualization of the tumor, and
2. accumulate in the tumor in sufficient concentration to provide adequate count rates for gamma-camera imaging.

The differential tissue distribution data for the radiolabelled pyrimidine base and nucleoside analogues has been expressed as percent injected radioactive dose incorporated per gram of tissue; percent injected

radioactive dose incorporated per whole organ; tissue to blood ratios; and specific activity (dpm or cps mg^{-1}) of each tissue, and are tabulated in the appendices. The tissue uptake has been expressed as a percentage of the injected radioactive dose because the absolute concentration of radiolabel in each tissue was important and the chemical identity of the radioactivity was not established. The tissue to whole blood ratios were used because it is the total radioactivity present in the circulating blood that comprises the background radiation detected by the gamma-camera.

1. Biodistribution of 6-[^{123}I]-Iodouracil

The distribution of 6-[^{123}I]-iodouracil was studied in male Wistar rats bearing intramuscular Walker 256 carcinosarcomas. The absolute uptake of radioactivity after intravenous injection of 6-[^{123}I]-iodouracil (0.73 μmol per rat) was low in all the tissues studied (Table XIV). Most of the radioactivity remained in the blood during the study. The blood contained 28% of the dose 15 minutes after injection and 2.5% after 8 hours. This preponderance of blood radioactivity was reflected in the low tissue : blood ratios observed for the other tissues. The liver, kidney and tumor accumulated 1% or more of the dose after 15 minutes, but did not concentrate the radioactivity from the blood. This was indicated by the low tissue : blood ratios observed for these tissues. The gradual rise in tissue : blood ratios for tumor and liver observed until 2 hours after injection may have been due to the decrease in blood radioactivity, rather than uptake and metabolic trapping by either organ, since the absolute concentration of radioactivity of both

TABLE XIV. Percent Dose of ^{123}I Incorporated per Whole Organ of Walker 256 Carcinosarcoma Bearing Wistar Rats after Injection of 6-[^{123}I]-Iodouracil.

Tissue		Time in minutes 15	30	60	120	240	480	960	1560
Blood	$\bar{X}$	28.72	18.15	10.76	5.52	2.97	2.55	0.11	0.11
	SD	2.48	5.70	4.26	3.68	1.37	1.25	0.05	0.07
Thyroid	$\bar{X}$	0.57	0.39	0.41	0.11	0.08	0.05	0.004	0.004
	SD	0.24	0.12	0.23	0.05	0.02	0.05	0.002	0.002
Liver	$\bar{X}$	2.66	2.04	1.39	0.93	0.46	0.23	0.022	0.025
	SD	0.13	0.22	0.18	0.36	0.18	0.14	0.010	0.014
Kidney	$\bar{X}$	0.98	0.80	0.97	0.23	0.13	0.06	0.006	0.010
	SD	0.30	0.34	0.23	0.09	0.06	0.05	0.004	0.005
GIT	$\bar{X}$	0.24	0.18	0.08	0.13	0.07	0.04	0.009	0.013
	SD	0.02	0.05	0.03	0.12	0.03	0.02	0.002	0.009
Stomach	$\bar{X}$	0.35	0.28	0.48	0.33	0.61	0.16	0.016	0.017
	SD	0.10	0.04	0.09	0.08	0.42	0.08	0.003	0.004
Tumor	$\bar{X}$	1.58	1.12	0.87	0.65	0.29	0.08	0.007	0.013
	SD	0.25	0.36	0.22	0.26	0.18	0.04	0.004	0.007

Three animals per time period.

the liver and the tumor decreased during that time period. The only tissues which demonstrated tissue : blood ratios greater than 1 were the stomach and the skin (Figure 9). This observation was probably due to the accumulation of radioiodide released from 6-[^{123}I]-iodouracil *in vivo*. The stomach can accumulate iodide in the gastric juice up to a concentration 40 times that found in the plasma[171]. Iodide is also known to concentrate in the inner layers of the epidermis of the skin and become organically bound in the hair[171]. The latter phenomenon seems to be peculiar to the rat. Thyroid accumulation of radioiodide was inhibited by prior addition of potassium iodide to the animals' drinking water. An increase in the plasma iodide level decreases the conversion of free iodide to organically bound iodide in the thyroid and saturates the iodide concentrating mechanism of the thyroid. Excess plasma iodide reduces but does not completely inhibit transport of iodide by the stomach and small intestine[151,171]. The most important route of iodide excretion is *via* the kidney into the urine.

Excretion of unchanged 6-[^{123}I]-iodouracil accounted for approximately one third of the urinary radioactivity up to 2 hours post injection (Table XV). The balance was due to free iodide and unidentified, polar metabolites retaining the radioiodine moiety. After 4 hours, the majority (91.6%) of the urinary radioactivity was excreted as free iodide. The low uptake of radioactivity by the liver, the major site of pyrimidine metabolism[172], may account for the relatively large proportion of unmetabolized 6-[^{123}I]-iodouracil found in the urine up to 4 hours after injection. 6-[^{123}I]-Iodouracil may be considered an analogue of orotic acid or uracil. The saturation capacity

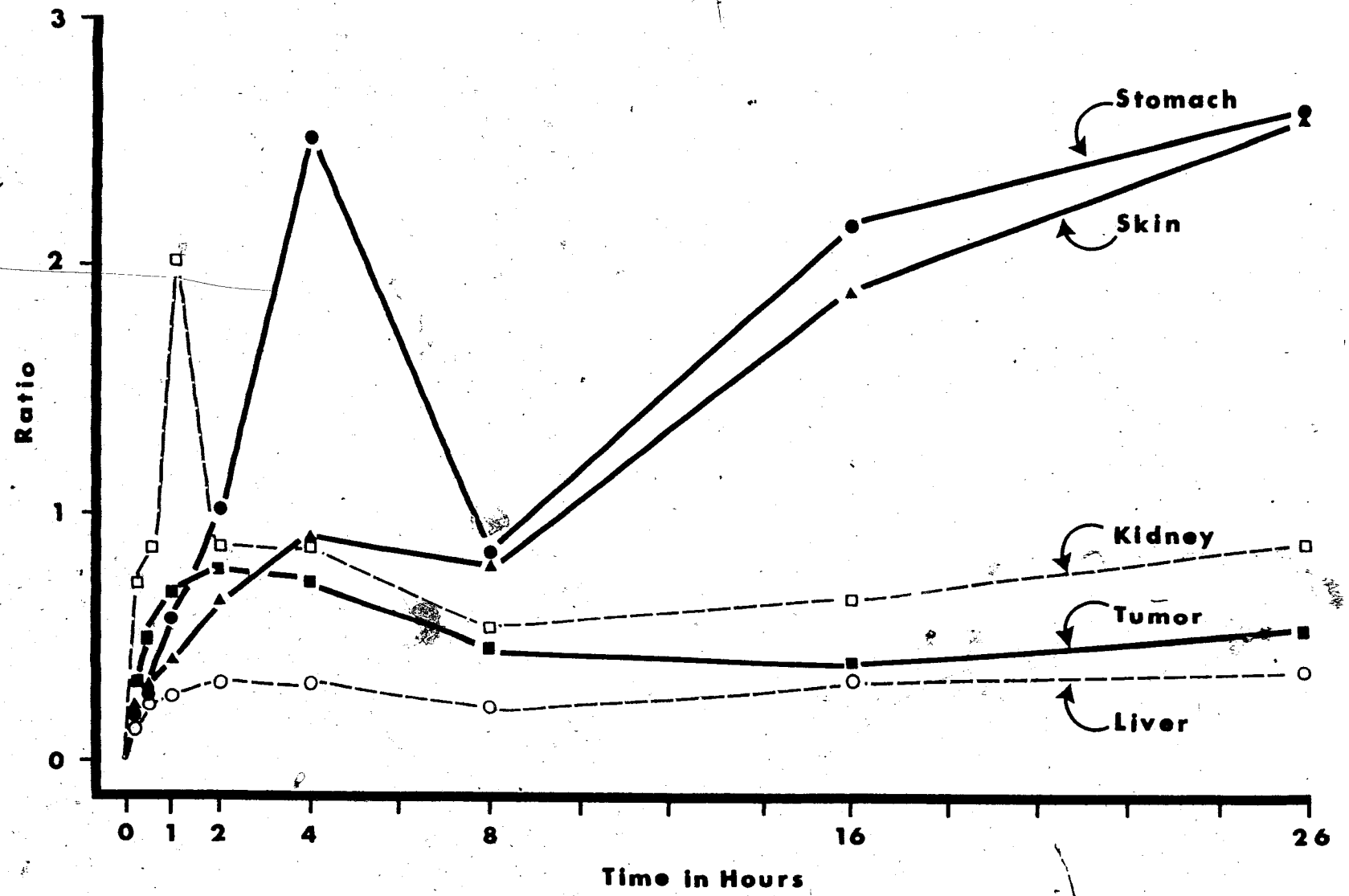

Figure 9. Tissue : Blood Ratios of ^{123}I in Wistar Rats Bearing Walker 256 Carcinosarcomas after Injection of 6-[^{123}I]-Iodouracil.

TABLE XV. Urinary Excretion Analysis after Intravenous Injection of 6-[^{123}I]-Iodouracil into Wistar Rats Bearing a Walker 256 Carcinosarcoma (n = 3).

Time (min) Post Injection	Proportion (%) of urinary radioactivity associated with: Iodide[1] $\bar{x}$ ± SD	6-IU[2] $\bar{x}$ ± SD	Unidentified[3] $\bar{x}$ ± SD
15	15.6 ± 9.4	33.1 ± 6.8	51.2 ± 13.2
30	6.8 ± 2.3	43.3 ± 20.6	49.9 ± 19.0
60	32.3 ± 16.1	27.7 ± 20.1	40.0 ± 4.3
120	32.3 ± 14.7	30.7 ± 19.5	37.0 ± 10.8
240	61.1 ± 14.9	9.4 ± 6.0	29.5 ± 9.2
480	91.6 ± 2.5	1.2 ± 0.5	7.2 ± 2.0
960	86.3 ± 4.2	1.7 ± 0.8	11.7 ± 3.8
1560	94.6 ± 2.0	0.7 ± 0.2	5.3 ± 1.1

1. Fraction of urinary ^{123}I retained on the AgCl-DEAE cellulose mini-column.
2. Fraction of urinary ^{123}I co-chromatographing with authentic 6-IU.
3. Fraction of urinary ^{123}I unaccounted for by 1) and 2).

of the normal rat liver for metabolizing orotic acid in the circulation was found to be approximately 5 mg kg^{-1} (33 μM)[173]. Uracil was not incorporated into the RNA of normal rat liver to the same extent as orotate, but was catabolized and excreted[174]. For example, more than 80% of 2 mg (18 μmol) of 2-[^{14}C]-uracil injected intraperitoneally into normal rats was degraded to CO_2 within 3 hours and 5% was recovered unchanged in the urine[174]. The injected dose (0.72 μmol) of 6-[^{123}I]-iodouracil would have been expected to be within the metabolic capacity of the normal rat liver based on uracil or orotic acid metabolism in the rat. However 6-[^{123}I]-iodouracil was not metabolized as efficiently as the reported metabolism of either orotic acid or uracil.

The tissue : blood ratios indicated that 6-[^{123}I]-iodouracil did not attain a concentration gradient of sufficient magnitude to allow non-invasive tumor imaging, a conclusion substantiated by the gamma ray camera studies. It was evident from the images obtained that the injected radioactivity was excreted quickly by the urinary system and accumulated in sufficient concentration to delineate the bladder within 5-10 minutes after injection. Sixty-five minutes post injection the kidneys and bladder were evident but the abdominal region was a diffuse area of relatively high activity (Plate 1). After 4 hours, only the stomach and bladder were evident and the image for 6-[^{123}I]-iodouracil closely resembled the image obtained 75 minutes after injection of sodium iodide-123 where the stomach (large focus of radioactivity) and the bladder (smaller focus of radioactivity) were the only tissues clearly delineated (Plate 1).

Another tissue distribution study was undertaken when 6-chlorouracil and 6-[^{123}I]-iodouracil were injected simultaneously to determine the effect that 6-chlorouracil may have had on the differential biological distribution of radioactivity after injection of 6-[^{123}I]-iodouracil. It was necessary to determine this effect since the removal of 6-chlorouracil from 6-[^{123}I]-iodouracil after purification was not always complete. The data in Table XVI compare the tissue : blood ratios for several tissues after the injection of 6-[^{123}I]-iodouracil with and without co-injection of 6-chlorouracil. The data indicate that co-injection of even an excess of 6-chlorouracil, on a molar basis with respect to 6-iodouracil, had little effect on the overall tissue distribution of 6-[^{123}I]-iodouracil.

6-[I-123]-IU
5×10^4 Counts
65 Minutes After Injection

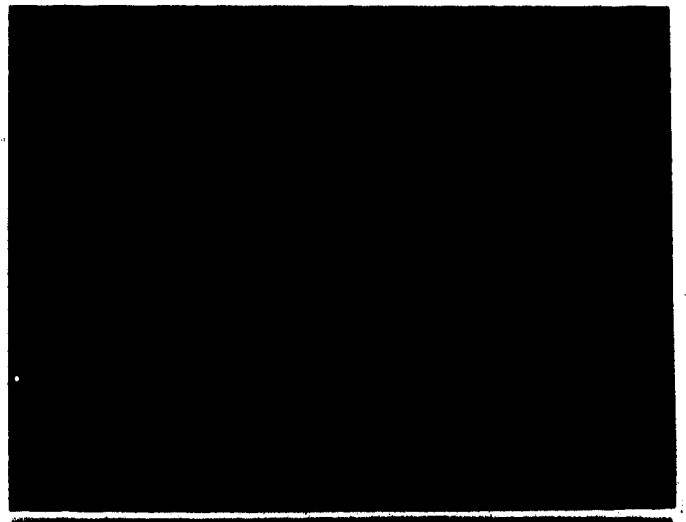

NaI-123
1×10^5 Counts
75 Minutes After Injection

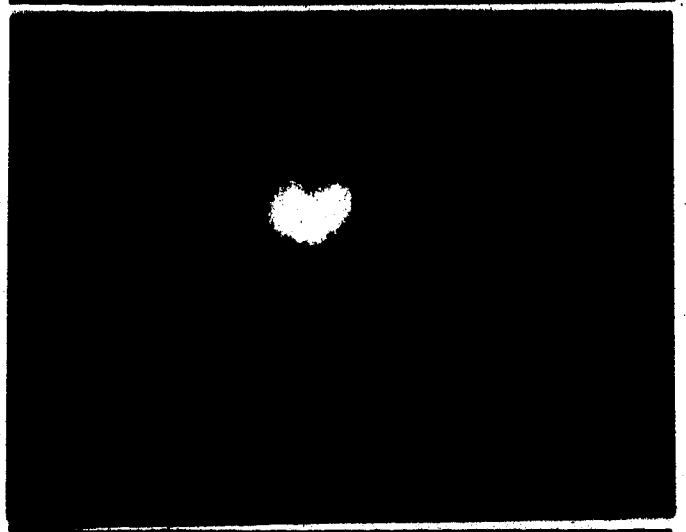

2'-[I-123]-IUdR
1×10^5 Counts
120 Minutes After Injection

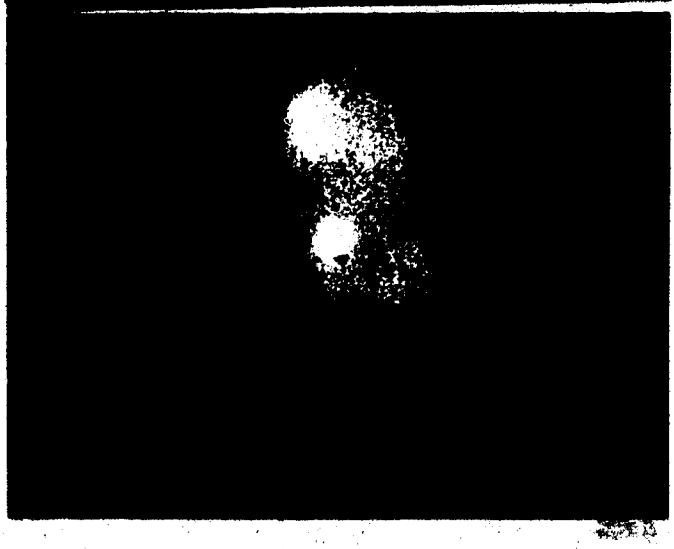

Plate I. Gamma Camera Images of Wistar Rats Bearing Intramuscular Walker 256 Carcinomas (Searle HP Camera with Pinhole Collimator)

TABLE XVI. Comparison of the Tissue to Blood Ratios of ^{123}I in Walker 256 Carcinosarcoma Bearing Wistar Rats after Injection of 6-[^{123}I]-Iodouracil with and without 6-Chlorouracil (n=3).

Tissue		6-[^{123}I]-IU								6-[^{123}I]-IU and 6-ClU							
		Time in minutes								Time in minutes							
		15	30	60	120	240	480	960	1560	15	30	60	120	240	480	960	1560
LIVER	$\bar{X}$	0.15	0.23	0.22	0.26	0.24	0.34	0.31	0.53	0.16	0.21	0.24	0.31	0.29	0.20	0.31	0.36
	SD	0.03	0.04	0.03	0.08	0.10	0.03	0.06	0.10	0.01	0.05	0.06	0.08	0.04	0.12	0.05	0.03
KIDNEY	$\bar{X}$	1.01	0.96	1.13	1.07	0.96	0.65	0.54	0.70	0.67	0.86	2.03	0.84	0.88	0.51	0.66	0.89
	SD	0.70	0.33	0.42	0.22	0.31	0.03	0.44	0.04	0.18	0.27	0.79	0.23	0.19	0.32	0.47	0.32
SPLEEN	$\bar{X}$	0.17	0.20	0.22	0.30	0.30	0.38	0.41	0.49	0.15	0.17	0.23	0.28	0.36	0.27	1.29	0.40
	SD	0.03	0.05	0.03	0.09	0.09	0.01	0.03	0.06	0.01	0.03	0.07	0.09	0.08	0.18	0.84	0.05
STOMACH	$\bar{X}$	0.19	0.32	0.58	1.49	1.32	1.75	1.47	5.86	0.15	0.21	0.55	1.00	2.53	0.80	2.17	2.63
	SD	0.06	0.17	0.32	1.04	0.42	0.54	0.02	1.50	0.04	0.06	0.25	0.51	1.35	0.32	1.08	1.20
TUMOR	$\bar{X}$	0.48	0.58	0.77	0.68	0.86	0.70	0.73	0.71	0.32	0.48	0.62	0.77	0.73	0.45	0.40	0.54
	SD	0.08	0.04	0.06	0.23	0.18	0.06	0.04	0.23	0.02	0.09	0.08	0.05	0.14	0.28	0.24	0.03
THYROID	$\bar{X}$	0.28	0.36	0.35	0.26	0.41	0.41	0.52	0.50	0.39	0.51	0.64	0.49	0.55	0.41	0.68	0.66
	SD	0.01	0.03	0.08	0.23	0.09	0.17	0.04	0.05	0.09	0.16	0.19	0.12	0.12	0.24	0.14	0.14
SKIN	$\bar{X}$	0.30	0.31	0.45	0.77	1.03	1.43	2.24	6.78	0.22	0.21	0.40	0.64	0.87	0.76	1.91	2.59
	SD	0.11	0.10	0.16	0.31	0.46	0.02	0.39	2.39	0.01	0.18	0.07	0.26	0.33	0.44	1.17	1.00

The low tissue utilization of 6-[^{123}I]-iodouracil by any of the tissues analyzed was reminiscent of the tissue distribution data reported for 5-iodouracil and 5-iodoorotic acid labelled with ^{131}I[175]. In these studies neither 5-[^{131}I]-iodouracil nor 5-[^{131}I]-iodoorotic acid demonstrated significant preferential concentration in either normal tissues or experimental tumors. Others[176] have reported poor utilization of 5-[^{3}H]-sodium orotate in normal tissues of rats bearing hepatomas with varying growth rates. Only the liver, kidney and hepatoma were reported to have incorporated radioactivity from the blood. In the same tumor models, 5-[^{3}H]-uracil demonstrated a similar qualitative pattern of tissue incorporation to that of 5-[^{3}H]-orotate, although the extent of uptake was quantitatively less.

2. Tissue Distribution of 6-[^{3}H]-2'-Fluoro-2'-deoxyuridine

The tissue distribution of 2'-FUdR was studied with the tritiated analogue 6-[^{3}H]-2'-FUdR rather than the ^{18}F labelled compound for convenience due to the short half-life of ^{18}F. Male Wistar rats inoculated with Walker 256 carcinomas were used as the tumor model.

The kidneys and liver rapidly accumulated radioactivity after intravenous injection of 6-[^{3}H]-2'-FUdR (3.5 pmol per rat) and accounted for greater than 3 and 32% respectively of the dose 15 minutes after injection (Table XVII). The blood contained 5% of the radioactive dose after 15 minutes and this level remained constant during the 6 hour time period examined. The remaining tissues examined, including the tumor, gave no evidence for accumulation of 6-[^{3}H]-2'-FUdR or its radiolabelled metabolites. The tissue : blood ratios for these tissues

TABLE XVII. Percent Dose of ^3H Incorporated per Whole Organ of Walker 256 Carcinosarcoma Bearing Wistar Rats after Injection of 6-[^3H]-2'-Fluoro-2'-deoxyuridine.

Tissue		Time in minutes					
		15	30	60	120	240	360
Blood	$\bar{X}$	5.06	5.22	4.49	4.29	4.31	4.29
	SD	0.78	0.68	0.53	0.21	0.35	0.33
Liver	$\bar{X}$	31.70	19.53	9.95	3.37	2.96	2.85
	SD	8.22	6.50	1.37	0.69	0.32	0.58
Spleen	$\bar{X}$	0.23	0.22	0.22	0.17	0.18	0.21
	SD	0.04	0.05	0.02	0.02	0.09	0.08
Kidney	$\bar{X}$	3.35	2.52	1.47	0.63	0.46	0.50
	SD	0.42	0.30	0.17	0.12	0.21	0.16
GIT	$\bar{X}$	0.29	0.27	0.23	0.23	0.16	0.22
	SD	0.12	0.10	0.08	0.08	0.09	0.07
Stomach	$\bar{X}$	0.41	0.37	0.38	0.31	0.20	0.36
	SD	0.11	0.08	0.09	0.08	0.03	0.10
Tumor	$\bar{X}$	0.41	0.28	0.24	0.30	0.27	0.26
	SD	0.19	0.17	0.20	0.09	0.10	0.14

Blood volume calculated as 6.5 % of body weight[177].

remained constant at each time period studied, indicating that blood perfusion rather than tissue uptake accounted for the majority of the radioactivity observed in the tissues (Table XVIII). Tumor : blood ratios at no time exceeded unity and were comparable, within experimental error, to the values calculated for the spleen, gastrointestinal tract or stomach. These latter tissues have high cell growth rates and would be expected to incorporate exogenously supplied nucleosides more readily than less actively growing tissues.

2'-Fluoro-2'-deoxyuridine has been shown to be a substrate for the erythrocyte nucleoside transport mechanism[178]. The mono- and diphosphate of 2'-fluoro-2'-deoxyuridine were shown to be substrates of a number of enzyme systems [76,77]. 2'-Fluoro-2'-deoxyuridine could therefore enter and be metabolized in the liver in a manner similar to that of uridine. The half-life of 5-[^{3}H]-uridine clearance from plasma was reported to be approximately 6 to 9 minutes[179,180]. This can be attributed to the rapid degradation of uridine in the liver, which catabolizes 70 to 90% of the uridine entering the organ[172,181]. The metabolites of 5-[^{3}H]-uridine were 5-[^{3}H]-uracil and [^{3}H]-water. A constant level of blood radioactivity was observed up to 4 hours after injection of 5-[^{3}H]-uridine.

The small dose (3.5 pmol per rat) of 6-[^{3}H]-2'-FUdR injected could have been cleared from the circulation very quickly by the liver, possibly on the first pass. If 6-[^{3}H]-2'-FUdR was metabolized in a manner analagous to 5-[^{3}H]-uridine, the tissue distribution of ^{3}H would not accurately reflect the tissue distribution of ^{18}F that would be obtained with 2'-[^{18}F]-FUdR. The radiolabelled catabolites of

TABLE XVIII. Tissue to Blood Ratios of ^3H in Various Organs in Walker 256 Carcinosarcoma Bearing Wistar rats after Injection of 6-[^3H]-2'-Fluoro-2'-deoxyuridine.

		Time in minutes					
		15	30	60	120	240	360
Liver	$\bar{X}$	9.58	5.77	3.06	1.03	0.97	0.92
	SD	3.24	2.57	0.60	0.19	0.16	0.55
Spleen	$\bar{X}$	1.07	1.01	1.05	0.80	0.70	1.10
	SD	0.16	0.20	0.13	0.11	0.06	0.52
Kidney	$\bar{X}$	6.18	4.53	2.75	1.24	1.07	1.11
	SD	0.86	0.52	0.11	0.23	0.36	0.41
Stomach	$\bar{X}$	0.94	0.76	0.89	0.74	0.53	0.97
	SD	0.27	0.12	0.24	0.20	0.05	0.32
Tumor	$\bar{X}$	1.00	0.87	0.82	0.69	0.62	0.76
	SD	0.10	0.08	0.18	0.15	0.13	0.09

2'-[^{18}F]-FUdR would be expected to be the fluorinated ribose analogue and fluoride-18 in contrast to 6-[^{3}H]-uracil and [^{3}H]-water, the analogous metabolites of 6-[^{3}H]-2'-FUdR. Therefore, the interpretation of the tissue distribution data of 6-[^{3}H]-2'-FUdR in relation to the suitability of 2'-[^{18}F]-FUdR for tumor imaging must be made with caution. The high levels of ^{3}H in the liver suggested that 6-[^{3}H]-FUdR was taken up and possibly metabolized in the liver. The very low fraction of ^{3}H in the tumor after injection of 6-[^{3}H]-2'-FUdR indicated that the absolute concentration of radioactivity in the tumor after injection of 2'-[^{18}F]-FUdR may be too low for accurate external visualization of the tumor.

3. Tissue Distribution of 2'-[^{36}Cl]-Chloro-2'-deoxyuridine

To allow for lengthy analytical procedures, 2'-ClUdR labelled with long-lived ^{36}Cl was used for the tissue distribution studies rather than the shorter-lived ^{34m}Cl radioisotope. The differential tissue distribution studies were conducted using male BDF_1 mice bearing a subpannicular Lewis Lung carcinoma as the tumor model. The tumors were used 8 to 10 days after implantation and ranged from 100 to 300 mg in size.

The injected radioactivity (7.78 kBq, 1.37 μmol per mouse) was removed rapidly from the blood with less than 1% of the dose remaining in the blood 2 hours after injection. The liver, spleen, kidney, gastrointestinal tract and tumor were the major organs to take up ^{36}Cl activity (Table XIX). Comparison of the tissue uptake of ^{36}Cl after injection of 2'-[^{36}Cl]-ClUdR indicated that the tumor, kidney and spleen accumulated the radioactivity more efficiently than the other tissues (Table XX).

TABLE XIX. Percent Dose of ^{36}Cl Incorporated per Whole Organ of Lewis Lung Carcinoma Bearing BDF_1 Mice after Injection of 2'-[^{36}Cl]-Chloro-2'-deoxyuridine.

Tissue		Time in minutes					
		15	30	60	90	120	180
Blood	$\bar{X}$	3.26	2.04	1.64	1.02	0.72	0.58
	SD	0.42	1.36	0.65	0.34	0.10	0.14
Liver	$\bar{X}$	3.61	1.85	1.52	0.89	0.53	0.54
	SD	0.86	0.18	0.82	0.33	0.15	0.10
Spleen	$\bar{X}$	2.12	1.76	1.48	1.07	0.60	0.58
	SD	0.52	0.18	0.35	0.68	0.20	0.13
Kidney	$\bar{X}$	1.23	0.69	0.53	0.30	0.21	0.28
	SD	0.23	0.07	0.21	0.08	0.03	0.21
GIT	$\bar{X}$	4.09	2.63	2.65	1.32	0.86	1.00
	SD	0.92	0.38	1.05	0.22	0.22	0.32
Stomach	$\bar{X}$	0.23	0.18	0.14	0.09	0.06	0.06
	SD	0.04	0.04	0.05	0.04	0.02	0.01
Tumor	$\bar{X}$	2.42	1.41	2.14	1.16	0.94	1.36
	SD	1.22	0.89	1.40	1.12	0.38	1.72

Five animals per 15, 30 and 120 minute time periods.
Six animals per 60, 90 and 180 minute time periods.

TABLE XX. Percent Dose of ^{36}Cl Incorporated per Gram Tissue of Lewis Lung Carcinoma Bearing BDF_1 Mice after Injection Of 2'-[^{36}Cl]-Chloro-2'-deoxyuridine.

		Time in minutes					
		15	30	60	90	120	180
Blood	$\bar{X}$	2.00	1.26	1.01	0.63	0.44	0.36
	SD	0.26	0.22	0.40	0.21	0.06	0.09
Liver	$\bar{X}$	2.53	1.38	1.10	0.69	0.32	0.41
	SD	0.67	0.23	0.47	0.21	0.17	0.07
Spleen	$\bar{X}$	14.02	14.08	8.83	6.05	4.28	3.82
	SD	3.08	2.49	2.68	1.83	1.09	1.26
Kidney	$\bar{X}$	6.76	4.01	3.08	1.89	1.30	1.60
	SD	0.73	0.56	1.33	0.50	0.22	1.34
GIT	$\bar{X}$	2.76	2.00	2.08	1.02	0.65	0.82
	SD	0.36	0.37	1.04	0.20	0.15	0.38
Stomach	$\bar{X}$	1.93	1.31	0.98	0.74	0.45	0.48
	SD	0.29	0.20	0.32	0.29	0.08	0.16
Tumor	$\bar{X}$	4.37	3.96	2.66	1.99	1.87	1.94
	SD	1.13	0.87	0.95	0.65	0.47	1.49

Five animals per 15, 30 and 120 minute time periods.
Six animals per 60, 90 and 180 minute time periods.

This is illustrated in Figure 10 in which the spleen, tumor and kidney tissue : blood ratios increased during the first hour after injection and remained high for the duration of the experiment.

Chromatographic analysis of the urinary contents of the bladder and determination of the total amount of radioactivity present in the bladder at each time period allowed the extent of metabolism of 2'-[^{36}Cl]-ClUdR and its urinary profile to be estimated (Table XXI). Most of the injected radioactive dose (69.7%) was recovered in the urine within 3 hours post injection. Catabolism of 2'-[^{36}Cl]-ClUdR occurred

TABLE XXI. Urinary Excretion Analysis After Intravenous Injection of 2'-[^{36}Cl]-Chloro-2'-deoxyuridine into Male BDF$_1$ Mice Bearing a Lewis Lung Carcinoma (n = 6).

Time (min) Post Injection	% of Injected Dose Recovered in Urine[1] $\bar{x} \pm SD$	Proportion[2] (%) of urinary radioactivity associated with: Chloride $\bar{x} \pm SD$	2'-ClUdR $\bar{x} \pm SD$	Unidentified $\bar{x} \pm SD$
15	12.7 ± 6.5	2.3 ± 2.4	95.0 ± 2.9	2.5 ± 3.0
30	31.1 ± 14.5	6.5 ± 2.9	88.1 ± 4.4	7.1 ± 4.3
60	42.7 ± 30.4	2.4 ± 1.3	92.0 ± 4.8	5.5 ± 4.2
90	53.3 ± 18.2	3.2 ± 1.3	90.8 ± 3.4	6.0 ± 3.4
120	56.3 ± 32.9	8.6 ± 4.0	84.4 ± 5.3	7.0 ± 4.5
180	69.7 ± 10.6	4.8 ± 5.0	85.3 ± 6.0	9.7 ± 5.5

1. Includes the urinary bladder and contents removed from each mouse during dissection and therefore represents the total radioactivity excreted into the urine during the time period in question minus urinary activity lost to the environment before sacrifice.

2. Proportions determined by silica gel tlc analysis of the urine.

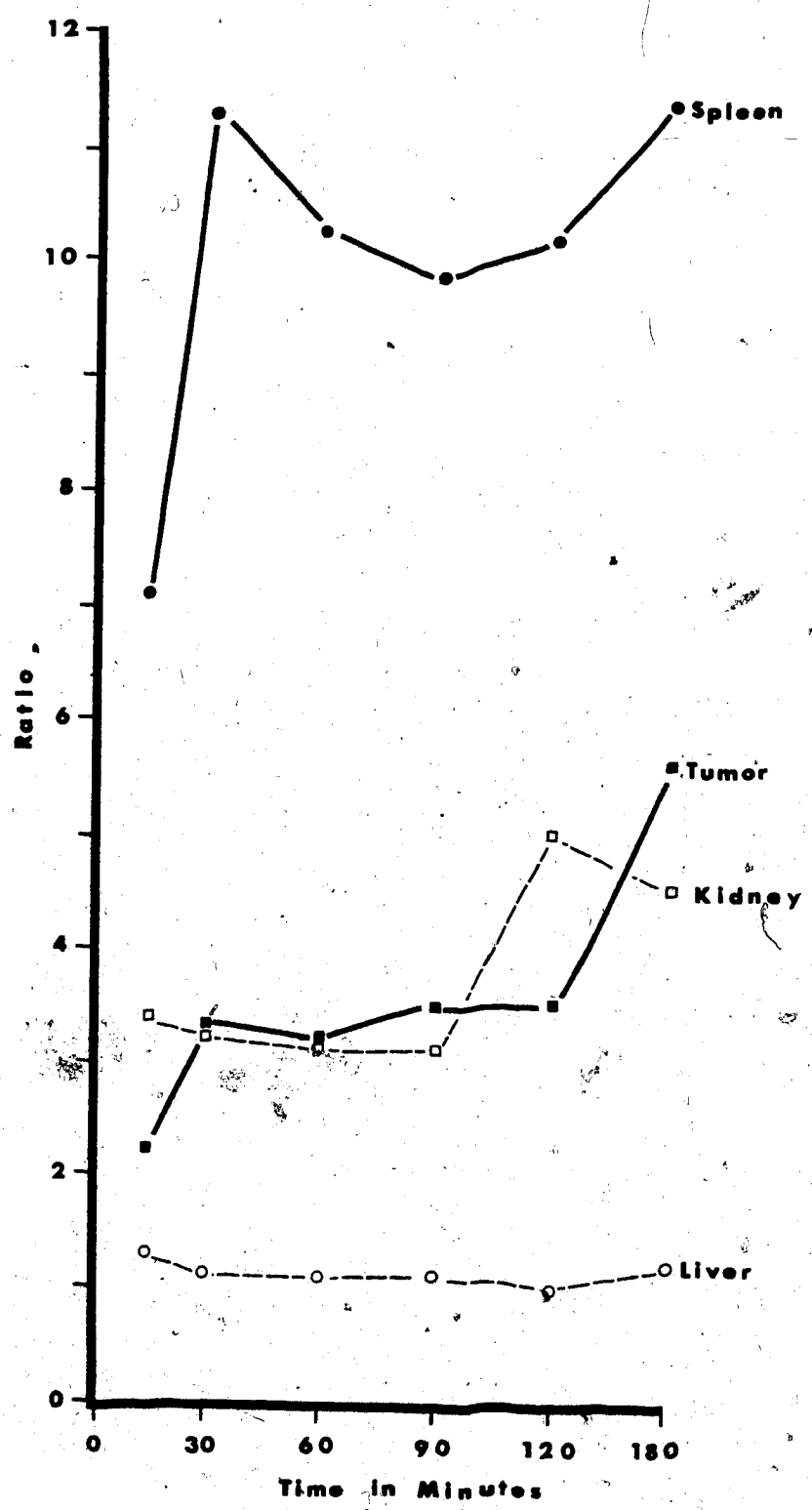

Figure 10. Tissue : Blood Ratios in BDF_1 Mice Bearing Lewis Lung Carcinomas After Injection of 2'-[^{36}Cl]-Chloro-2'-deoxyuridine.

slowly as was evident from the 3 hour urinary analysis which indicated that 85% of the excreted radioactivity was still associated with unmetabolized 2'-ClUdR. Further analysis of the data was limited as it could not be assumed that the urine collected represented the total amount formed during the time period. The values presented, therefore, underestimate the true rate of urinary excretion. With this in mind it is evident that 2'-[^{36}Cl]-ClUdR was rapidly excreted unchanged in the urine since at least 69% of the injected dose was found in the urine 3 hours post injection and that 85% of this radioactivity was still associated with 2'-ClUdR.

In contrast to 6-[^{3}H]-2'-FUdR, the injected dose of 2'-[^{36}Cl]-ClUdR (1.37 μmol per mouse) may have saturated the metabolic capacity of the mouse liver. The capacity of the rat liver to clear uridine on the first pass from the circulation is approximately 73% at concentrations (50 μM) many times greater than physiological levels[172]. However, a bolus injection of 1.37 μmol 2'-[^{36}Cl]-ClUdR would result in an initial molar concentration far greater than 50 μM (approximately 850 μM assuming blood volume is 6.5%[177] of a 25 g mouse). If one assumes that the mouse liver capacity for uridine was similar to that for the rat, the clearance of 2'-[^{36}Cl]-ClUdR from the blood would probably be less than 70% efficient. The low extraction efficiency would be consistent with the low concentration of ^{36}Cl activity in the liver and the rapid excretion of unchanged 2'-[^{36}Cl]-ClUdR in the urine. The low rate of metabolism of 2'-[^{36}Cl]-ClUdR would allow the other tissues such as the spleen and tumor an opportunity to incorporate 2'-[^{36}Cl]-ClUdR. An analysis of the acid soluble fraction of the spleen, tumor and kidneys

for phosphorylated metabolites would be necessary to determine whether these tissues had accumulated the ^{36}Cl by metabolic trapping of 2'-[^{36}Cl]-ClUdR. The ^{36}Cl activity in the kidneys could have been a reflection of the urinary excretion of 2'-[^{36}Cl]-ClUdR and its metabolites.

4. Tissue Distribution of 2'-[^{123}I]-2'-Iodo-2'-deoxyuridine

The tissue distribution of 2'-[^{123}I]-IUdR (2.35 pmol per rat) was studied using male Wistar rats bearing intramuscular Walker 256 carcinomas as the tumor model. Uptake of 2'-[^{123}I]-IUdR by the various tissues was very low. The blood, liver, spleen, kidney and thyroid accumulated the most radioactivity of the tissues examined 15 minutes after injection (Table XXII). The injected radioactivity was rapidly cleared from the blood which accounted for only 2% of the injected dose after 15 minutes. However the concentration of radioactivity in the blood remained at this level up to 8 hours post injection whereas the other tissues exhibited a gradual decrease in radioactivity level as a function of time. This was indicated by the general trend of decreasing tissue : blood levels as a function of time (Table XXIII). The skin and stomach were the only tissues to demonstrate consistently high tissue : blood ratios during the course of the experiment. This probably reflected uptake of free radioiodide released from 2'-[^{123}I]-IUdR *in vivo*.

Chromatographic analysis of the urine indicated that excretion of unchanged 2'-[^{123}I]-IUdR accounted for most of the early post injection radioactivity with 39% of the injected dose excreted as 2'-[^{123}I]-IUdR within 7 hours (Table XXIV). The balance of the urinary radioactivity

TABLE XXII. Percent Dose of ^{123}I Incorporated per Whole Organ of Walker 256 Carcinosarcoma Bearing Wistar Rats after Injection of 2'-[^{123}I]-Iodo-2'-deoxyuridine.

		Time in minutes							
Tissue		15	30	60	120	240	480	960	1560
Blood	$\bar{X}$	2.10	2.42	2.21	2.78	2.28	2.91	0.212	0.097
	SD	0.11	0.28	0.69	0.40	0.93	0.35	0.041	0.074
Liver	$\bar{X}$	12.10	10.51	7.01	4.21	1.95	1.32	0.103	0.072
	SD	0.31	1.25	1.59	0.58	0.17	0.30	0.016	0.020
Spleen	$\bar{X}$	1.09	1.36	1.00	0.52	0.23	0.13	0.007	0.005
	SD	0.15	0.05	0.26	0.07	0.08	0.01	0.001	0.002
Kidney	$\bar{X}$	1.32	1.17	0.66	0.46	0.24	0.17	0.010	0.005
	SD	0.20	0.11	0.15	0.07	0.02	0.02	0.003	0.002
Tumor	$\bar{X}$	0.22	0.55	0.38	0.40	0.21	0.12	0.015	0.003
	SD	0.08	0.20	0.04	0.05	0.09	0.01	0.004	0.002
Thyroid	$\bar{X}$	1.11	0.56	0.41	0.23	0.11	0.12	0.005	0.002
	SD	0.06	0.11	0.18	0.04	0.02	0.06	0.001	0.001

TABLE XXIII. Tissue:Blood Ratios of Various Tissues in Walker 256 Carcinosarcoma Bearing Wistar Rats after Injection of 2'-[^{123}I]-2'-Iodo-2'-deoxyuridine (n=3).

		Time in minutes							
Tissue		15	30	60	120	240	480	960	1560
Liver	$\bar{X}$	9.21	6.45	4.68	2.15	1.42	0.72	0.54	1.11
	SD	0.49	1.23	1.50	0.57	0.58	0.06	0.06	0.36
Spleen	$\bar{X}$	9.83	9.66	7.02	3.43	2.0[illegible]	0.85	0.61	0.95
	SD	1.46	0.92	1.58	1.00	0.9[illegible]	0.05	0.16	0.33
Kidney	$\bar{X}$	9.96	7.25	4.46	2.64	1.67	[illegible]	0.74	0.88
	SD	2.13	1.21	[illegible]	0.65	0.60	0.01	0.09	0.26
Stomach	$\bar{X}$	2.87	2.35	[illegible]	2.41	3.10	3.82	1.54	2.77
	SD	0.34	0.25	[illegible]	0.22	0.18	0.67	0.12	0.70
GIT	$\bar{X}$	8.46	4.62	[illegible]	1.91	1.43	0.83	0.74	0.90
	SD	2.48	0.78	0.82	0.46	0.27	0.12	0.06	0.26
Muscle	$\bar{X}$	1.35	1.22	0.90	0.71	0.37	0.22	0.22	0.36
	SD	0.09	0.09	0.11	0.20	0.09	0.01	0.03	0.18
Tumor	$\bar{X}$	3.52	4.13	4.35	2.86	2.24	1.12	1.00	1.02
	SD	0.11	0.59	0.80	0.7[illegible]	1.18	0.05	0.26	0.26
Thyroid	$\bar{X}$	11.96	6.95	4.76	2.12	1.40	0.78	0.74	0.73
	SD	1.80	0.96	1.87	0.41	0.68	0.07	0.18	0.38
Skin	$\bar{X}$	1.72	2.13	1.95	1.38	1.42	1.18	1.42	3.90
	SD	0.34	0.32	0.28	0.30	0.51	0.41	0.52	2.02

TABLE XXIV. Whole Body Elimination and Urinary Excretion Analysis After Intravenous Injection of 2'-[^{123}I]-Iodo-2'-deoxyuridine into Male Wistar Rats Bearing a Walker 256 Carcinosarcoma (n = 3).

Time (min) Post Injection	% of Total Dose Excreted[1] $\bar{x}$ ± SD	Proportion (%) of urinary radioactivity associated with:[2] 2'-IUdR $\bar{x}$ ± SD	Iodide $\bar{x}$ ± SD	Unidentified $\bar{x}$ ± SD
30	16.4 ± 5.2	79.3 ± 6.5	16.8 ± 3.2	4.0 ± 3.4
60	20.1 ± 6.7	78.2 ± 0.3	18.2 ± 3.4	3.4 ± 3.2
120	37.1 ± 6.7	73.6[3]	25.3	1.1
240	58.2 ± 7.9	36.6[4]	61.1	2.4
420	71.6 ± 5.4	15.1[4]	65.3	19.7
960	86.9 ± 3.7	-	-	-
1500	90.3 ± 2.8	-	-	-

1. Cumulative excretion of radioactivity from the whole body calculated as 100-fraction remaining in the body at each time period.
2. Determined by silica gel tlc analysis of the urine collected after induction of micturition at each time interval.
3. n = 2
4. n = 1

was attributable to radioiodide and possibly other polar metabolites retaining the ^{123}I moiety. Qualitative analysis of the urine radiochromatograms using the Berthold tlc scanner indicated that the majority of the urinary radioactivity was associated with two distinct peaks corresponding to 2'-IUdR and iodide. Seventy-two percent of the total dose was excreted within 7 hours and 90% was excreted within 25 hours after injection.

The whole body elimination of ^{123}I as a function of time after the injection of 2'-[^{123}I]-IUdR is compared (Figure 11) with the elimination profile of ^{123}I after injection of sodium iodide-123. The excretion profile of 2'-[^{123}I]-IUdR could not be resolved as a simple bi-exponential, in contrast to the two-compartment model calculated for the elimination of 2'-[^{82}Br]-BrUdR[164]. The complex elimination profile was due in part to the degradation of 2'-[^{123}I]-IUdR to radioiodide. Iodide also has a complex elimination profile due to the diversity of its metabolism, including active incorporation by the thyroid, stomach and skin of the rat[171]. The excretion profile of $Na^{123}I$ was similar to those reported by others[182].

The relative tissue concentrations of ^{123}I following injection of 2'-[^{123}I]-IUdR indicated that the tumor did not reach a sufficient tumor : background tissue ratio to allow tumor imaging. This was also evident from the gamma ray camera studies (Plate 1) in which the only distinguishable features were the liver and urinary bladder. The uptake of ^{123}I into the tumor leg versus the control leg was compared by computer analysis of the gamma-camera image recorded after injection of 2'-[^{123}I]-IUdR (Plate 2). The activity versus time profile (Plate 2A) plotted over the initial 24 minutes after injection of 2'-[^{123}I]-IUdR indicated that the concentration of ^{123}I in the tumor leg remained constant during the same time period for which the ^{123}I activity in the control leg showed a steady decline. This suggested that some of the ^{123}I in the tumor may have been trapped (perhaps metabolically) while the control muscle ^{123}I activity may have been due primarily to blood perfusion. The histogram (Plate 2B) also indicated that the level of ^{123}I activity in the tumor leg was greater than that in the control leg,

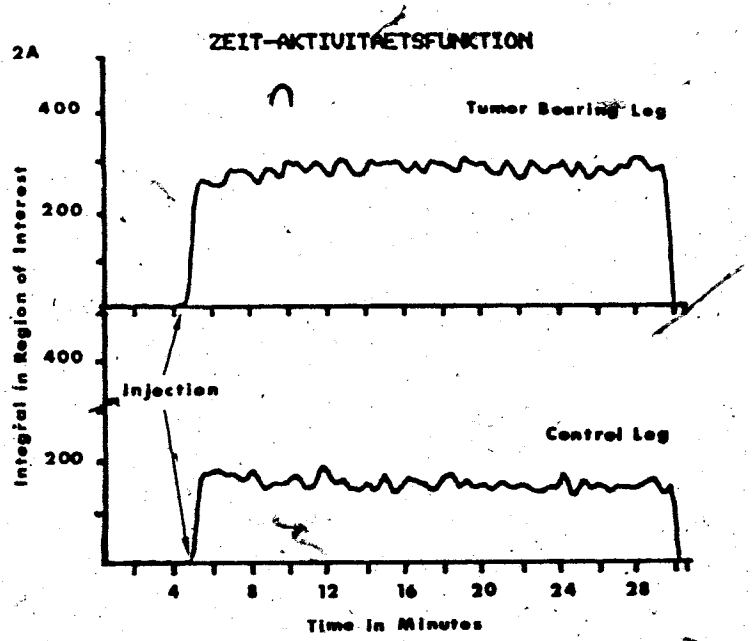

Plate 2. Time-Activity Profiles Comparing Tumor and Control Muscle (Leg) Activity Following Injection of 2'[I-123]-IUdR into a Wistar Rat Bearing an Intramuscular Walker 256 Carcinoma
A. Time versus Activity Profile of Tumor and Control Muscle Immediately Following Injection
B. Histogram Comparing Tumor and Control Muscle Activity 30 Minutes After Injection

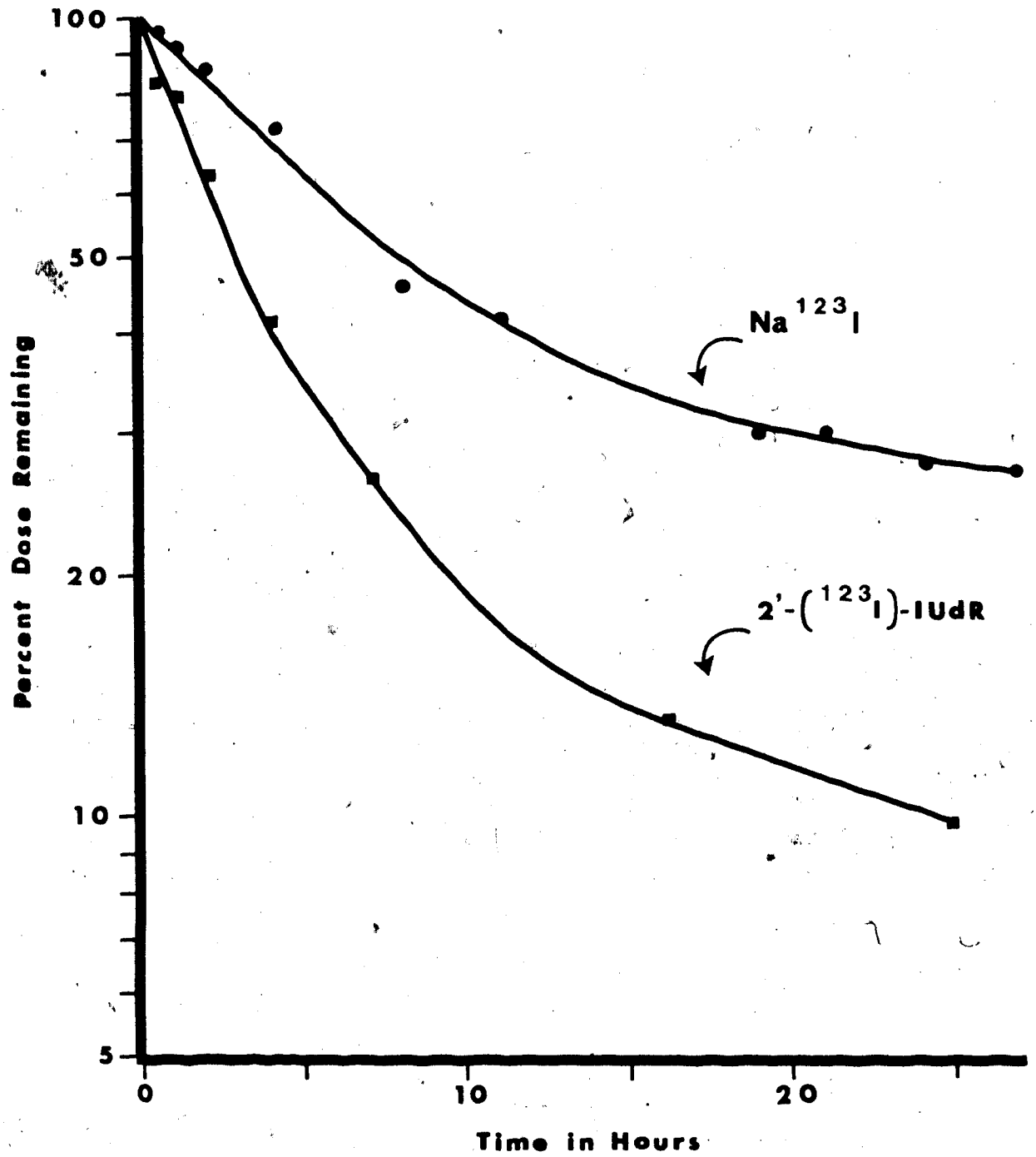

Figure 11. Whole Body Radioactivity Profile After Intravenous Injection of 2'-[^{123}I]-IUdR or ^{123}I-NaI in Wistar Rats.

30 minutes after injection of 2'-[^{123}I]-IUdR. The difference in uptake between the tumor and the muscle detected by the gamma-camera was not as great as the tumor : muscle ratios calculated from the tissue distribution data (15 min = 2.6 and 30 min = 3.3). Delineation of the tumor was poor with 2'-[^{123}I]-IUdR (Plates 1 and 2B).

Substitution of the 2'-hydroxyl influences the conformation assumed by nucleoside analogues but it is difficult to predict what the effect of a given substituent would be. The furanose ring conformation exists in a dynamic equilibrium between two pucker conformations in which either the C-2'(S) or the C-3'(N) atom is furthest away from the plane of the other atoms of the ribose ring[183,184]. The unsubstituted ribosides favor a conformational equilibrium approximately 50% N and 50% S while the deoxynucleosides favor a predominantly S equilibrium[185]. The effect which the C-2' or C-3' substituent has on the conformational equilibria of nucleoside analogues has been attributed to steric repulsion, electrostatic interactions (substituent electronegativity and polarity), hydrogen bonding and other factors[186]. None of these factors alone completely accounts for the conformational preferences assumed by the analogues studied[17,186].

Fluorine has a van der Waals radius (1.35 Å) between that of hydrogen (1.20 Å) and oxygen (1.40 Å) but is more electronegative than either functional group (F = 4.0, O = 3.5, H = 2.1). Chlorine (1.80 Å) is larger than oxygen but is less electronegative (3.0) while bromine (1.95 Å) and iodine (2.16 Å) are larger than oxygen and compare more favorably with the methyl group (2.0 Å) in both size and electronegativity (Br = 2.8, I = 2.4 and CH_3 = 2.5)[187].

The data presented by Cushley et al.[18] and Guschelbauer and Jankowski[17] indicated that the conformational equilibria (relative contributions of the N and S states as determined by the $J_{1',2'}$ coupling constants) of 2'-IUdR, 2'-BrUdR and 2'-ClUdR was between the conformational equilibria favored by uridine and 2'-deoxyuridine. The conformational equilibrium assumed by 2'-FUdR favored the N state to a greater extent than that observed for uridine. The 2'-halogenated deoxyuridine analogues are therefore considered to be analogues of uridine rather than 2'-deoxyuridine.

The rapid blood clearance and high liver radioactivity after injection of 2'-[^{123}I]-IUdR and 6-[^{3}H]-2'-FUdR was qualitatively similar to the profile presented by 5-[^{3}H]-uridine[180]. Unlike uridine, 2'-[^{123}I]-IUdR and 2'-[^{36}Cl]-ClUdR were not rapidly metabolized and large proportions of the early urinary radioactivity was due to unchanged nucleoside (2'-[^{123}I]-IUdR = 73.6% after 2 hours and 2'-[^{36}Cl]-ClUdR = 85.3% after 3 hours). The rapid clearance and constant decrease of ^{36}Cl activity from the blood was in contrast to the kinetics of 6-[^{3}H]-2'-FUdR and 2'-[^{123}I]-IUdR in the blood stream. Caution must be exercised when comparing the tissue distribution of 2'-[^{36}Cl]-ClUdR to 6-[^{3}H]-2'-FUdR and 2'-[^{123}I]-IUdR since the former was studied in a mouse model and the latter in a rat model. Differences in size and metabolism must be considered as factors in any observed differences. After this work was completed, it was learned that cultured Walker 256 carcinosarcoma cells lack NBMPR binding sites, which suggests that these cells have either an atypical or an uncharacterized nucleoside transport mechanism[188]. Therefore, the low tumor uptake of 6-[^{3}H]-2'-FUdR and 2'-[^{123}I]-IUdR observed for the rat Walker 256 carcinosarcoma may not be characteristic

of the analogues but rather characteristic of the tumor. This suggests that other tumor models should be tested before the analogues are considered unsuitable. In addition, 2'-FUdR should be tested with a ^{18}F label since the distribution of radioactivity after injection of 2'-FUdR analogues labelled with ^{3}H or ^{14}C in the base would be different than the distribution of ^{18}F activity.

The value of a tumor delineating agent is determined by its degree of tumor specificity, which is a function of the absolute amount of radioactivity in the tumor and the ratio between the radioactivity in the tumor and the blood and surrounding tissues. Both of these parameters are dynamic, changing with time after injection. In order to compare the relative utility of tumor localizing agents, it has been suggested that a tumor index be applied which would consider the effect of the changing concentration of radioactivity in the tumor and in the background. The tumor index proposed by Emrich et al.[146] is calculated as the tumor uptake (percent injected dose incorporated per gram tumor) multiplied by the tumor : blood ratio. Blood represents a ubiquitous background value, but other more specific background tissues for specific tumors have been used. The tumor indices for the nucleoside and base analogues tested, using whole blood as the background tissue, are given in Table XXV. In terms of tumor index, 2'-[^{36}Cl]-ClUdR would be predicted to be the best tumor imaging agent of the nucleosides in the series. The index also predicts that the best time for imaging would be between 15 and 30 minutes, which is well within the effective half-life of ^{34m}Cl labelled 2'-ClUdR. The comparison between 2'-ClUdR and the other analogues must take into consideration the differences

in specific activity and tumor models used for these studies, as discussed previously.

TABLE XXV. Tumor Index[1] in Relation to Time After Administration.

Radiopharmaceutical	Time after administration (min)										
	15	30	60	90	120	180	240	360	480	960	1560
6-[^{123}I]-IU	0.18	0.22	0.23	-	0.18	-	0.09	-	0.03	0.001	0.002
6-[^{3}H]-2'-FUdR	0.31	0.24	0.18	-	0.12	-	0.10	0.15	-	-	-
2'-[^{36}Cl]-ClUdR	9.60	12.72	8.17	6.91	6.56	10.84	-	-	-	-	-
2'-[^{123}I]-IUdR	1.90	2.99	2.96	-	1.63	-	0.73	-	0.27	0.016	0.007

1. Tumor indices calculated as proposed by Emrich *et al.*[146].

V. SUMMARY AND CONCLUSIONS

A summary of the experimental results is presented in Table XXVI a-c. The recovery of anhydrous hydrogen fluoride-18 for the synthesis of 2'-[^{18}F]-FUdR was most successful when the ^{20}Ne(d,α)^{18}F nuclear reaction was used. Carrier anhydrous hydrogen fluoride was required to recover appreciable yields of ^{18}F with the result that the specific activity of the ^{18}F recovered was low. The chemical and radiochemical yields obtained did not provide sufficient 2'-[^{18}F]-FUdR for tissue distribution studies.

The ^{34}S(p,n)^{34m}Cl nuclear reaction provided the best compromise between radiochemical yield and specific activity for the production of ^{34m}Cl. The ^{34m}Cl could be recovered from the target gas and 2'-[^{34m}Cl]-ClUdR could be synthesized within two half-lives of ^{34m}Cl. The short time required for the preparation of 2'-[^{34m}Cl]-ClUdR would allow sufficient time for use of 2'-[^{34m}Cl]-ClUdR as a tumor imaging agent. The yield of ^{34m}Cl could have been increased further through the use of an enriched ^{34}S target material. Hydrogen sulfide was not an ideal target material due to the production of elemental sulfur during irradiation. The use of a solid target could perhaps obviate the problems associated with a gaseous H_2S target, thereby giving an increased recovery of ^{34m}Cl from the target material.

2'-[^{123}I]-Iodo-2'-deoxyuridine was synthesized in high yield in the presence of a small amount of carrier iodide. No-carrier-added 2'-[^{123}I]-IUdR was synthesized in low radiochemical yield. The presence of sodium hydroxide or sodium chloride in the reaction mixture interfered with the synthesis of radioiodinated 2'-IUdR.

6-[^{123}I]-Iodouracil was readily synthesized by iodide-123 exchange on 6-chlorouracil in the presence of carrier iodide. The yield of

6-[^{123}I]-iodouracil was dependent upon the iodide concentration which limited the product specific activity. No-carrier-added 6-[^{123}I]-iodouracil could not be synthesized by this method.

The tissue distribution data for 2'-[^{123}I]-IUdR, 6-[^{3}H]-2'-FUdR and 6-[^{123}I]-iodouracil in the Walker 256 carcinosarcoma tumor model indicated that the low tumor uptake of radioactivity and the high blood and background radioactivity would preclude the use of these agents for tumor imaging. The tissue distribution studies for 2'-[^{36}Cl]-ClUdR in the Lewis Lung carcinoma tumor model indicated higher tumor uptake and lower background radioactivity for 2'-[^{36}Cl]-ClUdR than observed for the other analogues.

More than one tumor model should be used to evaluate radiolabelled nucleosides for tumor imaging before definitive conclusions regarding their applicability are drawn. This conclusion is based upon the observed differences in the uptake patterns of the labelled compounds by the Walker 256 and the Lewis Lung tumor models. It has also recently been suggested that cultured Walker 256 carcinosarcoma cells lack NBMPR binding sites which indicates that these cells either do not transport nucleosides or transport them via an undemonstrated transport mechanism. Therefore, tumor models which demonstrate more typical nucleoside transport capabilities than the Walker 256 model may be more suitable for evaluating nucleoside analogues as potential tumor imaging agents.

TABLE XXVIa. Summary of Results: Radionuclide Production.

Product	Nuclear Reaction	Target Material	Recovery Conditions	Recovery %[1]
^{18}F	$^{20}Ne(d,\alpha)^{18}F$	Neon	^{18}F eluted from target with normal saline and distilled from conc. H_2SO_4.	54.7
^{18}F	$^{20}Ne(d,\alpha)^{18}F$	Neon	^{18}F eluted from target with anhydrous HF.	69.0
^{34m}Cl	$^{34}S(p,n)^{34m}Cl$	H_2S	^{34m}Cl removed from target gas on anion exchange resin.	14.4

[1]. Values obtained under optimum conditions.

TABLE XXVIb. Summary of Results: Radiochemical Synthesis.

Product	Molar Ratio halide:substrate	Time min	Temp °C	Yield %
6-[^{36}Cl]-Chlorouracil	1.1	31	152	77.1
6-[^{123}I]-Iodouracil	1.0	118	150	55.4
6-[^{3}H]-2,2'-Cyclouridine	-	16	153	83.7
2'-[^{18}F]-FUdR	49.0	61	185	0.4
2'-[^{36}Cl]-ClUdR	1.0	30	163	29.8
2'-[^{34m}Cl]-ClUdR	1.1	10	140	36.0
2'-[^{123}I]-IUdR	0.5	25	135	84.0
2'-[^{123}I]-IUdR	NCA	15	133	21.0
2'-[^{125}I]-IUdR	0.5	16	148	47.0

TABLE XXVIc. Summary of Results: Tissue Distribution.

Analogue	Tumor Uptake % / organ[1] (min)[2]	Tumor:Blood Ratio[1] (min)[2]	Emrich Tumor Ratio[1] (min)[2]
6-[^{123}I]-Iodouracil	1.58 (15)	0.86 (240)	0.23 (60)
6-[^{3}H]-2'-FUdR	0.41 (15)	1.00 (15)	0.31 (15)
2'-[^{36}Cl]-ClUdR	2.42 (30)	5.58 (180)	12.72 (30)
2'-[^{123}I]-IUdR	0.55 (30)	4.35 (60)	2.99 (30)

[1]. Maximum values observed.
[2]. Time after injection.

VI. BIBLIOGRAPHY

1. Houghton PJ, Houghton JA and Taylor DM: Effects of Cytotoxic Agents on TdR Incorporation and Growth Delay in Human Colonic Tumour Xenografts. Brit. J. Cancer 36: 206, 1977.

2. Denekamp J: Tumour Regression as a Guide to Prognosis: A Study with Experimental Animals. Brit. J. Radiol. 50: 271, 1977.

3. Robins AB and Taylor DM: Iodine-123-iododeoxyuridine: A Potential Indicator of Tumour Response to Treatment. Int. J. Nucl. Med. Biol. 8: 53, 1981.

4. Crawford E, Friedkin M, Fowler J, Gallagher B, MacGregor R, Wolf A, Wodinsky I and Goldin A: 6-[F-18]Fluorouridylate as a Probe for Measuring RNA Synthesis and Tumor Growth Rates in vivo. J. Nucl. Med. 19: 702, 1978.

5. McCready VR: Tumour Localization. Brit. Med. Bull. 36: 209, 1980.

6. DeNardo GL, Krohn KA and DeNardo SJ: [illegible]rison of Oncophi[illegible] Radiopharmaceuticals, *I-Fibrinogen, [illegible]Ga-Citrate, ^{111}In-[illegible] and *I-Bleomycin in Tumor-Bearing Mice. Cancer 40: 2923, 1[illegible].

7. Larson SM, Milder MS and Johnston GS: Interpretation of the ^{67}Ga Photoscan. J. Nucl. Med. 14: 208, 1973.

8. Houghton PJ and Taylor DM: Fractional Incorporation of [^{3}H]-Thymidine and DNA Specific Activity as Assays of Inhibition of Tumour Growth. Brit. J. Cancer 35: 68, 1977.

9. Christman D, Crawford EJ, Friedkin M and Wolf AP: Detection of DNA Synthesis in Intact Organisms with Positron-Emitting [Methyl-^{11}C]Thymidine. Proc. Nat. Acad. Sci. USA 69(4): 988, 1972.

10. Crawford EJ, Christman D, Atkins H, Friedkin M and Wolf AP: Scintigraphy with Positron-Emitting Compounds. I. Carbon-11 Labeled Thymidine and Thymidylate. Int. J. Nucl. Med. Biol. 5: 61, 1978.

11. Prusoff WH, Jaffe JJ and Gunther H: Studies in the Mouse of the Pharmacology of 5-Iododeoxyuridine, An Analogue of Thymidine. Biochem. Pharmacol. 3: 110, 1960.

12. Shani J, Wolf W, Schlesinger T, Atkins HL, Bradley-Moore PR, Casella V, Fowler JS, Greenberg D, Ido T, Lambrecht RM, MacGregor R, Mantescu C, Neirinckx R, Som P, Wolf AP, Wodinsky I and Meany K: Distribution of ^{18}F-5-Fluorouracil in Tumor Bearing Mice and Rats. Int. J. Nucl. Med. Biol. 5: 19, 1978.

13. Abrams DN, Knaus EE and Wiebe LI: Tumor Uptake of Radiolabelled Pyrimidine Bases and Pyrimidine Nucleosides in Animal Models. I. 6-[^{3}H]-5-Fluorouracil. Int. J. Nucl. Med. Biol. 6: 97, 1979.

14. Abrams DN, Knaus EE, Lentle BC and Wiebe LI: Tumor Uptake of Radiolabelled Pyrimidine Bases and Pyrimidine Nucleosides in Animal Models: II. 6-[^{3}H]-5-Fluoro-2'-deoxyuridine. Int. J. Nucl. Med. Biol. 6: 103, 1979.

15. Abrams DN, Knaus EE, McQuarrie SA and Wiebe LI: "^{18}F-5-Fluoro-2'-deoxyuridine as a Radiopharmaceutical for Diagnostic Oncology". In The Chemistry of Radiopharmaceuticals, Heindel ND, Burns HD, Honda T and Brady LW (Eds), Masson Publishing USA, N.Y., 1978, p. 205.

16. Hartmann KU and Heidelberger C: Studies on Fluorinated Pyrimidines. XIII. Inhibition of Thymidylate Synthetase. J. Biol. Chem. 236: 3006, 1961.

17. Guschlbauer W and Jankowski K: Nucleoside Conformation is Determined by the Electronegativity of the Sugar Substituent. Nucleic Acids Res. 8(6): 1421, 1980.

18. Cushley RJ, Codington JF and Fox JJ: Nucleosides. XLIX. Nuclear Magnetic Resonance Studies of 2'- and 3'-Halogenonucleosides. The Conformations of 2'-deoxy-2'-fluorouridine and 3'-deoxy-3'-fluoro-β-D-arabinofuranosyluracil. Can. J. Chem. 46: 1131, 1968.

19. Horwitz JP and Tomson AJ: Some 6-Substituted Uracils. J. Org. Chem. 26: 3392, 1961.

20. Griff ERN: "The Beginnings of Nuclear Medicine". In Goldens Diagnostic Radiology: Diagnostic Nuclear Medicine, Gottschalk A and Potchen EJ (Eds), The Williams and Wilkins Co., Baltimore, MD, USA, 1976, p. 1.

21. Edwards CL: Tumor-Localizing Radionuclides in Retrospect and Prospect. Seminars in Nucl. Med. IX(3): 186, 1979.

22. Freedman GS: Radionuclide Tomography. Seminars in Nucl. Med. IX(3): 201, 1979.

23. Kreel L: Diagnostic Imaging: Introduction. Brit. Med. Bull. 36(3): 205, 1980.

24. Britton KE: Dynamic Radionuclide Imaging. Brit. Med. Bull. 36(3): 215, 1980.

25. Alavi A, Reivich M, Greenberg J, Hand P, Rosenquist A, Rintlemann W, Christman D, Fowler J, Goldman A, MacGregor R and Wolf A: Mapping of Functional Activity in Brain with ^{18}F-Fluoro-Deoxyglucose. Seminars in Nucl. Med. XI(1): 24, 1981.

26. Winchell HS: Mechanism for Localization of Radiopharmaceuticals in Neoplasms. Seminars in Nucl. Med. VI(4): 371, 1976.

27. Dendy PP, Sharp PF, Keyes WI and Mallard JR: Radionuclide Emission Imaging - Single-Photon Techniques Including Radiopharmaceutical Developments. Brit. Med. Bull. 36(3): 223, 1980.

28. Wolf AP: Special Characteristics and Potential for Radiopharmaceuticals for Positron Emission Tomography. Seminars in Nucl. Med. XI(1): 2, 1981.

29. Myers MJ, Keyes WI and Mollard JR: "An Analysis of Tomographic Scanning Systems", In Proc. of IAEA Symposium on Medical Radioisotope Scintigraphy, Monte Carlo, Monaco, October 1972.

30. Counsell RE and Ice RD: "The Design of Organ Imaging Radiopharmaceuticals". In Drug Design VI, Ariens EJ (Ed), Academic Press, New York, 1975, p. 171.

31. Wagner HN Jr and Emmons H: "Characteristics of An Ideal Radiopharmaceutical". In Radioactive Pharmaceuticals, Andrews GA, Knisley RM and Wagner HN (Eds), US Atomic Energy Commission, Oak Ridge, Tennessee, 1966, p. 1.

32. deKleijn JP: "Fluorine-18 Labelled Compounds", Free University of Amsterdam, Ph.D. Thesis, 1978.

33. Browne E, Dairiki JM and Doebler RE: Table of Isotopes, Lederer CM and Shirley VS (Eds), Wiley Interscience, Wiley and Sons Inc., Toronto, 7th ed., 1978.

34. Lambrecht RM and Wolf AP: "Cyclotron Production of Radiohalogens and Their Use in Excitation Labeling". In Radiopharmaceuticals, Subramanian G, Rhodes BA, Cooper JF and Sodd VJ (Eds), Soc. Nucl. Med., New York, 1975, p. 111.

35. Lambrecht RM and Wolf AP: "Cyclotron and Short-Lived Halogen Isotopes for Radiopharmaceutical Applications". In Radiopharmaceuticals and Labelled Compounds Vol. I, IAEA, Vienna, 1973, p. 275.

36. Elsevier's Dictionary of Nuclear Science and Technology, 2nd ed, Clason WE (Ed), Elsevier Publishing Company, Amsterdam, 1970.

37. Henderson JF and Paterson ARP: Nucleotide Metabolism. An Introduction, Academic Press, New York, 1973.

38. Bloch A: The Structure of Nucleosides in Relation to Their Biological and Biochemical Activity: A Summary. Ann. N.Y. Acad. Sci. 255: 576, 1975.

39. Hurst DT: An Introduction to the Chemistry and Biochemistry of Pyrimidines, Purines and Pteridines, John Wiley and Sons, Chichester, England, 1980.

40. Gots JS: Metabolic Pathways Map 1: Pyrimidines and Purines, Calbiochem-Behring Corp. SR#4110, Doc. No. 4950-578.

40a. Michal G: Biochemical Pathways, Boehringer Mannheim GMBH, 1978.

41. Roy-Burman P: Analogues of Nucleic Acid Components. Mechanism of Action, Springer-Verlag, Berlin, 1970, pp. 36-39.

42. Cory JG, Breland JC and Carter GL: Effect of 5-Fluorouracil on RNA Metabolism in Novikov Hepatoma Cells. Cancer Res. 39: 4905, 1979.

43. Enzyme Nomenclature: Recommendations of the International Union of Pure and Applied Chemistry and the International Union of Biochemistry, Elsevier Scientific Publishing Co., Netherlands, 1973.

44. Hall TC: Basis for Clinical Resistance to Antitumor Nucleoside Analogs. Ann. N.Y. Acad. Sci. 255: 235, 1975.

45. Physiological and Regulatory Functions of Adenosine and Adenine Nucleotides. Bauer HP and Drummond GI (Eds), Raven Press, New York, New York, 1979.

46. Cooper GM and Greer S: Irreversible Inhibition of Dehalogenation of 5-Iodouracil by 5-Diazouracil and Reversible Inhibition by 5-Cyanouracil. Cancer Res. 30: 2937, 1970.

47. Paterson ARP: "Adenosine Transport". In Physiological and Regulatory Functions of Adenosine and Adenine Nucleotides. Bauer HP and Drummond GI (Eds), Raven Press, New York, 1979, p. 305.

48. Paterson ARP, Kolassa N and Cass CE: Transport of Nucleoside Drugs in Animal Cells. Pharmacol. Ther. 12: 515, 1981.

49. Plageman PGW, Wohlheuter RM and Erbe J: Facilitated Transport of Inosine and Uridine in Cultured Mammalian Cells is Independent of Nucleoside Phosphorylases. Biochim. Biophys. Acta 640: 448, 1981.

50. Hunting D, Hordern J and Henderson JF: Quantitative Analysis of Purine and Pyrimidine Metabolism in Chinese Hamster Ovary Cells. Can. J. Biochem. 59: 838, 1981.

51. Michelson AM: The Chemistry of Nucleosides and Nucleotides, Academic Press Inc., London, 1963.

52. Bloch A: "The Design of Biologically Active Nucleosides". In Drug Design IV, Ariens EJ (Ed), Academic Press, New York, 1973, p. 286.

53. Jurovčik M and Holý A: Metabolism of Pyrimidine L-Nucleosides. Nucleic Acids Res. 3(8): 2143, 1976.

54. Holmes WL: Studies on the Mode of Action of Analogues of Orotic Acid: 6-Uracilsulfonic Acid, 6-Uracilsulfonamide and 6-Uracil Methyl Sulfone. J. Biol. Chem. 223: 677, 1956.

55. Byrd RA, Dawson WH, Ellis PD and Dunlap RB: ^{19}F Nuclear Magnetic Resonance Investigation of the Ternary Complex Formed Between Native Thymidylate Synthetase, 5-Fluoro-2'-deoxyuridylate and 5,10-Methylenetetrahydrofolate. J. Am. Chem. Soc. 99: 6139, 1977.

56. Notari RE, Witiak DT, DeYoung JL and Lin AJ: Comparative Kinetics of Cytosine Nucleosides. Influence of a 6-Methyl Substituent on Degradation Rates and Pathways in Aqueous Buffers. J. Med. Chem. 15(12): 1207, 1972.

57. Wataya Y, Kawada R, Itadani A, Hayatsu H, Bruice TW, Garrett C, Matsuda A and Santi DV: Use of α-Secondary Isotope Effects in Nucleophile Promoted Reactions of Pyrimidine Derivatives; Evidence for Transient 5,6-Dihydropyrimidine Intermediates. Nucleic Acids Res. Symp. Ser. 8: 555, 1980.

58. Gut J, Morávek J, Párkányi C, Prystaš M, Škoda J and Šorm F: Nucleic Acid Components and Their Analogs. III. Antimicrobial Effect of Some Pyrimidine Analogs and Related Compounds. Collect. Czech. Chem. Commun. 24(2): 3154, 1959.

59. Holý A, Bald RW and Šorm F: Nucleic Acid Components and Their Analogs. CXLVI. Preparation of Some Nucleotide Derivatives of 6-Methyluridine, 3-(β-D-Ribofuranosyl)uracil and 3-(β-D-Ribofuranosyl)-6-methyluracil. Investigations of Their Template Activity and Behaviour Towards Some Nucleolytic Enzymes. Collect. Czech. Chem. Commun. 37: 592, 1972.

60. Holý A: A Synthesis of 6-Methyl-2'-deoxyuridine. Tetrahedron Letters, 1147, 1973.

61. Chang PK: Synthesis of Some Hydroxylamine Derivatives of Pyrimidines and Purines. J. Med. Chem. 8: 884, 1965.

62. Wempen I and Fox JJ: Pyrimidines. II. Synthesis of 6-Fluorouracil. J. Med. Chem. 7: 207, 1964.

63. Etzold VG, Baerwolff D, Langen P, Cech D and Meinert H: Synthese und Reactivitaet von 6-Fluor-thymin. J. Prakt. Chemie 313: 602, 1971.

64. Horwitz JP and Tomson AJ: Some 6-Substituted Uracils. J. Org. Chem. 26: 3392, 1961.

65. Bergman ED, Cohen S and Shahak I: Organic Fluorine Compounds. Part XI. Ethyl Fluoroacetoacetates and Fluoropyrimidines. J. Chem. Soc., 3278, 1959.

66. Škoda J, Cihák A, Gut J, Prystaš M, Pískala A, Párkányi C and Šorm F: Nucleic Acid Components and Their Analogues. XXIII. Inhibitors of Growth of Escherichia coli by Derivatives of Pyrimidine, 5-Azauracil, 6-Azauracil and Some Simpler Models of These Derivatives. Collect. Czech. Chem. Commun. 27(2): 1736, 1962.

67. Wempen I and Fox JJ: Pyrimidines. I. The Synthesis of 6-Fluorocytosine and Related Compounds. J. Med. Chem. 6: 688, 1963.

68. Israel M, Protopapa HK, Schlein HN and Modest EJ: Pyrimidine Derivatives. V. Synthesis of Substituted Pyrimidines from 4-Amino-6-chloro-2-methylthiopyrimidine. J. Med. Chem. 7: 5, 1964.

69. von Janta-Lipinski M and Langen P: Synthesis of 6-Substituted Thymine Nucleosides. Nucleic Acids Res. Symp. Ser. 9: 41, 1981.

70. Pichat L, Godbillon J and Herbert M: Préparations de Iodo-6 Thymine, Thymine-(^{3}H-6) et Thymidine-(^{3}H-6). Bull. Soc. Chim., 2719, 1973.

71. Codington JF, Doerr I, Van Praag D, Bendich A and Fox JJ: Nucleosides. XIV. Synthesis of 2'-Deoxy-2'-fluorouridine. J. Am. Chem. Soc. 83: 5030, 1961.

72. Codington JF, Doerr IL and Fox JJ: Nucleosides. XVIII. Synthesis of 2'-Fluorothymidine, 2'-Fluorodeoxyuridine, and Other 2'-Halogeno-2'-deoxy Nucleosides. J. Org. Chem. 29: 558, 1964.

73. Codington JF, Doerr IL and Fox JJ: Nucleosides. XIX. Structure of the 2'-Halogeno-2'-deoxypyrimidine Nucleosides. J. Org. Chem. 29: 564, 1964.

74. Brown DM, Parihar DB, Reese CB and Todd A: Deoxynucleosides and Related Compounds. Part VII. The Synthesis of 2'-Deoxyuridine and of Thymidine. J. Chem. Soc., 3035, 1958.

75. Fox JJ: Personal Communication.

76. Pinto D, Sarocchi-Landousy M-T and Guschlbauer W: 2'-Deoxy-2'-fluorouridine-5'-triphosphates: A Possible Substrate for E. Coli RNA Polymerase. Nucleic Acids Res. 6(3): 1041, 1979.

77. Reyes P and Heidelberger C: Fluorinated Pyrimidines. XXV. The Inhibition of Thymidylate Synthetase from Ehrlich Ascites Carcinoma Cells by Pyrimidine Analogs. Biochim. Biophys. Acta. 103: 177, 1965.

78. Janik B, Kotick MP, Kreiser TH, Reverman LF, Sommer RG and Wilson DP: Synthesis and Properties of Poly 2'-Fluoro-2'-deoxyuridylic acid. Biochem. Biophys. Res. Commun. 46: 1153, 1972.

79. DeClercq E, Stollar BD, Hobbs J, Fukui T, Kakiuchi N and Ikehara M: Interferon Induction by Two 2'-Modified Double-Helical RNAs, Poly(2'-fluoro-2'-deoxyinosinic acid) . Poly(cytidylic acid) and Poly(2'-chloro-2'-deoxyinosinic acid) . Poly(cytidylic acid). Eur. J. Biochem. 107: 279, 1980.

80. Stubbe J and Kozarich JW: Fluoride, Pyrophosphate, and Base Release from 2'-Deoxy-2'-fluoronucleoside 5'-Diphosphates by Ribonucleoside Diphosphate Reductase. J. Biol. Chem. 255: 5511, 1980.

81. Thelander L, Larsson B, Hobbs J and Eckstein F: Active Site of Ribonucleoside Diphosphate Reductase from Escherichia coli. J. Biol. Chem. 251: 1398, 1976.

82. Burchenal JH, Currie VE, Dowling MD, Fox JJ and Krakoff IH: Experimental and Clinical Studies on Nucleoside Analogs as Antitumor Agents. Ann. N.Y. Acad. Sci. 255: 202, 1975.

83. Hobbs J, Sternbach H and Eckstein F: Poly 2'-Deoxy-2'-chloro-uridylic and -cytidylic Acids. FEBS Letters 15: 345, 1971.

84. Hobbs J, Sternbach H, Sprinzl M and Eckstein F: Polynucleotides Containing 2'-Chloro-2'-deoxyribose. Biochemistry 11: 4336, 1972.

85. Watanabe KA, Reichman U, Chu CK, Hollenberg DH and Fox JJ: Nucleosides.116. 1-(β-D-Xylofuranosyl)-5-fluorocytosines with a Leaving Group on the 3' Position. Potential Double-Barreled Masked Precursors of Anticancer Nucleosides. J. Med. Chem. 23: 1088, 1980.

86. Ikehara M, Fukui T and Kakiuchi N: Synthesis and Properties of Poly(2'-chloro- and 2'-bromo-2'-deoxyadenylic acid). Nucleic Acids Res. Spec. Publ. No. 3, s135, 1977.

87. Brown DJ: The Pyrimidines, Interscience Publishers, New York, 1962.

88. Palmer MH: The Structure and Reactions of Heterocyclic Compounds, Edward Arnold (Publishers) Ltd., London, 1967, pp. 76-88.

89. Robins MJ: Chemical Transformations of Naturally Occurring Nucleosides to Otherwise Difficultly Accessible Structures. Ann. N.Y. Acad. Sci. 255: 104, 1975.

90. Shannahoff DH and Sanchez RA: 2,2'-Anhydropyrimidine Nucleosides. Novel Syntheses and Reactions. J. Org. Chem. 38: 593, 1973.

91. Moffatt JG: "Transformations of the Sugar Moiety of Nucleosides". In Nucleoside Analogues. Chemistry, Biology and Medical Applications, Walker RT, DeClercq E and Eckstein F (Eds), Plenum Press, London, 1979, pp. 71-164.

92. Brown DM, Todd A and Varadarajan S: Nucleotides. XXXVII. The Structure of Uridylic Acids a and b, and A Synthesis of Spongouridine (3-β-D-Arabinofuranosyluracil). J. Chem. Soc., 2388, 1956.

93. Hampton A and Nichol AW: Nucleotides. V. Purine Ribonucleoside 2',3'-Cyclic Carbonates. Preparation and Use for the Synthesis of 5'-Monosubstituted Nucleosides. Biochemistry 5: 2076, 1966.

94. Verheyden JPH, Wagner D and Moffatt JG: Synthesis of Some Pyrimidine 2'-Amino-2'-deoxynucleosides. J. Org. Chem. 36: 250, 1971.

95. Ogilvie KK and Iwacha D: Conversion of Uridine 2',3'-Carbonates to Anhydrouridines. Can. J. Chem. 47: 495, 1969.

96. Fox JJ, Miller N and Wempen I: Nucleosides. XXIX. 1-β-D-Arabinofuranosyl-5-fluorocytosine and Related Arabino Nucleosides. J. Med. Chem. 9: 101, 1966.

97. Brown DM, Parihar DB and Todd A: Deoxynucleosides and Related Compounds. Part VIII. Some Further Transformations of O^2: 2'-Cyclouridine. J. Chem. Soc., 4242, 1958.

98. Fox JJ and Miller NC: Nucleosides. XVI. Further Studies of Anhydronucleosides. J. Org. Chem. 28: 936, 1963.

99. Kikugawa K, Ichino M and Ukita T: Reactions of Methyl Iodide on 2,2'-Anhydro-1-(β-D-arabinofuranosyl)uracil and 2,3'-Anhydro-1-(β-D-xylofuranosyl)uracil. Chem. Pharm. Bull. 17: 785, 1969.

100. Mengel R and Guschlbauer W: A Simple Synthesis of 2'-Deoxy-2'-fluorocytidine by Nucleophilic Substitution of 2,2'-Anhydrocytidine with Potassium Fluoride/Crown Ether. Angew. Chem. Int. Ed. Engl. 17: 525, 1978.

101. Långström B: "On the Synthesis of ^{11}C-Compounds". University of Uppsala, Ph.D. Thesis, 1980.

102. Chase GD and Rabinowitz JL: Principles of Radioisotope Methodology, Burgess Publishing Co., Minneapolis, 3rd ed., 1971.

103. Tewson TJ and Welch MJ: Re: Terminology Concerning Specific Activity of Radiopharmaceuticals. J. Nucl. Med. 22(4): 392, 1981.

104. Wolf AP: Re: Terminology Concerning Specific Activity of Radiopharmaceuticals. J. Nucl. Med. 22(4): 392, 1981.

105. Graham LS, MacDonald NS, Robinson GD and Llacer J: Effect of Positron Energy on Spatial Resolution. J. Nucl. Med. 14: 401, 1973.

106. Clark JC and Silvester DJ: A Cyclotron Method for the Production of Fluorine-18. Int. J. Appl. Radiat. Isotopes 17: 151, 1966.

107. Nusynowitz ML, Feldman MH and Maier JG: A Simple Method of Producing ^{18}F Fluoride for the Study of Bone Disease. J. Nucl. Med. 6: 473, 1965.

108. Patomäki L: Production of ^{18}F for Bone Scanning. Acta Radiol. Ther. Physiol. Biol. 7: 71, 1968.

109. Fry BW, Whitford GM and Pashley DH: A Method for Increasing the Amount of ^{18}F at the Laboratory by Recovery During Transport from the Reactor. Int. J. Appl. Radiat. Isotopes 29: 123, 1978.

110. Hsieh TH, Fan KW, Chuang JT and Yang MH: Preparation of Carrier-Free Fluorine-18. Int. J. Appl. Radiat. Isotopes 28: 251, 1977.

111. Dunson GL, Jones AE and Crofford WM: ^{18}F Production, Processing and Patient Use. J. Nucl. Med. 11: 316, 1970.

112. Tilbury RS, Dahl JR, Mamacos JP and Laughlin JS: Fluorine-18 Production for Medical Use by Helium-3 Bombardment of Water. Int. J. Appl. Radiat. Isotopes 21: 277, 1970.

113. Nozaki T, Iwamoto M and Ido T: Yield of ^{18}F for Various Reactions from Oxygen and Neon. Int. J. Appl. Radiat. Isotopes 25: 393, 1974.

114. Lambrecht RM, Neirinckx R and Wolf AP: Cyclotron Isotopes and Radiopharmaceuticals. XXIII. Novel Anhydrous ^{18}F-Fluorinating Intermediates. Int. J. Appl. Radiat. Isotopes 29: 175, 1978.

115. Lambrecht RM, Mantescu C, Fowler JS and Wolf AP: Novel ^{18}F Intermediates for the Synthesis of Radiopharmaceuticals. J. Nucl. Med. 13: 785, 1972.

116. Nozaki T, Tanaka Y, Shimamura A and Karasawa T: The Preparation of Anhydrous HF^{18}. Int. J. Appl. Radiat. Isotopes 19: 27, 1968.

117. Firnau G, Nahmias C and Garnett S: The Preparation of [^{18}F] 5-Fluoro-DOPA with Reactor-Produced Fluorine-18. Int. J. Appl. Radiat. Isotopes 24: 182, 1973.

118. Gnade BE, Schwaiger GP, Liotta CL and Fink RW: Preparation of Reactor-produced Carrier-free ^{18}F-fluoride as the Potassium 18-Crown-6 Complex for Synthesis of Labelled Organic Compounds. Int. J. Appl. Radiat. Isotopes 32: 91, 1981.

119. Gately SJ, Hichwa RD, Shaughnessy WJ and Nickles RJ: ^{18}F-Labeled Lower Fluoroalkanes; Reactor-produced Gaseous Physiological Tracers. Int. J. Appl. Radiat. Isotopes 32: 211, 1981.

120. Ido T, Irie T and Kasida Y: Isotope Exchange with ^{18}F on Superconjugate System. J. Label. Compd. Radiopharm. XVI: 153, 1979.

121. Gately JS and Shaughnessy WJ: Synthesis of ^{18}F-3-Deoxy-3-fluoro-D-glucose with Reactor-produced ^{18}F. Int. J. Appl. Radiat. Isotopes 31: 339, 1980.

122. Firnau G, Chirakal R, Sood S and Garnett ES: Radiofluorination with Xenon Difluoride: L-6[F-18]Fluoro-DOPA. J. Label. Cmpd. Radiopharm. XVIII(1-2): 7, 1981.

123. Neirinckx RD, Lambrecht RM and Wolf AP: Cyclotron Isotopes and Radiopharmaceuticals. XXV. An Anhydrous ^{18}F-Fluorinating Intermediate: Trifluoromethyl Hypofluorite. Int. J. Appl. Radiat. Isotopes 29: 323, 1978.

124. Straatman M: "Fluorine-18 Production and Chemistry". In Medical Radionuclide Production Vol. 1, Noujaim AA, McQuarrie SA and Wiebe LI (Eds), University of Alberta, Maria Design Symp., Banff, 1980.

125. Donnerhack A and Sattler EL: The Preparation of Fluorine-18 with an Electron Linear Accelerator for Applications in Medical and Biological Investigations. Int. J. Appl. Radiat. Isotopes 31: 279, 1980.

126. Yagi M and Amano R: Production of ^{18}F by Means of Photonuclear Reactions and Preparation of Anhydrous $H^{18}F$. Int. J. Appl. Radiat. Isotopes 31: 559, 1980.

127. Palmer A: Recoil Labelling of Fluorine-18 Labelled Chlorofluoromethanes and Tetrafluoromethane. Int. J. Appl. Radiat. Isotopes 29: 545, 1978.

128. Brinkman GA and Visser J: ^{18}F-Recoil Labelling of CF_3Cl. Int. J. Appl. Radiat. Isotopes 30: 517, 1979.

129. Anbar M and Neta P: Formation of F^{18}-Labeled Fluoro-Organic Compounds by the $F^{19}(n,2n)$ Reaction. J. Chem. Phys. 37: 2757, 1962.

130. Lebowitz E, Richards P and Baranosky J: ^{18}F Recoil Labeling. Int. J. Appl. Radiat. Isotopes 23: 392, 1972.

131. Malcolme-Lawes DJ: The Production of High Specific Activity $^{34m}Cl^-$ by Fast Neutron Irradiation of Chlorocarbons. Int. J. Appl. Radiat. Isotopes 29: 698, 1978.

132. Szilard L and Chalmers TA: Chemical Separation of the Radioactive Element From its Bombarded Isotope in the Fermi Effect. Nature 134: 462, 1934.

133. Anbar M and Neta P: The Preparation of Carrier-Free ^{36}Cl and ^{82}Br. Int. J. Appl. Radiat. Isotopes 14: 634, 1963.

134. Machulla H-J, Stoecklin G, Kupfernagel Ch, Freundlieb Ch, Hoeck A, Vyska K and Feinendegen LE: Comparative Evaluation of Fatty Acids Labeled with C-11, Cl-34m, Br-77 and I-123 for Metabolic Studies of the Myocardium: Concise Communication. J. Nucl. Med. 19: 298, 1978.

135. Bell R and Stoecklin G: The Preparation of Carrier-Free Chlorine-36 via Ligand Recoil in $K_2[ReCl_6]$ and $K_3[RhCl_6]$. Radiochim. Acta. 13: 57, 1970.

136. Brinkman GA and Visser J: Production of $^{34m}Cl^-$. Int. J. Appl. Radiat. Isotopes 30: 515, 1979.

137. Black A and Morgan A: Preparation of Some Chlorine-38 Labelled Chlorinated Hydrocarbons by Neutron Irradiation and Gas Chromatography. Int. J. Appl. Radiat. Isotopes 21: 5, 1970.

138. Zatolokin BV, Konstantinov IO and Krasnov NN: Thick Target Yields of ^{34m}Cl and ^{38}Cl Produced by Various Charged Particles on Phosphorous, Sulfur and Chlorine Targets. Int. J. Appl. Radiat. Isotopes 27: 159, 1976.

139. Ediss C and Abrams DN: Implementation of the Coincidence Method for Determining ^{125}I Activity with an Estimate of Error. J. Radioanal. Chem. 65: 341, 1981.

140. Sheppard G: The Radiochromatography of Labelled Compounds. Amersham/Searle Information Series Review 14, 1973.

141. Helus F, Wolber G, Sahm U, Abrams D and Maier-Borst W: ^{18}F Production Methods. J. Label. Cmpd. Radiopharm. XVI: 214, 1979.

142. Helus F, Maier-Borst W, Sahm U and Wiebe LI: F-18 Cyclotron Production Methods. Radiochem. Radioanal. Letters 38: 395, 1979.

143. Lee YW, Knaus EE and Wiebe LI: Synthesis of 2'-[^{82}Br]-2'-Deoxyuridine. J. Label. Compd. Radiopharm. XVII: 269, 1979.

144. Helus F, Sinn H, Maier-Borst W and Sahm U: ^{123}I-Trapping Mittels Goldfolie. Radiochem. Radioanal. Letters 32: 311, 1978.

145. Brown DM, Parihar DB, Todd A and Varadarajan S: Deoxynucleosides and Related Compounds. Part VI. The Synthesis of 2-Thiouridine and of 3'-Deoxyuridine. J. Chem. Soc., 3028, 1958.

146. Emrich D, von zur Mühlen A, Willgeroth F and Lammich A: Comparison of Tumor Uptake and Kinetics of Different Radiopharmaceuticals Under Experimental Conditions. Acta Radiol. (Ther) (Stockholm) 11: 566, 1972.

147. Hewitt HB: "The Choice of Animal Tumors for Experimental Studies of Cancer Therapy". In Advances in Cancer Research Vol. 27, Klein G and Weinhouse S (Eds), Academic Press, New York, 1978, p. 149.

148. Sugiura K and Stock CC: Studies in a Tumor Spectrum. III. The Effect of Phosphoramides on the Growth of a Variety of Mouse and Rat Tumors. Cancer Res. 15: 38, 1955.

148a. The transplantation technique described is a modification of the method originally demonstrated to the author by Dr. A.R.P.Paterson.

149. Earle WR: A Study of the Walker Rat Mammary Carcinoma 256, In Vivo and In Vitro. Am. J. Cancer 24: 566, 1935.

150. Haynie TP, Konikowski T and Glenn JH: Experimental Models for Evaluation of Radioactive Tumor-localizing Agents. Sem. Nucl. Med. 6: 347, 1976.

151. Wolff J and Chaikoff IL: Plasma Inorganic Iodide as a Homeostatic Regulator of Thyroid Function. J. Biol. Chem. 174: 555, 1948.

152. Wiebe LI and Ediss C: "Methyl Salicylate as a Medium for Radioassay of ^{36}Chlorine Using a Liquid Scintillation Spectrometer". In Liquid Scintillation: Science and Technology, Academic Press Inc., New York, 1976.

153. Wiebe LI, McQuarrie SA, Ediss C, Maier-Borst W and Helus F: Liquid Scintillation Counting of Radionuclides Emitting High Energy Beta Radiation. J. Radioanal. Chem. 60: 385, 1980.

154. Straatman M: "Cyclotron Targetry Description". In Medical Radionuclide Production Vol. 1, Noujaim AA, McQuarrie SA and Wiebe LI (Eds), University of Alberta, Maria Design Symp., Banff, 1980.

155. Casella V, Ido T, Wolf AP, Fowler JS, MacGregor RR and Ruth TJ: Anhydrous F-18 Labeled Elemental Fluorine for Radiopharmaceutical Preparation. J. Nucl. Med. 21: 750, 1980.

156. Fitshen J, Beckmann R, Holm U and Neuert H: Yield and Production of ^{18}F by ^{3}He Irradiation of Water. Int. J. Appl. Radiat. Isotopes 28: 781, 1977.

157. Crouzel C and Comar D: Production of Carrier-Free ^{18}F-Hydrofluoric Acid. Int. J. Appl. Radiat. Isotopes 29: 407, 1978.

158. The program used to perform these calculations was written by H. Gasper of the German Cancer Research Center.

159. Andersen HH and Ziegler JF: Hydrogen Stopping Powers and Ranges in All Elements, Pergamon Press Inc., New York, 1977.

160. Cotton AF and Wilkinson G: Advanced Inorganic Chemistry, A Comprehensive Text, John Wiley and Sons, New York, 1980, p. 523.

161. Cohen BL, Reynolds HL and Zucker A: Comparison of Nitrogen- and Proton-Induced Nuclear Reactions. Phys. Rev. 96: 1617, 1954.

162. Fulmer CB and Goodman CD: (p,α) Reactions Induced by Protons in the Energy Range of 9.5-23 MeV. Phys. Rev. 117: 1339, 1960.

163. Ediss C: Personal Communication.

164. Lee YW, Knaus EE and Wiebe LI: Tumor Uptake of Radiolabeled Pyrimidine Bases and Pyrimidine Nucleosides in Animal Models. III. 2'-[^{82}Br]-Bromo-2'-deoxyuridine. Int. J. Nucl. Med. Biol. 6: 109, 1979.

165. March J: Advanced Organic Chemistry: Reactions, Mechanisms and Structure, McGraw-Hill Book Company, New York, 1968, pp. 488-520.

166. Fieser LF and Fieser M: Reagents for Organic Synthesis Vol. 1, John Wiley and Sons, Inc., New York, 1967, pp. 390-392.

167. Robins MJ: "Chemistry of Naturally Occurring Pyrimidine Nucleosides and Analogues". In Nucleoside Analogues. Chemistry, Biology and Medical Applications, Walker RT, DeClercq E and Eckstein F (Eds), Plenum Press, London, 1979, pp. 165-192.

168. Fieser LF and Fieser M: Reagents for Organic Synthesis Vol. 4, John Wiley and Sons, Inc., New York, 1974, p. 91.

169. Fieser LF and Fieser M: Reagents for Organic Synthesis Vol. 2, John Wiley and Sons, Inc., New York, 1969, p. 453.

170. Abrams DN, Knaus EE, Mercer JR and Wiebe LI: 2'-Fluoro-2'-Deoxyuridine. J. Label. Compd. Radiopharm. XVI: 12, 1979.

171. Gross J: "Iodine and Bromine". In Mineral Metabolism Vol. II(B), Comar CL and Broomer F (Eds), Academic Press, New York, 1962.

172. Gasser T, Moyer JD and Handschumacher RE: Novel Single-Pass Exchange of Circulating Uridine in Rat Liver. Science 213: 777, 1981.

173. Ord MG and Stocken LA: Uptake of Orotate and Thymidine by Normal and Regenerating Rat Livers. Biochem. J. 132: 47, 1972.

174. Rutman RJ, Cantarow A and Paschkis KE: The Catabolism of Uracil In Vivo and In Vitro. J. Biol. Chem. 210: 321, 1954.

175. Prusoff WH, Holmes WL and Welch AD: Nonutilization of Radioactive Iodinated Uracil, Uridine and Orotic Acid by Animal Tissues In Vivo. Canc. Res. 13: 221, 1953.

176. Lea MA, Bullock J, Khalil FL and Morris HP: Incorporation of Precursors and Inhibitors of Nucleic Acid Synthesis into Hepatomas and Liver of the Rat. Cancer Res. 34: 3414, 1974.

177. Wang L: Plasma Volume, Cell Volume, Total Blood Volume and F cells Factor in the Normal and Splenectomized Sherman Rat. Am. J. Physiol. 196: 188, 1959.

178. Gati WP, Knaus EE and Wiebe LI: Interaction of 2'-Halogeno-2'-deoxyuridines with the Human Nucleoside Transport Mechanism. Mol. Pharmacol. (in press).

179. Singh IJ and Tonna EA: Estimation of the Turnover Rates of ^{3}H-Uridine in Mouse Skeletal Tissues During Aging. Exp. Gerontol. 16: 317, 1981.

180. Dahnke H-G and Mosebach K-O: In-vivo-Untersuchungen zur Metabolisierung der Pyrimidinnucleoside. Hoppe-Seyler's Z. Physiol. Chem. 356: 1565, 1975.

181. Moyer JD, Oliver JT and Handschumacher RE: Salvage of Circulating Pyrimidine Nucleosides in the Rat. Cancer Res. 41: 3010, 1981.

182. Zaltzman S, Baron J, Werner A and Chaichik S: Exposure to Radioiodine in the Preconception and Conception Periods. Isr. J. Med. Sci. 16: 856, 1980.

183. Guschlbauer W: Conformational Analysis of Ribonucleosides From Proton-Proton Coupling Constants. Biochim. Biophys. Acta. 610: 47, 1980.

184. Danyluk SS: "Nuclear Magnetic Resonance Studies of Nucleoside Conformational Properties". In Nucleoside Analogues, Walker RT, DeClercq E and Eckstein F (Eds), Plenum Press, London, 1979, pp. 15-34.

185. Olson WK and Sussman JL: How Flexible is the Furanose Ring? I. A Comparison of Experimental and Theoretical Studies. J. Am. Chem. Soc. 104: 270, 1982.

186. Klimke G, Cuno I, Lüdemann H-D, Mengel R and Robins MJ: Xylose Conformations of 9-β-D-Xylofuranosyladenine Analogues Modified at the 2',3' or 5'-Positions and Lyxose Conformations of 9-β-D-Lyxofuranosyl adenine. Z. Naturforsch. 35: 865, 1980.

187. Pauling L: The Nature of the Chemical Bond, Cornell University Press, New York, 3rd ed., 1960.

188. Paterson ARP: Personal Communication.

VII. APPENDICES

APPENDIX 1. Tissue Distribution of 6-[I-123]-Iodouracil in Walker 256 Carcinoma Bearing Wistar Rats

Percent Dose Incorporated per Gram of Tissue

		TIME IN MINUTES 15	30	60	120	240	480	960	1560
BLOOD	$\bar{X}$	1.605	0.989	0.596	0.317	0.172	0.153	0.006	0.007
	SD	0.164	0.320	0.195	0.208	0.077	0.073	0.002	0.005
THYROID	$\bar{X}$	0.637	0.487	0.391	0.143	0.088	0.056	0.005	0.004
	SD	0.198	0.172	0.178	0.062	0.025	0.044	0.002	0.003
HEART	$\bar{X}$	0.467	0.285	0.196	0.103	0.056	0.034	0.002	0.002
	SD	0.044	0.085	0.058	0.061	0.022	0.028	0.000	0.002
LUNG	$\bar{X}$	0.668	0.420	0.271	0.160	0.102	0.059	0.004	0.006
	SD	0.051	0.119	0.069	0.089	0.037	0.043	0.001	0.005
LIVER	$\bar{X}$	0.257	0.202	0.135	0.086	0.048	0.026	0.002	0.002
	SD	0.018	0.037	0.019	0.030	0.016	0.018	0.001	0.002
SPLEEN	$\bar{X}$	0.243	0.166	0.130	0.078	0.058	0.035	0.012	0.003
	SD	0.030	0.035	0.030	0.023	0.017	0.021	n=2	0.002
KIDNEY	$\bar{X}$	1.089	0.835	1.130	0.236	0.151	0.071	0.004	0.005
	SD	0.378	0.362	0.313	0.087	0.069	0.058	0.002	0.003
GIT	$\bar{X}$	0.200	0.145	0.112	0.099	0.074	0.041	0.004	0.006
	SD	0.011	0.028	0.020	0.054	0.019	0.018	0.001	0.005
TESTES	$\bar{X}$	0.097	0.088	0.099	0.097	0.084	0.047	0.004	0.003
	SD	0.014	0.020	0.016	0.037	0.012	0.031	0.001	0.002
STOMACH	$\bar{X}$	0.238	0.192	0.294	0.247	0.390	0.116	0.013	0.014
	SD	0.071	0.016	0.062	0.043	0.226	0.067	0.004	0.004
TUMOUR	$\bar{X}$	0.520	0.455	0.364	0.237	0.121	0.062	0.002	0.004
	SD	0.055	0.082	0.078	0.138	0.049	0.050	0.001	0.003
MUSCLE	$\bar{X}$	0.175	0.111	0.083	0.043	0.027	0.017	0.001	0.001
	SD	0.021	0.025	0.024	0.025	0.008	0.011	n=2	0.001
SKIN	$\bar{X}$	0.357	0.276	0.229	0.167	0.133	0.097	0.011	0.015
	SD	0.036	n=2	0.037	0.036	0.017	0.054	0.005	0.005
BONE	$\bar{X}$	0.194	0.145	0.110	0.074	0.053	0.035	0.023	0.003
	SD	0.024	0.029	0.021	0.025	0.013	0.023	n=2	0.002

Percent Dose Incorporated per Whole Organ

		TIME IN MINUTES 15	30	60	120	240	480	960	1560
BLOOD	$\bar{X}$	28.722	18.154	10.757	5.525	2.969	2.552	0.111	0.113
	SD	2.483	5.697	4.263	3.678	1.374	1.250	0.046	0.073
THYROID	$\bar{X}$	0.571	0.389	0.413	0.110	0.075	0.054	0.004	0.004
	SD	0.236	0.119	0.230	0.050	0.021	0.054	0.002	0.002
HEART	$\bar{X}$	0.392	0.256	0.148	0.088	0.046	0.027	0.002	0.002
	SD	0.050	0.079	0.055	0.053	0.019	0.021	0.000	0.001
LUNG	$\bar{X}$	1.022	0.588	0.344	0.230	0.125	0.072	0.005	0.008
	SD	0.096	0.156	0.097	0.119	0.045	0.047	0.002	0.007
LIVER	$\bar{X}$	2.665	2.045	1.386	0.931	0.457	0.233	0.022	0.025
	SD	0.133	0.223	0.182	0.355	0.176	0.140	0.010	0.014
SPLEEN	$\bar{X}$	0.193	0.136	0.098	0.056	0.040	0.027	0.004	0.002
	SD	0.029	0.020	0.018	0.014	0.013	0.016	n=2	0.001
KIDNEY	$\bar{X}$	0.981	0.796	0.966	0.227	0.134	0.064	0.006	0.010
	SD	0.299	0.341	0.231	0.090	0.065	0.054	0.004	0.005
GIT	$\bar{X}$	0.238	0.183	0.085	0.131	0.070	0.038	0.009	0.013
	SD	0.018	0.047	0.030	0.117	0.027	0.016	0.002	0.009
TESTES	$\bar{X}$	0.139	0.139	0.192	0.145	0.131	0.076	0.013	0.011
	SD	0.010	0.039	0.090	0.055	0.024	0.048	0.002	0.007
STOMACH	$\bar{X}$	0.354	0.284	0.477	0.333	0.609	0.161	0.016	0.017
	SD	0.103	0.038	0.089	0.077	0.424	0.080	0.003	0.004
TUMOUR	$\bar{X}$	1.577	1.118	0.869	0.652	0.289	0.075	0.007	0.013
	SD	0.252	0.359	0.220	0.264	0.182	0.042	0.004	0.007

Blood volume calculated as 6.5 % of body weight
Three animals per data point

APPENDIX 2. Tissue Distribution of 6-[I-123]-Iodouracil in Walker 256 Carcinoma Bearing Wistar Rats

		Tissue Specific Activity in cps/mg								Tissue to Blood Ratios							
		TIME IN MINUTES								TIME IN MINUTES							
		15	30	60	120	240	480	960	1560	15	30	60	120	240	480	960	1560
BLOOD	$\bar{X}$	11.459	7.064	4.259	2.266	1.227	1.093	0.046	0.049	1.000	1.000	1.000	1.000	1.000	1.000	1.000	1.000
	SD	1.172	2.285	1.396	1.483	0.547	0.524	0.017	0.034	0.0	0.0	0.0	0.0	0.0	0.0	0.0	0.0
THYROID	$\bar{X}$	4.547	3.480	2.793	1.019	0.631	0.403	0.032	0.032	0.391	0.512	0.641	0.491	0.549	0.406	0.675	0.661
	SD	1.415	1.225	1.274	0.445	0.178	0.312	0.018	0.019	0.087	0.157	0.187	0.116	0.125	0.238	0.137	0.142
HEART	$\bar{X}$	3.332	2.036	1.401	0.738	0.401	0.244	0.015	0.015	0.291	0.290	0.332	0.334	0.331	0.251	0.341	0.307
	SD	0.313	0.609	0.414	0.435	0.160	0.203	0.003	0.011	0.003	0.015	0.042	0.022	0.031	0.162	0.043	0.035
LUNG	$\bar{X}$	4.771	3.000	1.938	1.146	0.726	0.421	0.032	0.041	0.417	0.429	0.465	0.526	0.610	0.444	0.706	0.794
	SD	0.364	0.851	0.493	0.636	0.261	0.304	0.008	0.035	0.019	0.022	0.087	0.051	0.063	0.270	0.064	0.130
LIVER	$\bar{X}$	1.838	1.443	0.963	0.611	0.344	0.186	0.015	0.017	0.161	0.214	0.237	0.307	0.291	0.197	0.312	0.362
	SD	0.127	0.261	0.133	0.218	0.117	0.128	0.007	0.011	0.006	0.048	0.057	0.084	0.037	0.119	0.049	0.027
SPLEEN	$\bar{X}$	1.734	1.182	0.930	0.555	0.415	0.247	0.085	0.018	0.151	0.173	0.229	0.285	0.360	0.274	0.176	0.398
	SD	0.211	0.252	0.214	0.168	0.122	0.152	n=2	0.012	0.008	0.030	0.068	0.091	0.081	0.178	n=2	0.053
KIDNEY	$\bar{X}$	7.777	5.965	8.072	1.686	1.080	0.504	0.026	0.039	0.668	0.859	2.027	0.840	0.879	0.507	0.663	0.890
	SD	2.700	2.586	2.235	0.618	0.493	0.417	0.015	0.023	0.184	0.271	0.786	0.228	0.193	0.315	0.468	0.324
GIT	$\bar{X}$	1.429	1.035	0.797	0.706	0.531	0.296	0.028	0.045	0.125	0.158	0.201	0.325	0.506	0.329	0.632	0.891
	SD	0.079	0.199	0.146	0.384	0.133	0.128	0.006	0.035	0.012	0.061	0.070	0.039	0.250	0.199	0.086	0.077
TESTES	$\bar{X}$	0.692	0.629	0.704	0.696	0.603	0.338	0.028	0.025	0.061	0.099	0.179	0.350	0.551	0.369	0.632	0.579
	SD	0.097	0.142	0.117	0.263	0.083	0.219	0.006	0.012	0.009	0.048	0.065	0.108	0.205	0.236	0.082	0.162
STOMACH	$\bar{X}$	1.698	1.372	2.098	1.764	2.788	0.826	0.093	0.103	0.148	0.207	0.547	1.001	2.529	0.803	2.172	2.634
	SD	0.506	0.116	0.445	0.310	1.611	0.481	0.028	0.031	0.036	0.061	0.248	0.509	1.349	0.315	1.085	1.205
TUMOR	$\bar{X}$	3.711	3.251	2.596	1.690	0.867	0.444	0.016	0.027	0.324	0.479	0.625	0.768	0.731	0.449	0.400	0.539
	SD	0.395	0.587	0.559	0.987	0.352	0.360	0.007	0.020	0.017	0.086	0.077	0.052	0.135	0.276	0.244	0.034
MUSCLE	$\bar{X}$	1.246	0.791	0.594	0.308	0.193	0.119	0.010	0.010	0.110	0.115	0.141	0.140	0.166	0.129	0.160	0.195
	SD	0.148	0.177	0.174	0.179	0.058	0.079	n=2	0.006	0.016	0.017	0.017	0.010	0.031	0.079	n=2	0.019
SKIN	$\bar{X}$	2.548	1.311	1.633	1.195	0.952	0.696	0.075	0.104	0.223	0.206	0.398	0.638	0.874	0.756	1.908	2.588
	SD	0.255	1.205	0.265	0.257	0.118	0.385	0.033	0.036	0.011	0.183	0.071	0.262	0.334	0.444	1.169	1.002
BONE	$\bar{X}$	1.388	1.038	0.785	0.530	0.377	0.247	0.150	0.021	0.121	0.153	0.193	0.268	0.331	0.265	0.445	0.443
	SD	0.172	0.205	0.149	0.179	0.092	0.163	n=2	0.015	0.008	0.029	0.049	0.080	0.084	0.163	n=2	0.041

APPENDIX 3. Tissue Distribution of 6-[I-123]-Iodouracil Co-injected with 6-ClU in walker 256 Carcinoma Bearing Wistar Rats

		Percent Dose Incorporated per Gram of Tissue								Percent Dose Incorporated per Whole Organ							
		TIME IN MINUTES								TIME IN MINUTES							
		15	30	60	120	240	480	960	1560	15	30	60	120	240	480	960	1560
BLOOD	$\bar{X}$	1.454	1.025	0.882	0.389	0.364	0.166	0.015	0.006	19.854	13.991	12.039	5.305	4.969	2.261	0.208	0.082
	SD	0.210	0.309	0.339	0.155	0.114	0.011	0.006	0.002	2.863	4.217	4.628	2.121	1.551	0.145	0.078	0.033
THYROID	$\bar{X}$	0.412	0.365	0.291	0.160	0.141	0.070	0.008	0.003	0.213	0.205	0.152	0.069	0.059	0.041	0.004	0.001
	SD	0.061	0.088	0.067	n=2	0.011	0.031	0.003	0.001	0.039	0.036	0.053	n=2	0.021	0.006	0.002	0.000
HEART	$\bar{X}$	0.439	0.344	0.284	0.117	0.116	0.046	0.005	0.002	0.353	0.301	0.231	0.092	0.090	0.049	0.004	0.002
	SD	0.048	0.083	0.095	0.030	0.041	0.022	0.002	0.001	0.050	0.073	0.083	0.026	0.038	0.007	0.001	0.001
LUNG	$\bar{X}$	0.673	0.480	0.423	0.200	0.198	0.107	0.011	0.005	0.994	0.665	0.590	0.288	0.302	0.161	0.015	0.006
	SD	0.076	0.088	0.138	0.059	0.026	0.008	0.004	0.002	0.130	0.113	0.202	0.061	0.087	0.006	0.005	0.001
LIVER	$\bar{X}$	0.215	0.228	0.189	0.092	0.080	0.057	0.005	0.003	2.486	2.490	1.936	1.076	0.762	0.564	0.059	0.033
	SD	0.016	0.032	0.058	0.005	0.015	0.009	0.003	0.001	0.046	0.197	0.602	0.156	0.116	0.038	0.025	0.007
SPLEEN	$\bar{X}$	0.243	0.191	0.186	0.107	0.103	0.063	0.006	0.003	0.166	0.120	0.125	0.074	0.065	0.169	0.005	0.002
	SD	0.009	0.019	0.053	0.003	0.014	0.005	0.002	0.001	0.019	0.023	0.036	0.005	0.005	0.220	0.002	0.001
KIDNEY	$\bar{X}$	1.372	0.940	0.903	0.396	0.341	0.108	0.014	0.004	1.165	0.881	0.844	0.360	0.293	0.097	0.013	0.004
	SD	0.732	0.246	0.166	0.077	0.117	0.007	n=2	0.002	0.492	0.167	0.124	0.076	0.094	0.002	n=2	0.002
GIT	$\bar{X}$	0.178	0.177	0.183	0.150	0.175	0.101	0.009	0.005	0.234	0.183	0.215	0.174	0.221	0.132	0.008	0.005
	SD	0.030	0.032	0.019	0.043	0.072	0.034	0.004	0.001	0.025	0.072	0.023	0.042	0.134	0.069	0.004	0.002
TESTES	$\bar{X}$	0.106	0.121	0.159	0.133	0.150	0.080	0.011	0.004	0.160	0.191	0.250	0.215	0.212	0.123	0.018	0.006
	SD	0.013	0.036	0.032	0.025	0.028	0.005	0.004	0.001	0.022	0.054	0.056	0.031	0.042	0.005	0.005	0.002
STOMACH	$\bar{X}$	0.270	0.293	0.441	0.489	0.454	0.290	0.022	0.037	0.416	0.406	0.664	0.744	0.596	0.384	0.032	0.045
	SD	0.045	0.086	0.019	0.268	0.052	0.094	0.008	0.023	0.065	0.122	0.030	0.412	0.070	0.112	0.011	0.029
TUMOR	$\bar{X}$	0.691	0.584	0.666	0.271	0.322	0.116	0.011	0.004	1.041	0.726	0.879	0.447	0.402	0.332	0.024	0.016
	SD	0.039	0.135	0.224	0.147	0.156	0.014	0.003	0.001	0.248	0.271	0.160	0.307	0.141	0.059	0.008	0.005
MUSCLE	$\bar{X}$	0.196	0.134	0.112	0.049	0.058	0.025	0.003	0.002								
	SD	0.051	0.016	0.042	0.016	0.003	0.002	0.001	0.001								
SKIN	$\bar{X}$	0.423	0.299	0.361	0.268	0.343	0.236	0.034	0.037								
	SD	0.083	0.028	0.045	0.042	0.050	0.014	0.011	0.007								
BONE	$\bar{X}$	0.194	0.164	0.169	0.115	0.099	0.065	0.007	0.003								
	SD	0.025	0.008	0.043	0.019	0.009	0.005	0.002	0.001								

Blood volume calculated as 6.5 % of body weight
Three animals per data point

APPENDIX 4. Tissue Distribution of 6-[I-123]-Iodouracil Co-injected with 6-ClU in Walker 256 Carcinoma Bearing Rats

		Tissue Specific Activity in cps/mg								Tissue to Blood Ratios							
		TIME IN MINUTES								TIME IN MINUTES							
		15	30	60	120	240	480	960	1560	15	30	60	120	240	480	960	1560
BLOOD	$\bar{X}$	4.812	3.391	2.918	1.286	1.204	0.548	0.050	0.020	1.000	1.000	1.000	1.000	1.000	1.000	1.000	1.000
	SD	0.694	1.022	1.122	0.514	0.376	0.035	0.019	0.008	0.0	0.0	0.0	0.0	0.0	0.0	0.0	0.0
THYROID	$\bar{X}$	1.362	1.208	0.962	0.353	0.466	0.230	0.026	0.010	0.283	0.360	0.349	0.255	0.406	0.413	0.516	0.502
	SD	0.200	0.292	0.223	0.313	0.037	0.103	0.011	0.003	0.006	0.028	0.075	0.228	0.094	0.168	0.035	0.052
HEART	$\bar{X}$	1.454	1.139	0.938	0.387	0.384	0.154	0.017	0.008	0.303	0.340	0.328	0.311	0.318	0.285	0.334	0.404
	SD	0.159	0.276	0.313	0.100	0.137	0.072	0.006	0.003	0.013	0.031	0.031	0.041	0.025	0.141	0.008	0.032
LUNG	$\bar{X}$	2.226	1.588	1.398	0.661	0.654	0.355	0.036	0.017	0.464	0.479	0.491	0.529	0.566	0.649	0.715	0.893
	SD	0.250	0.292	0.458	0.195	0.087	0.025	0.014	0.005	0.025	0.052	0.052	0.074	0.117	0.013	0.006	0.228
LIVER	$\bar{X}$	0.711	0.753	0.624	0.305	0.264	0.189	0.016	0.010	0.151	0.229	0.221	0.257	0.241	0.344	0.307	0.531
	SD	0.052	0.105	0.192	0.018	0.051	0.029	0.008	0.002	0.032	0.035	0.030	0.076	0.105	0.034	0.059	0.105
SPLEEN	$\bar{X}$	0.803	0.633	0.614	0.353	0.340	0.210	0.021	0.010	0.170	0.196	0.218	0.299	0.298	0.382	0.412	0.488
	SD	0.029	0.063	0.176	0.009	0.046	0.017	0.008	0.003	0.033	0.049	0.031	0.092	0.087	0.014	0.028	0.060
KIDNEY	$\bar{X}$	4.539	3.111	2.988	1.311	1.128	0.358	0.032	0.014	1.010	0.962	1.128	1.072	0.960	0.654	0.545	0.701
	SD	2.422	0.813	0.548	0.256	0.388	0.022	0.029	0.006	0.705	0.327	0.422	0.216	0.313	0.029	0.445	0.041
GIT	$\bar{X}$	0.587	0.586	0.606	0.495	0.577	0.333	0.029	0.016	0.126	0.178	0.242	0.445	0.518	0.600	0.564	0.872
	SD	0.099	0.107	0.063	0.142	0.237	0.111	0.015	0.002	0.042	0.032	0.133	0.241	0.307	0.165	0.136	0.308
TESTES	$\bar{X}$	0.350	0.401	0.526	0.441	0.497	0.264	0.036	0.013	0.075	0.122	0.193	0.379	0.425	0.482	0.727	0.663
	SD	0.043	0.118	0.106	0.083	0.093	0.017	0.013	0.005	0.021	0.041	0.051	0.162	0.073	0.030	0.075	0.063
STOMACH	$\bar{X}$	0.893	0.970	1.460	1.619	1.501	0.961	0.074	0.122	0.191	0.319	0.581	1.494	1.323	1.748	1.466	5.861
	SD	0.150	0.285	0.064	0.888	0.173	0.313	0.028	0.076	0.063	0.173	0.315	1.041	0.425	0.541	0.024	1.499
TUMOR	$\bar{X}$	2.285	1.931	2.202	0.895	1.064	0.384	0.036	0.013	0.482	0.577	0.769	0.680	0.863	0.701	0.728	0.708
	SD	0.129	0.447	0.741	0.486	0.517	0.047	0.011	0.004	0.079	0.038	0.065	0.231	0.181	0.062	0.045	0.232
MUSCLE	$\bar{X}$	0.649	0.444	0.369	0.162	0.191	0.082	0.009	0.007	0.140	0.136	0.127	0.129	0.168	0.150	0.187	0.348
	SD	0.169	0.053	0.140	0.054	0.009	0.006	0.004	0.003	0.059	0.023	0.011	0.035	0.044	0.014	0.003	0.147
SKIN	$\bar{X}$	1.400	0.990	1.194	0.887	1.136	0.781	0.111	0.123	0.301	0.313	0.449	0.769	1.030	1.426	2.243	6.778
	SD	0.276	0.093	0.148	0.139	0.164	0.046	0.035	0.023	0.109	0.103	0.157	0.314	0.456	0.025	0.386	2.393
BONE	$\bar{X}$	0.642	0.542	0.560	0.381	0.328	0.214	0.022	0.010	0.136	0.168	0.202	0.329	0.293	0.391	0.454	0.534
	SD	0.082	0.026	0.142	0.064	0.029	0.018	0.007	0.004	0.035	0.039	0.038	0.140	0.108	0.022	0.069	0.053

APPENDIX 5. Tissue Distribution of 6-[H-3]-2'-Fluoro-2'-deoxyuridine in Walker 256 Carcinoma Bearing Rats

		Percent Dose Incorporated per Gram of Tissue						Percent Dose Incorporated per Whole Organ					
		TIME IN MINUTES						TIME IN MINUTES					
		15	30	60	120	240	360	15	30	60	120	240	360
BLOOD	$\bar{X}$	0.311	0.321	0.277	0.264	0.265	0.264	5.057	5.221	4.493	4.292	4.309	4.286
	SD	0.048	0.042	0.033	0.013	0.021	0.020	0.777	0.679	0.529	0.213	0.349	0.326
HEART	$\bar{X}$	0.273	0.268	0.233	0.169	0.166	0.201	0.215	0.209	0.185	0.143	0.140	0.164
	SD	0.050	0.069	0.037	0.027	0.031	0.016	0.034	0.066	0.023	0.023	0.022	0.025
LUNGS	$\bar{X}$	0.326	0.306	0.228	0.210	0.158	0.215	0.440	0.403	0.320	0.297	0.251	0.272
	SD	0.064	0.026	0.019	0.043	0.043	0.066	0.085	0.034	0.038	0.056	0.111	0.078
LIVER	$\bar{X}$	2.907	1.795	0.834	0.273	0.256	0.299	31.696	19.528	9.950	3.373	2.957	2.848
	SD	0.774	0.633	0.094	0.057	0.033	0.072	8.215	6.496	1.369	0.689	0.324	0.584
SPLEEN	$\bar{X}$	0.329	0.320	0.287	0.212	0.186	0.295	0.228	0.216	0.221	0.174	0.180	0.206
	SD	0.044	0.057	0.017	0.032	0.005	0.156	0.037	0.049	0.019	0.025	0.089	0.083
KIDNEY	$\bar{X}$	1.911	1.441	0.762	0.326	0.279	0.288	3.351	2.521	1.467	0.629	0.463	0.501
	SD	0.300	0.119	0.119	0.051	0.081	0.084	0.424	0.296	0.173	0.117	0.213	0.155
TESTES	$\bar{X}$	0.201	0.210	0.176	0.179	0.153	0.181	0.309	0.322	0.271	0.302	0.254	0.306
	SD	0.054	0.017	0.084	0.038	0.035	0.021	0.131	0.059	0.163	0.074	0.068	0.037
GIT	$\bar{X}$	0.258	0.262	0.247	0.233	0.168	0.194	0.286	0.270	0.234	0.228	0.163	0.215
	SD	0.029	0.045	0.031	0.029	0.039	0.026	0.119	0.101	0.085	0.085	0.087	0.071
STOMACH	$\bar{X}$	0.285	0.243	0.241	0.195	0.141	0.252	0.409	0.366	0.378	0.310	0.200	0.360
	SD	0.066	0.025	0.046	0.052	0.018	0.072	0.110	0.082	0.094	0.081	0.026	0.104
TUMOR	$\bar{X}$	0.308	0.279	0.225	0.181	0.164	0.201	0.408	0.279	0.243	0.300	0.267	0.263
	SD	0.041	0.045	0.038	0.035	0.026	0.024	0.188	0.172	0.196	0.087	0.097	0.138
MUSCLE	$\bar{X}$	0.229	0.214	0.190	0.156	0.125	0.189						
	SD	0.037	0.024	0.031	0.026	0.023	0.022						
BONE	$\bar{X}$	0.169	0.141	0.131	0.108	0.085	0.095						
	SD	0.020	0.022	0.032	0.026	0.018	0.018						
SKIN	$\bar{X}$	0.384	0.263	0.177	0.177	0.141	0.151						
	SD	0.202	0.050	0.009	0.027	0.052	0.031						

Blood volume calculated as 6.5 % of body weight

Five animals per data point

APPENDIX 6. Tissue Distribution of 6-[H-3]-2'-Fluoro-2'-deoxyuridine in Walker 256 Carcinoma Bearing Wistar Rats

		Tissue Specific Activity in dpm/mg						Tissue to Blood Ratios					
		TIME IN MINUTES						TIME IN MINUTES					
		15	30	60	120	240	360	15	30	60	120	240	360
BLOOD	$\bar{X}$	27.635	28.529	24.554	23.456	23.546	23.421	1.000	1.000	1.000	1.000	1.000	1.000
	SD	4.247	3.713	2.890	1.162	1.906	1.784	0.0	0.0	0.0	0.0	0.0	0.0
HEART	$\bar{X}$	24.281	23.802	20.653	15.016	14.759	17.865	0.891	0.846	0.855	0.644	0.632	0.768
	SD	4.460	6.102	3.261	2.387	2.744	1.461	0.200	0.240	0.202	0.123	0.145	0.105
LUNGS	$\bar{X}$	28.970	27.143	20.245	18.681	13.997	19.129	1.052	0.962	0.828	0.793	0.599	0.826
	SD	5.695	2.320	1.663	3.840	3.799	5.880	0.155	0.131	0.049	0.130	0.177	0.287
LIVER	$\bar{X}$	258.159	159.407	74.099	24.278	22.696	26.528	9.575	5.769	3.061	1.032	0.971	1.148
	SD	68.738	56.225	8.308	5.092	2.942	6.429	3.240	2.568	0.599	0.192	0.160	0.239
SPLEEN	$\bar{X}$	29.206	28.441	25.470	18.789	16.478	26.232	1.068	1.007	1.048	0.800	0.703	1.101
	SD	3.911	5.021	1.554	2.881	0.423	13.894	0.159	0.201	0.131	0.108	0.055	0.523
KIDNEY	$\bar{X}$	169.734	127.959	67.692	28.978	24.740	25.582	6.182	4.527	2.747	1.240	1.066	1.112
	SD	26.624	10.610	10.534	4.570	7.200	7.452	0.856	0.517	0.108	0.226	0.359	0.408
TESTES	$\bar{X}$	17.807	18.661	15.646	15.896	13.579	16.061	0.653	0.662	0.635	0.683	0.586	0.689
	SD	4.802	1.467	7.443	3.352	3.145	1.874	0.197	0.088	0.294	0.168	0.173	0.100
GIT	$\bar{X}$	22.900	23.272	21.951	20.696	14.880	17.252	0.822	0.821	0.899	0.887	0.642	0.735
	SD	2.590	4.019	2.741	2.573	3.491	2.319	0.068	0.147	0.119	0.146	0.196	0.062
STOMACH	$\bar{X}$	25.327	21.552	21.373	17.309	12.541	22.420	0.935	0.765	0.890	0.739	0.532	0.971
	SD	5.827	2.201	4.045	4.591	1.627	6.407	0.270	0.116	0.237	0.201	0.049	0.325
TUMOR	$\bar{X}$	27.383	24.790	20.001	16.106	14.547	17.846	0.997	0.868	0.823	0.690	0.623	0.764
	SD	3.630	4.027	3.405	3.082	2.336	2.127	0.100	0.077	0.175	0.146	0.130	0.093
MUSCLE	$\bar{X}$	20.364	19.022	16.840	13.880	11.099	16.764	0.739	0.668	0.692	0.591	0.470	0.715
	SD	3.270	2.144	2.740	2.333	2.007	1.969	0.078	0.026	0.132	0.094	0.067	0.053
BONE	$\bar{X}$	14.978	12.532	11.676	9.562	7.569	8.421	0.550	0.442	0.478	0.410	0.322	0.358
	SD	1.774	1.995	2.823	2.343	1.605	1.606	0.089	0.072	0.121	0.110	0.065	0.046
SKIN	$\bar{X}$	34.078	23.315	15.734	15.738	12.501	13.400	1.285	0.839	0.647	0.670	0.542	0.581
	SD	17.922	4.410	0.800	2.436	4.606	2.764	0.764	0.227	0.070	0.093	0.240	0.164

APPENDIX 7. Tissue Distribution of 2'-[Cl-36]-2'-Chloro-2'-deoxyuridine in Lewis Lung Carcinoma Bearing BDF1 Mice

		Percent Dose Incorporated per Gram of Tissue						Percent Dose Incorporated per Whole Organ					
		TIME IN MINUTES						TIME IN MINUTES					
		15	30	60	90	120	180	15	30	60	90	120	180
BLOOD	$\bar{X}$	2.004	1.257	1.011	0.630	0.443	0.356	3.257	2.043	1.643	1.024	0.719	0.579
	SD	0.259	0.218	0.400	0.211	0.064	0.089	0.422	1.355	0.649	0.343	0.104	0.145
HEART	$\bar{X}$	2.523	1.555	1.093	1.020	0.532	0.461	0.340	0.189	0.125	0.119	0.064	0.055
	SD	0.370	0.238	0.285	0.565	0.102	0.085	0.054	0.015	0.022	0.076	0.008	0.008
LUNGS	$\bar{X}$	2.733	1.720	1.121	1.010	0.625	0.569	0.445	0.271	0.177	0.158	0.100	0.092
	SD	0.524	0.411	0.377	0.462	0.236	0.234	0.107	0.042	0.044	0.082	0.048	0.043
LIVER	$\bar{X}$	2.533	1.384	1.096	0.691	0.319	0.412	3.614	1.852	1.523	0.894	0.533	0.541
	SD	0.671	0.231	0.473	0.210	0.172	0.074	0.861	0.181	0.821	0.333	0.150	0.098
SPLEEN	$\bar{X}$	14.025	14.076	8.829	6.052	4.280	3.821	2.122	1.758	1.476	1.072	0.603	0.583
	SD	3.077	2.486	2.676	1.831	1.086	1.259	0.515	0.180	0.352	0.677	0.204	0.132
KIDNEY	$\bar{X}$	6.765	4.006	3.077	1.893	1.300	1.598	1.229	0.689	0.528	0.305	0.212	0.275
	SD	0.732	0.560	1.332	0.497	0.222	1.343	0.230	0.067	0.213	0.077	0.028	0.210
TESTES	$\bar{X}$	1.976	1.531	1.622	1.142	0.666	0.752	0.194	0.142	0.156	0.110	0.062	0.071
	SD	0.543	0.279	0.475	0.263	0.335	0.346	0.059	0.021	0.052	0.024	0.024	0.034
GIT	$\bar{X}$	2.762	2.003	2.077	1.022	0.653	0.821	4.092	2.630	2.648	1.316	0.857	1.001
	SD	0.363	0.366	1.036	0.201	0.152	0.382	0.925	0.383	1.046	0.224	0.218	0.324
STOMACH	$\bar{X}$	1.934	1.309	0.977	0.743	0.447	0.481	0.230	0.180	0.143	0.094	0.064	0.060
	SD	0.293	0.203	0.317	0.293	0.075	0.156	0.038	0.042	0.050	0.044	0.015	0.012
TUMOR	$\bar{X}$	4.371	3.963	2.657	1.990	1.872	1.944	2.423	1.410	2.137	1.158	0.936	1.361
	SD	1.126	0.871	0.952	0.653	0.470	1.488	1.217	0.888	1.403	1.115	0.381	1.716
MUSCLE	$\bar{X}$	2.170	1.599	1.143	0.826	0.408	0.469						
	SD	0.424	0.760	0.459	0.270	0.069	0.120						
BONE	$\bar{X}$	1.721	1.038	0.742	0.557	0.416	0.562						
	SD	0.462	0.154	0.218	0.220	0.148	0.412						
SKIN	$\bar{X}$	2.515	1.658	1.180	0.830	0.444	0.483						
	SD	0.486	0.301	0.457	0.296	0.142	0.167						

Blood volume calculated as 6.5 % of body weight
Five animals per 15, 30 and 120 min data point
Six animals per 60, 90 and 180 min data point

APPENDIX 8. Tissue Distribution of 2'-[Cl-36]-2'-Chloro-2'-deoxyuridine in Lewis Lung Carcinoma Bearing BDF1 Mice

		Tissue Specific Activity in cpm/mg						Tissue to Blood Ratios					
		TIME IN MINUTES						TIME IN MINUTES					
		15	30	60	90	120	180	15	30	60	90	120	180
BLOOD	$\bar{X}$	9.291	5.830	4.68	2.920	2.315	1.653	1.000	1.000	1.000	1.000	1.000	1.000
	SD	1.203	1.010	1.853	0.977	0.697	0.414	0.0	0.0	0.0	0.0	0.0	0.0
HEART	$\bar{X}$	11.698	7.210	5.067	4.729	3.022	2.139	1.258	1.240	1.155	1.728	1.263	1.388
	SD	1.717	1.100	1.323	2.620	1.427	0.393	0.049	0.110	0.277	1.202	0.174	0.589
LUNGS	$\bar{X}$	12.672	7.970	5.197	4.683	3.595	2.637	1.358	1.360	1.176	1.695	1.488	1.845
	SD	2.430	1.910	1.749	2.143	1.965	1.087	0.127	0.100	0.335	0.956	0.438	1.490
LIVER	$\bar{X}$	11.743	6.420	5.082	3.205	2.331	1.912	1.271	1.110	1.118	1.106	0.995	1.199
	SD	3.110	1.070	2.195	0.971	1.090	0.344	0.338	0.150	0.312	0.080	0.269	0.275
SPLEEN	$\bar{X}$	65.019	65.260	40.933	28.057	23.242	17.716	7.118	11.280	10.285	9.869	10.226	11.422
	SD	14.267	11.530	12.405	8.490	9.476	5.835	1.928	1.680	5.288	2.716	3.729	5.031
KIDNEY	$\bar{X}$	31.361	18.570	14.265	8.776	9.702	7.410	3.402	3.210	3.063	3.062	4.952	4.542
	SD	3.391	2.600	6.175	2.302	9.051	6.227	0.425	0.350	0.665	0.310	5.978	3.413
TESTES	$\bar{X}$	9.161	7.100	7.519	5.294	3.982	3.488	1.000	1.220	1.796	1.981	1.868	2.380
	SD	2.519	1.290	2.201	1.221	2.590	1.605	0.301	0.130	0.767	0.839	1.623	1.797
GIT	$\bar{X}$	12.805	9.290	9.628	4.740	3.782	3.808	1.345	1.600	1.993	1.714	1.578	2.393
	SD	1.685	1.700	4.802	0.933	1.954	1.770	0.138	0.220	0.356	0.449	0.350	1.141
STOMACH	$\bar{X}$	8.967	6.070	4.531	3.447	2.367	2.232	0.965	1.060	1.032	1.282	1.033	1.417
	SD	1.360	0.940	1.468	1.357	0.789	0.721	0.082	0.240	0.397	0.759	0.229	0.564
TUMOR	$\bar{X}$	20.265	18.370	12.319	9.224	8.365	9.014	2.196	3.210	3.074	3.471	3.502	5.578
	SD	5.220	4.040	4.413	3.028	4.608	6.898	0.554	0.840	1.594	1.535	1.571	3.992
MUSCLE	$\bar{X}$	10.059	7.410	5.299	3.828	2.185	2.172	1.089	1.230	1.130	1.372	0.934	1.402
	SD	1.964	3.510	2.130	1.250	0.770	0.554	0.211	0.360	0.133	0.539	0.045	0.528
BONE	$\bar{X}$	7.976	4.810	3.440	2.582	2.225	2.606	0.870	0.830	0.773	0.915	0.944	1.979
	SD	2.141	0.710	1.012	1.021	0.949	1.909	0.278	0.060	0.189	0.337	0.215	2.281
SKIN	$\bar{X}$	11.658	7.680	5.468	3.849	2.584	2.240	1.259	1.320	1.186	1.337	1.073	1.543
	SD	2.253	1.390	2.121	1.373	1.413	0.775	0.226	0.080	0.291	0.399	0.303	1.095

APPENDIX 9. Tissue Distribution of 2′-[I-123]-2′-Iodo-2′-deoxyuridine in Walker 256 Carcinoma Bearing Rats

		Percent Dose Incorporated per Gram Tissue								Percent Dose Incorporated per Whole Organ							
		TIME IN MINUTES								TIME IN MINUTES							
		15	30	60	120	240	480	960	1560	15	30	60	120	240	480	960	1560
BLOOD	$\bar{X}$	0.154	0.177	0.162	0.204	0.167	0.213	0.016	0.007	2.098	2.417	2.211	2.785	2.280	2.912	0.212	0.097
	SD	0.008	0.021	0.051	0.029	0.068	0.025	0.003	0.005	0.114	0.281	0.693	0.397	0.934	0.346	0.041	0.074
HEART	$\bar{X}$	0.465	0.411	0.284	0.223	0.107	0.090	0.006	0.003	0.396	0.330	0.256	0.205	0.091	0.076	0.005	0.003
	SD	0.024	0.014	0.097	0.016	0.017	0.016	0.001	0.001	0.051	0.024	0.069	0.013	0.006	0.022	0.001	0.001
LUNG	$\bar{X}$	0.871	0.755	0.410	0.284	0.188	0.174	0.012	0.006	0.496	0.767	0.684	0.470	0.261	0.269	0.012	0.005
	SD	0.256	0.208	0.096	0.048	0.030	0.030	0.004	0.004	0.418	0.225	0.154	0.150	0.087	0.057	0.002	0.002
LIVER	$\bar{X}$	1.414	1.136	0.722	0.430	0.213	0.155	0.008	0.007	12.100	10.514	7.014	4.206	1.947	1.315	0.103	0.072
	SD	0.065	0.222	0.209	0.070	0.015	0.031	0.002	0.002	0.310	1.250	1.593	0.585	0.174	0.300	0.016	0.020
SPLEEN	$\bar{X}$	1.513	1.698	1.101	0.685	0.299	0.181	0.009	0.006	1.086	1.365	0.996	0.519	0.232	0.134	0.007	0.005
	SD	0.259	0.055	0.308	0.135	0.008	0.029	0.003	0.002	0.146	0.047	0.263	0.066	0.079	0.008	0.001	0.002
KIDNEY	$\bar{X}$	1.520	1.267	0.695	0.530	0.252	0.179	0.012	0.005	1.316	1.174	0.655	0.465	0.242	0.167	0.010	0.005
	SD	0.261	0.057	0.125	0.088	0.024	0.020	0.003	0.002	0.204	0.107	0.150	0.071	0.018	0.020	0.003	0.002
STOMACH	$\bar{X}$	0.440	0.414	0.398	0.492	0.511	0.824	0.024	0.017	0.667	0.601	0.613	0.776	0.774	1.321	0.034	0.026
	SD	0.042	0.038	0.140	0.080	0.189	0.236	0.005	0.008	0.018	0.067	0.239	0.123	0.294	0.342	0.008	0.011
GIT	$\bar{X}$	1.290	0.809	0.528	0.384	0.231	0.179	0.011	0.006	0.335	0.886	0.644	0.444	0.317	0.274	0.011	0.005
	SD	0.330	0.073	0.184	0.062	0.078	0.047	0.002	0.003	0.110	0.239	0.173	0.048	0.076	0.165	0.003	0.003
TESTES	$\bar{X}$	0.087	0.115	0.124	0.134	0.113	0.109	0.011	0.005	0.138	0.178	0.202	0.212	0.158	0.171	0.018	0.007
	SD	0.006	0.018	0.027	0.017	0.019	0.013	0.002	0.003	0.025	0.025	0.053	0.027	0.051	0.026	0.004	0.004
TUMOR	$\bar{X}$	0.541	0.724	0.680	0.572	0.325	0.238	0.016	0.007	0.218	0.548	0.377	0.403	0.206	0.120	0.015	0.003
	SD	0.045	0.041	0.139	0.098	0.040	0.018	0.005	0.003	0.077	0.198	0.043	0.053	0.091	0.014	0.004	0.002
THYROID	$\bar{X}$	1.829	1.219	0.760	0.425	0.204	0.168	0.011	0.005	1.108	0.561	0.411	0.229	0.114	0.122	0.005	0.002
	SD	0.185	0.072	0.403	0.035	0.011	0.034	0.003	0.002	0.057	0.109	0.176	0.040	0.016	0.056	0.001	0.001
MUSCLE	$\bar{X}$	0.207	0.216	0.142	0.147	0.057	0.046	0.003	0.002								
	SD	0.007	0.012	0.036	0.061	0.010	0.006	0.001	0.001								
BONE	$\bar{X}$	0.218	0.205	0.157	0.157	0.088	0.093	0.008	0.004								
	SD	0.025	0.005	0.046	0.038	0.024	0.007	0.002	0.002								
SKIN	$\bar{X}$	0.264	0.374	0.309	0.277	0.214	0.259	0.022	0.021								
	SD	0.050	0.018	0.076	0.036	0.031	0.123	0.010	0.001								

Blood volume calculated as 6.5 % body weight
Three animals per data point

APPENDIX 10. Tissue Distribution of 2′-[I-123]-2′-Iodo-2′-deoxyuridine in Walker 256 Carcinoma Bearing Wistar Rats

		Tissue Specific Activity in cps/mg								Tissue to Blood Ratios							
		TIME IN MINUTES								TIME IN MINUTES							
		15	30	60	120	240	480	960	1560	15	30	60	120	240	480	960	1560
BLOOD	$\bar{X}$	0.170	0.196	0.179	0.225	0.184	0.236	0.017	0.008	1.000	1.000	1.000	1.000	1.000	1.000	1.000	1.000
	SD	0.009	0.023	0.056	0.032	0.076	0.028	0.003	0.006	0.0	0.0	0.0	0.0	0.0	0.0	0.0	0.0
HEART	$\bar{X}$	0.513	0.454	0.314	0.246	0.118	0.099	0.007	0.004	3.028	2.339	1.775	1.100	0.694	0.418	0.379	0.615
	SD	0.026	0.015	0.107	0.018	0.018	0.017	0.002	0.001	0.132	0.208	0.310	0.107	0.192	0.023	0.068	0.250
LUNGS	$\bar{X}$	0.962	0.834	0.452	0.314	0.208	0.192	0.013	0.007	5.688	4.262	2.649	1.414	1.217	0.812	0.757	0.897
	SD	0.282	0.229	0.106	0.054	0.033	0.033	0.004	0.004	1.787	1.005	0.718	0.340	0.329	0.040	0.094	0.219
LIVER	$\bar{X}$	1.561	1.254	0.797	0.475	0.235	0.172	0.009	0.007	9.209	6.450	4.680	2.150	1.424	0.725	0.537	1.110
	SD	0.072	0.245	0.230	0.077	0.016	0.034	0.002	0.003	0.490	1.229	1.495	0.572	0.576	0.058	0.059	0.364
SPLEEN	$\bar{X}$	1.671	1.875	1.216	0.756	0.330	0.200	0.010	0.006	9.827	9.659	7.018	3.428	2.039	0.848	0.611	0.949
	SD	0.286	0.061	0.340	0.149	0.009	0.032	0.003	0.002	1.457	0.923	1.575	1.005	0.933	0.053	0.162	0.327
KIDNEY	$\bar{X}$	1.678	1.399	0.767	0.585	0.278	0.198	0.013	0.006	9.958	7.247	4.458	2.637	1.667	0.841	0.744	0.880
	SD	0.288	0.063	0.139	0.097	0.026	0.022	0.004	0.002	2.126	1.210	0.838	0.647	0.601	0.010	0.088	0.260
STOMACH	$\bar{X}$	0.485	0.457	0.439	0.543	0.564	0.910	0.026	0.019	2.866	2.351	2.493	2.411	3.103	3.815	1.538	2.770
	SD	0.047	0.042	0.155	0.089	0.209	0.261	0.005	0.009	0.337	0.254	0.506	0.225	0.177	0.670	0.125	0.700
GIT	$\bar{X}$	1.424	0.894	0.583	0.424	0.254	0.198	0.013	0.006	8.465	4.624	3.337	1.914	1.432	0.832	0.741	0.900
	SD	0.364	0.080	0.203	0.068	0.086	0.052	0.002	0.003	2.479	0.783	0.818	0.463	0.272	0.120	0.055	0.257
TESTES	$\bar{X}$	0.096	0.127	0.137	0.148	0.125	0.120	0.012	0.005	0.568	0.651	0.788	0.657	0.783	0.511	0.697	0.702
	SD	0.007	0.020	0.030	0.019	0.021	0.014	0.003	0.003	0.016	0.063	0.095	0.038	0.445	0.007	0.044	0.127
TUMOR	$\bar{X}$	0.597	0.799	0.751	0.632	0.359	0.262	0.017	0.007	3.515	4.127	4.351	2.856	2.239	1.118	0.995	1.021
	SD	0.050	0.046	0.153	0.108	0.044	0.019	0.006	0.004	0.112	0.587	0.803	0.746	1.182	0.049	0.255	0.258
THYROID	$\bar{X}$	2.019	1.346	0.839	0.470	0.225	0.186	0.013	0.005	11.963	6.950	4.764	2.123	1.401	0.784	0.744	0.734
	SD	0.204	0.080	0.445	0.038	0.012	0.038	0.003	0.003	1.801	0.959	1.869	0.410	0.681	0.069	0.180	0.383
MUSCLE	$\bar{X}$	0.229	0.238	0.157	0.163	0.063	0.051	0.004	0.002	1.350	1.223	0.895	0.707	0.366	0.218	0.220	0.360
	SD	0.008	0.013	0.040	0.067	0.011	0.006	0.001	0.001	0.090	0.086	0.109	0.198	0.094	0.006	0.028	0.183
BONE	$\bar{X}$	0.241	0.227	0.173	0.173	0.097	0.102	0.008	0.004	1.420	1.169	0.976	0.766	0.549	0.437	0.490	0.539
	SD	0.028	0.005	0.051	0.042	0.026	0.008	0.002	0.002	0.135	0.121	0.080	0.112	0.082	0.023	0.105	0.084
SKIN	$\bar{X}$	0.292	0.413	0.341	0.306	0.236	0.286	0.025	0.023	1.722	2.134	1.954	1.382	1.419	1.182	1.424	3.903
	SD	0.055	0.020	0.084	0.040	0.034	0.136	0.012	0.001	0.339	0.321	0.279	0.302	0.508	0.411	0.519	2.023